UILU-ENG-87-2007

CIVIL ENGINEERING STUDIES
STRUCTURAL RESEARCH SERIES NO. 536

ISSN: 0069-4274

SEISMIC DAMAGE ANALYSIS AND DESIGN OF UNREINFORCED MASONRY BUILDINGS

By
Y-H. KWOK
and
A. H-S. ANG

Technical Report of Research
Supported by the
NATIONAL SCIENCE FOUNDATION
(under Grants ECE 85-11972
and CEE 83-12438)

UNIVERSITY OF ILLINOIS
at URBANA-CHAMPAIGN
JUNE 1987

50272-101

REPORT DOCUMENTATION PAGE	1. REPORT NO.	2.	3. Recipient's Accession No.

4. Title and Subtitle

SEISMIC DAMAGE ANALYSIS AND DESIGN OF UNREINFORCED MASONRY BUILDINGS

5. Report Date
JUNE 1987

6.

7. Author(s)
Y-H. Kwok and A. H-S. Ang

8. Performing Organization Rept. No.
SRS 536

9. Performing Organization Name and Address

Department of Civil Engineering
University of Illinois
208 N. Romine Street
Urbana, IL 61801

10. Project/Task/Work Unit No.

11. Contract(C) or Grant(G) No.

(C) NSF ECE 85-11972
(G) NSF CEE 83-12438

12. Sponsoring Organization Name and Address

National Science Foundation
Washington, D.C.

13. Type of Report & Period Covered

Technical Report

14.

15. Supplementary Notes

16. Abstract (Limit: 200 words)

A model for evaluating the structural damage to masonry buildings subjected to earthquake ground motion is proposed. Damage is expressed as a combination of the effects of excessive deformation and repeated loadings. The model parameters for unreinforced brick masonry are obtained from cyclic load tests of masonry wall specimens. A random vibration method using a nonlinear hysteretic restoring force model to describe the load-deformation behavior of masonry is adopted to evaluate the response statistics required for damage assessment. The proposed damage model is calibrated using the damages of a number of masonry buildings damaged during past earthquakes.

A simplified method for damage assessment is also proposed, in which seismic damage is expressed as a function of the seismic loading to the structural resistance. The validity of the simplified method is thoroughly examined relative to the random vibration method. A damage-limiting design method, based essentially on the equivalent lateral load procedure, is developed in which the base shear coefficient is expressed explicitly as a function of a tolerable damage level. Two design examples indicate the effectiveness of the design method.

17. Document Analysis a. Descriptors

Reliability
Earthquake
Masonry Structures

b. Identifiers/Open-Ended Terms

c. COSATI Field/Group

18. Availability Statement	19. Security Class (This Report)	21. No. of Pages
	UNCLASSIFIED	104
	20. Security Class (This Page)	22. Price
	UNCLASSIFIED	

(See ANSI-Z39.18) *See Instructions on Reverse*

OPTIONAL FORM 272 (4-77)
(Formerly NTIS-35)
Department of Commerce

ACKNOWLEDGMENTS

This report is based on the doctoral dissertation of Dr. Y-H. Kwok submitted in partial fulfillment for the Ph.D. degree at the University of Illinois at Urbana-Champaign. The study is part of a cooperative study in earthquake engineering with the Institute of Engineering Mechanics, Harbin, China; in this regard, Professors Y. Hu and J. Jiang, Ms. J. Xia, and Mr. Q. Lu provided valuable assistance in the collection and analysis of the experimental data used in this study.

The financial supports of the National Science Foundation under Grants CEE 83-12438 and ECE 85-11972 are gratefully acknowledged.

TABLE OF CONTENTS

Page

LIST OF TABLES

LIST OF FIGURES

Page

CHAPTER 1

INTRODUCTION

1.1 Objective and Scope

Masonry has been a building material since ancient times and is still used extensively in many countries for low and medium-rise buildings. It is a brittle material, and like plain concrete, is much stronger in compression than it is in tension. Because of its low cost and ease of construction, this has not precluded its use in seismically active areas; occasionally it is reinforced to resist tensile stresses. However, in places where steel reinforcement is not easily available or is expensive, as in rural areas of China or India, unreinforced masonry structures continue to be used extensively. The performance of these structures during earthquakes, such as the 1976 Tangshan earthquake, has generally been poor.

The aim of structural design is to provide safe and economical structures. In the case of structures subjected to seismic loads, the building should not collapse, even when it is subjected to severe ground shaking. Also, the additional cost necessary for earthquake resistance should not be higher than the expected cost of repair in the event of an earthquake. Thus, the design of earthquake-resistant structures should be guided by considerations of potential damage to a structure. This is recognized in the philosophy underlying many seismic building codes. Limiting the potential damage to some tolerable level is implied in many codes; however, lacking a quantitative measure for damage, it has not been considered explicitly in structural design.

The objective of this study, therefore, is to (i) develop a quantitative measure of damage for unreinforced brick masonry structures, (ii) calibrate this damage measure to actual observed damage, and (iii) develop a design procedure for low-rise unreinforced masonry buildings that explicitly limits the

potential seismic damage to a specified tolerable level.

Damage from earthquakes depends on the seismic loading and the structural capacity. Seismic loading, which may be described by the intensity of the ground motion, its sequence, duration, and frequency content, is highly unpredictable. It is appropriate that this should be modeled as a stochastic process so that the uncertainty in the loading can be accounted for. The determination of the structural response, therefore, requires a random vibration approach. The response of a masonry building to a given loading is dependent on its load-deformation characteristics. Under a strong seismic loading that can cause damage, the load-deformation relation of masonry is nonlinear. Energy is also dissipated through hysteresis under repeated cyclic loading. Being a brittle material, the strength of masonry deteriorates rapidly after reaching its ultimate strength. Thus, to accurately predict the response to seismic loading, the load-deformation model for masonry should reflect the above characteristics.

The load-deformation behavior of a masonry wall is affected by the presence of other structural components, such as out-of-plane walls and framing beams and columns, and by nonstructural components. Experiments on unreinforced concrete block walls by Woodward (1986) indicate that the behavior of walls intersecting at a corner can be adequately predicted by considering each wall independently. The influence of frames and nonstructural components on the load-deformation behavior of a wall will depend on their relative strengths and stiffnesses, and associated interaction under cyclic loading. In many cases, the influence of nonstructural components on the load-deformation behavior is uncertain, and when damaged under cyclic loading, their effect on the overall structural behavior is nominal. In this study, damage will be correlated with the in-plane response of masonry shear walls without frames.

For the damage measure to be meaningful, it has to be calibrated against observed seismic damage of masonry structures. For this purpose, damage data on unreinforced brick masonry buildings damaged during recent earthquakes in the People's Republic of China (PRC) are used. These are two to four-story

residential or office buildings in which unreinforced masonry shear walls are the primary structural components for resisting both vertical and lateral loads.

It has been observed that masonry buildings tend to be more severely damaged in the lower stories. This is clearly undesirable because collapse, or even severe damage, to the lower stories would be tantamount to the total failure of the entire building. Thus, not only should the overall damage be limited to a desired level, but damage should also be uniformly distributed throughout the building height.

1.2 Review of Related Studies

Masonry walls are often the vertical load-bearing as well as the lateral load-resisting components of a masonry structure. Hence, much experimental work has focussed on the shear resistance of masonry walls subjected to vertical and lateral loads (Benjamin and Williams, 1958; Scrivener, 1969; Sinha and Hendry, 1969; Turnsek and Cacovic, 1970; Borchelt, 1970; Williams, 1971; Meli, 1972; Williams and Scrivener, 1973; Priestley and Bridgeman, 1974; Mayes et al., 1976; Hegemier, et al., 1978; Zhu et al., 1980; Woodward, 1986; Xia, et al., 1986). The diversity in the types of masonry and methods of construction is reflected in the above experimental research which includes clay brick and concrete block masonry, reinforced and unreinforced walls, subjected to monotonic and cyclic loadings. Since there is as yet no consensus on the most appropriate testing procedures that would give the best estimate of the actual shear strength, various configurations of test specimens and testing methods were used. Most of the researchers attempted to correlate the experimentally determined shear strength with parameters such as the vertical compressive load, and the masonry tensile strength. While quantitative relations are thus obtained for a specific type of masonry, differences in masonry type and testing procedures make it possible only to obtain general qualitative conclusions about the effects of various parameters on shear strength (see Mayes and Clough, 1975 for a review).

Yang et al. (1981) compiled extensive data on unreinforced masonry structures damaged during six earthquakes in the PRC. Structural damage to walls was classified into five categories from collapse to no damage. The equivalent base shear coefficients that will induce wall shear stresses equal to the allowable shear stresses in the walls were calculated. Correlating the computed base shear coefficients with different degrees of damage, design base shear coefficients were obtained that will ensure no severe damage.

1.3 Organization of Report

Chapter 2 proposes a seismic damage model for masonry. Damage is represented by a damage index which is a function of the maximum deformation and absorbed hysteretic energy. Using results from cyclic load tests, the necessary model parameters are obtained for unreinforced brick masonry.

In Chapter 3, a nonlinear restoring force model for masonry is developed. The model is capable of stiffness degradation and strength deterioration beyond the ultimate load. Model parameters are determined for unreinforced brick masonry. Using this model, a random vibration approach to obtain the statistics of the maximum displacement and dissipated energy is described.

In Chapter 4, the damage indices for forty five buildings subjected to ground motions from five earthquakes in the PRC are computed. These damage indices are correlated with the observed damages, thus establishing limits on the damage index corresponding to different levels of damage.

Chapter 5 develops a damage-limiting design procedure based on an alternate method to obtain the damage index. Damage is expressed as the ratio of the seismic load to the structural capacity. Using this method, a modification to the equivalent lateral load procedure is proposed in which the base shear coefficient is obtained as a function of the limiting damage level. The design method is illustrated with two examples. The designs based on the proposed method are compared with those based on existing building codes. The reliability of the proposed design method is evaluated.

1.4 Summary of Notations

a	=	restoring force model parameter
C_s, C_s'	=	base shear and adjusted base shear coefficient, respectively
D	=	damage index
D_e	=	component of damage caused by dissipated energy
D_L	=	tolerable damage level
D_s	=	overall structural damage index
D_u	=	component of damage caused by excessive deformation
D_{ult}	=	ultimate damage capacity
e_p	=	mean maximum potential energy
E_m	=	elastic modulus of masonry
F_{u_m}	=	distribution function of the maximum displacement
F_{u_p}	=	distribution function of the peak displacement
f_m	=	compressive strength of masonry
f_{mo}	=	compressive strength of mortar
f_{mu}	=	compressive strength of masonry units
G_m	=	shear modulus of masonry
k_{eu}	=	equivalent linearized stiffness
k_i	=	initial wall stiffness used in response analysis
k_{ic}	=	computed initial wall stiffness
N	=	number of stories
n_i	=	number of peaks in the i-th time interval
q, q_n	=	restoring force and normalized restoring force, respectively
q_u	=	ultimate shear capacity of masonry
S	=	covariance matrix
s_0	=	shot noise spectral ordinate
S_D	=	sum of story damage indices

T = first natural period of a structure

T_g = predominant period of ground motion

t_d = duration of strong ground motion

u_f = failure deformation

u_m, u_{mn} = maximum and normalized maximum deformation, respectively

u, u_n = displacement and normalized displacement, respectively

u_p = peak displacement

u_u, u_{ue} = ultimate and equivalent ultimate displacement respectively

z = hysteretic displacement

α = ratio of failure displacement to ultimate displacement

α_1, α_2, β, γ, η, ν, ρ = parameters of the restoring force model

ϵ = parameter of damage index

ς_g = ground damping ratio

λ = ratio of k_i to secant stiffness at ultimate load

λ_c = ratio of k_{ic} to secant stiffness at ultimate load

μ = coefficient of friction between masonry unit and mortar

σ_a = root-mean-square (rms) acceleration

σ_b = bond strength of masonry

σ_c = vertical compressive stress

σ_{cr} = critical tensile stress of masonry

$\sigma_{D_{ult}}$ = standard deviation of ultimate damage index

σ_u, $\sigma_{\dot{u}}$ = rms displacement and velocity, respectively

σ_E = standard deviation of absorbed energy

τ, τ_{all} = masonry shear strength and allowable shear stress, respectively

ϕ_D = damage distribution vector

ϕ_i = first mode displacement of the i-th story

ϕ_i' = first mode interstory displacement of the i-th story

ω_g = predominant ground motion frequency

$E[\ ]$ = expected value

$\int dE$ = cumulative hysteretic energy

$Var[\ ]$ = variance

CHAPTER 2

DAMAGE MODEL OF MASONRY

2.1 Introduction

The in-plane shear resistance of masonry walls provide the major lateral load resistance of most masonry structures. Seismic damage to masonry structures during an earthquake is caused mainly by shear and to a lesser extent by bending or overturning moment. Shear failure in masonry walls is initiated by cracking from diagonal tension or bond slip at the joints. Crack propagation eventually leads to a decrease in load carrying capacity. Hence, shear failure of masonry, especially of unreinforced masonry, is essentially brittle. This would suggest that damage to masonry structures is primarily a function of the deformation. In addition, under cyclic loading, masonry walls (especially those with reinforcement) have some ability to dissipate hysteretic energy. Masonry walls will fail when cyclically loaded under load control (Xia, et al., 1986), indicating that energy dissipation can also cause damage.

A damage model for masonry is proposed expressing damage as a function of the maximum deformation and the dissipated energy. Since masonry is composed of masonry units (clay bricks, concrete blocks, etc.) and mortar, the parameters of the damage model should be specific to the type of masonry construction. In this study, the damage model parameters are obtained for unreinforced brick masonry from test data of brick walls cyclically loaded to failure.

2.2 Proposed Damage Model

In accordance with the behavior of masonry described above, seismic damage to masonry can be expressed as a function of the damage caused by

excessive deformation and that due to energy dissipation. This is expressed in terms of a damage index,

$$D = D_u + D_e \tag{2.1}$$

or

$$D^2 = D_u^2 + D_e^2 \tag{2.2}$$

in which $D_u = \frac{u_m}{u_f}$ and $D_e = \epsilon \frac{\int dE}{q_u u_f}$,

where: u_m = the maximum response deformation,

u_f = the deformation at failure,

$\int dE$ = the cumulative hysteretic energy,

q_u = the ultimate shear capacity,

and, ϵ = a constant.

Equations 2.1 and 2.2 give linear and circular damage surfaces, respectively. Structural damage is thus expressed as a function of the response quantities u_m and $\int dE$ and the structural parameters u_f, q_u, and ϵ. Collapse certainly means failure; however, under cyclic loading, walls are able to resist lateral loads through friction even after severe cracking (Xia, et al., 1986), and thus are able to deform substantially before collapse. When this occurs, however, the masonry wall would have lost its integrity as a structural component because of severe cracking, such that any out-of-plane motion, as would occur in an earthquake, will easily cause total collapse. Moreover, frictional lateral resistance is not consistently evident in all walls tested. Hence, even without collapse, an unreinforced masonry wall of a low-rise structure can be considered to have failed when its residual lateral load resistance is mainly through friction.

2.2.1 Determination of Damage Model Parameters

The proposed damage model (Eq. 2.1 or 2.2) contains three parameters; namely, u_f, q_u, and ϵ which have to be determined from experimental data.

Many early experimental programs involved wall specimens of various configurations subjected to monotonically increasing loads. Later, pseudo-static cyclic load tests were used to study the hysteretic behavior and degradation of strength and stiffness under repeated loading. However, to simulate conditions during an earthquake, dynamic cyclic testing is required. For examples, experiments by Williams and Scrivener (1973) and Mayes, et al. (1976) have indicated that pseudo-static tests may not always produce conservative estimates of ultimate strength or stiffness degradation. To date, dynamic cyclic load tests are still not common because of the need for elaborate testing equipment.

Ultimate Shear Capacity, q_u -- A shear wall may fail either in flexure or in shear. To determine the shear capacity in the flexural failure mode, it is necessary to obtain the moment capacity of a shear wall. The ability of an unreinforced wall to resist moments will depend on the tensile strength of masonry and the vertical compressive load. The tensile strength of masonry is small; hence, the moment resistance of an unreinforced wall is due mainly to gravity loads. Flexural failure of shear walls in low-rise unreinforced masonry buildings during an earthquake is not as common as shear failure (except in the top story where the compressive load is low).

In the shear mode of failure, the ultimate shear capacity of unreinforced masonry is the product of the shear strength, τ, and the wall area. Two analytical formulations for estimating the shear strength are

$$\tau = \sigma_b + \mu \sigma_c \tag{2.3}$$

and

$$\tau = \frac{\sigma_{cr}}{\xi} \left(1. + \frac{\sigma_c}{\sigma_{cr}} \right)^{\frac{1}{2}} \tag{2.4}$$

where: σ_b = the bond strength,

μ = the coefficient of friction between a masonry unit and the mortar,

σ_c = the vertical compressive stress,

σ_{cr} = the critical tensile stress of masonry,

and, ξ = a factor depending on the wall geometry and load distribution (equals 1.5 for a laterally loaded cantilever rectangular section).

Equation 2.3 assumes that the shear strength is due to bond and friction between the masonry units and mortar. It gives good estimates of the shear strength when the mortar strength is low, resulting in failure along cracks running stepwise through the mortar joints. Values of σ_b and μ for brick masonry have been obtained by Benjamin and Williams, (1958), Zelga, (1965), Murthy and Hendry, (1966), Sinha and Hendry, (1969), Pieper and Trautsch, (1970), and Zhu, et al., (1980), and for concrete block masonry by Woodward, (1986). Depending on the strength of the masonry units and the mortar, values of σ_b range between 0.5 and 5.0 kg/cm^2, whereas the coefficient of friction varies from 0.3 to 1.0.

Equation 2.4 assumes that failure occurs when the principal tensile stress in masonry exceeds a critical value (Borchelt, 1970, Turnsek and Cacovic, 1970). It has been observed to give good estimates of the shear strength when the bond between the masonry units and mortar is strong (as when the mortar strength is high and workmanship is good), allowing the principal tensile strength to reach its critical value without a bond slip. Failure is characterized by diagonal cracks running through both the masonry units and mortar.

Test data of cyclically loaded unreinforced brick masonry walls from Zhu, et al., (1980), Ref. 27, and Xia, et al. (1986) are used to obtain the parameters σ_b, μ, and σ_{cr} of Eqs. 2.3 and 2.4. The test data available are for low strength bricks with compressive strength, f_{mu} = 75 to 100 kg/cm^2. Bond between masonry units and mortar can be expected to depend on the mortar strength, water retentivity of the mortar, initial rate of absorption of the masonry unit, and workmanship.

For Eq. 2.3, regression analysis gives μ = 0.5 and

$$\sigma_b = 0.056\,(f_{mo})^{0.8} \tag{2.5}$$

Fig. 2.1 shows the variation of σ_b with the mortar strength, f_{mo}. Using Eqs. 2.3 and 2.5, the ratio of the experimental to the calculated ultimate shear capacities has a mean of 1.02 and a coefficient of variation (cov) of 0.11.

Figure 2.2 shows the variation of σ_{cr} with f_{mo}. In this case, regression gives

$$\sigma_{cr} = 0.20 (f_{mo})^{0.7} \tag{2.6}$$

Using Eqs. 2.4 and 2.6, the ratio of the experimental to the calculated shear capacities has a mean and cov of 1.02 and 0.23, respectively. Also shown for comparision in Fig. 2.2 are the σ_{cr} values obtained by Turnsek and Cacovic (1970) from monotonically increasing lateral load tests on cantilever walls. The higher values for σ_{cr} is likely to be associated with higher strength bricks ($f_{mu} = 200$ kg/cm^2) and monotonic (instead of cyclic) loading.

Failure Displacement, u_f, and ϵ -- The displacement at failure, u_f, may be defined as a multiple of the ultimate displacement, u_u, corresponding to q_u. Because of deterioration in the load carrying capacity for $u > u_u$, especially for unreinforced walls, the recording of loads and displacements for $u > u_u$ is difficult. Therefore, for simplicity u_f is assumed to be a constant multiple of u_u, i.e.,

$$u_f = \alpha u_u \tag{2.7}$$

in which α is a constant. The ultimate displacement, u_u, may be obtained as

$$u_u = \lambda_c \frac{q_u}{k_{ic}} \tag{2.8}$$

where k_{ic} is the computed initial stiffness of the wall.

To obtain k_{ic}, the elastic and shear moduli of masonry, E_m and G_m, are required. The elastic modulus is a function of the elastic moduli of the masonry units and the mortar, and the ratio of the thickness of the masonry units to the thickness of the mortar joints (Sahlin, 1971). However, for practical purposes, it is common to relate E_m to the masonry strength, f'_m. For

brick masonry, E_m may vary from $400 f'_m$ to $1000 f'_m$ with a mean of $700 f'_m$ (Shalin, 1971), whereas the shear modulus may be assumed to be

$$G_m = 0.4 E_m \tag{2.9}$$

The factor λ_c was computed for all the test data in which u_u can be obtained; the results are summarized in Fig. 2.3, indicating a negative correlation between λ_c and the vertical compressive stress σ_c. Regression analysis gives the relationship

$$\lambda_c = 1./(0.052 + 0.82\, \sigma_c/ f'_m) \tag{2.10}$$

For each wall specimen tested to failure ($D \geq 1.0$), the value of α can be computed for a given ϵ. Failure was assumed to have occurred when the load test had to be terminated because of significant reduction in the load carrying capacity or when the residual lateral load resistance was largely frictional. The parameter ϵ can be chosen so that α will have minimum variance. This gives $\alpha = 1.47$ and $\epsilon = 0.075$ for Eq. 2.1 and $\alpha = 1.30$ and $\epsilon = 0.122$ for Eq. 2.2.

2.3 Ultimate Damage Index

With the appropriate model parameters determined above, the damage index for each test specimen can be computed using Eq. 2.1 or 2.2. The computed damage index, D_{ult}, for each test specimen is a measure of its capacity to resist damage when subjected to cyclic loads. For both equations, D_{ult} can be assumed to be distributed according to the Weibull distribution (see Fig. 2.4). Using Eq. 2.1, the mean and cov of D_{ult} are 0.99 and 0.31 respectively, whereas Eq. 2.2 gives a mean of 0.99 and a cov of 0.30. Since Eq. 2.2 does not seem to give a significantly better measure of damage (as seen from the cov of D_{ult}) and in view of the relative simplicity of Eq. 2.1 over Eq. 2.2, the former will be used subsequently for the assessment of seismic damage to unreinforced brick masonry structures.

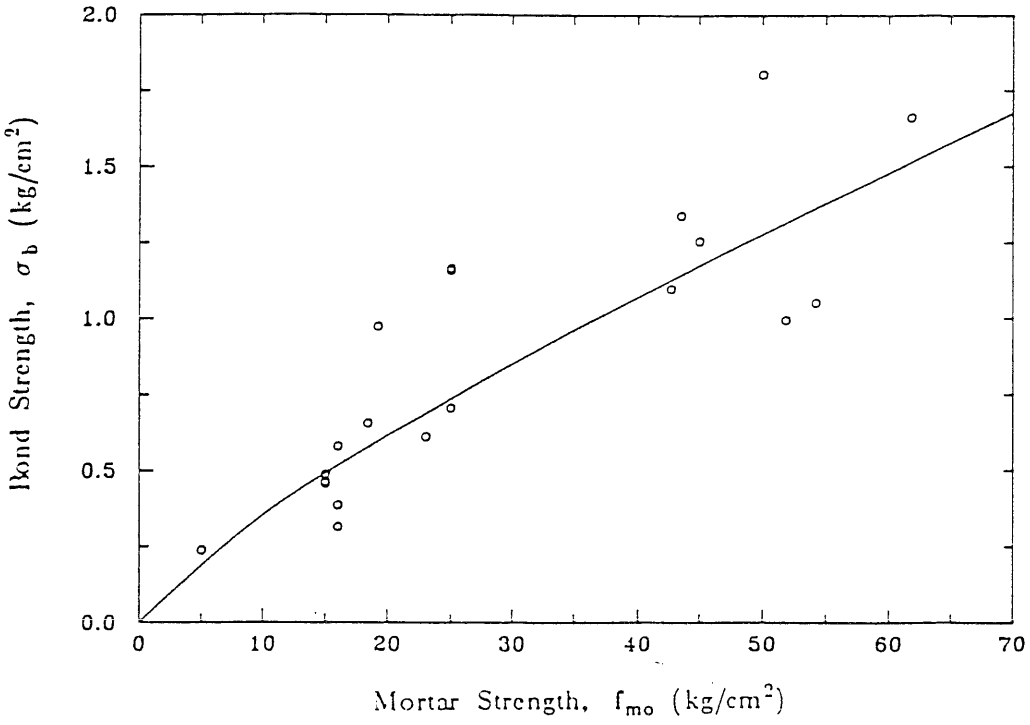

Fig. 2.1 Bond Strength versus Mortar Strength

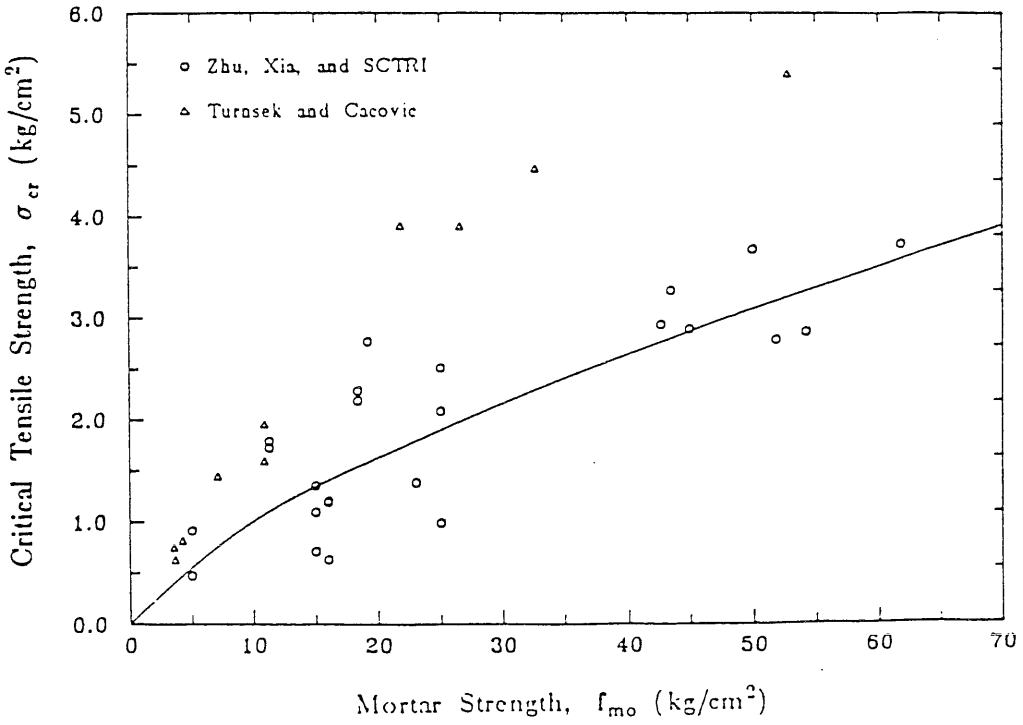

Fig. 2.2 Critical Tensile Strength versus Mortar Strength

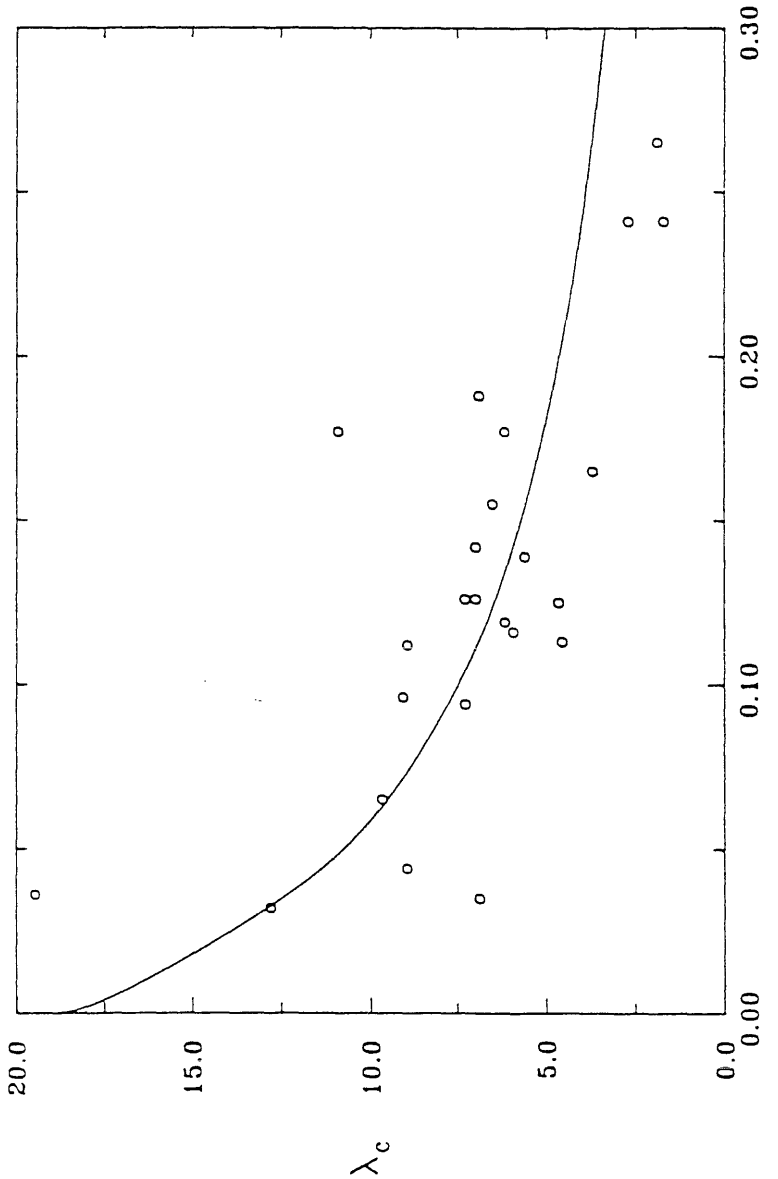

Fig. 2.3 λ_c versus σ_c/f_m

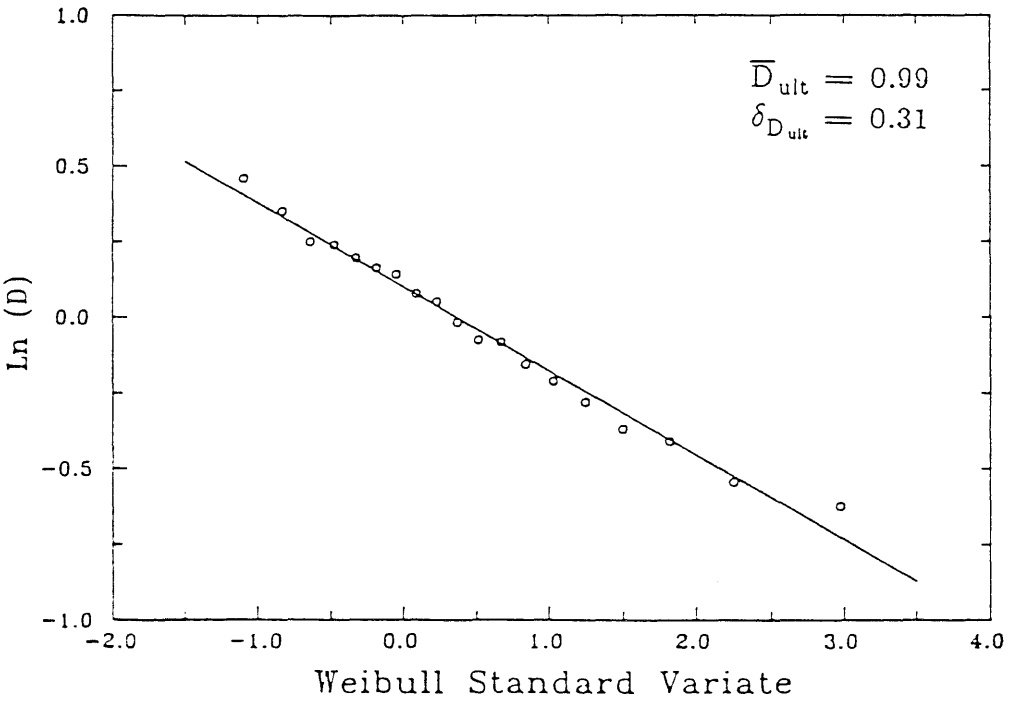

Fig. 2.4a Distribution of Ultimate Damage Index defined by Eq. 2.1a

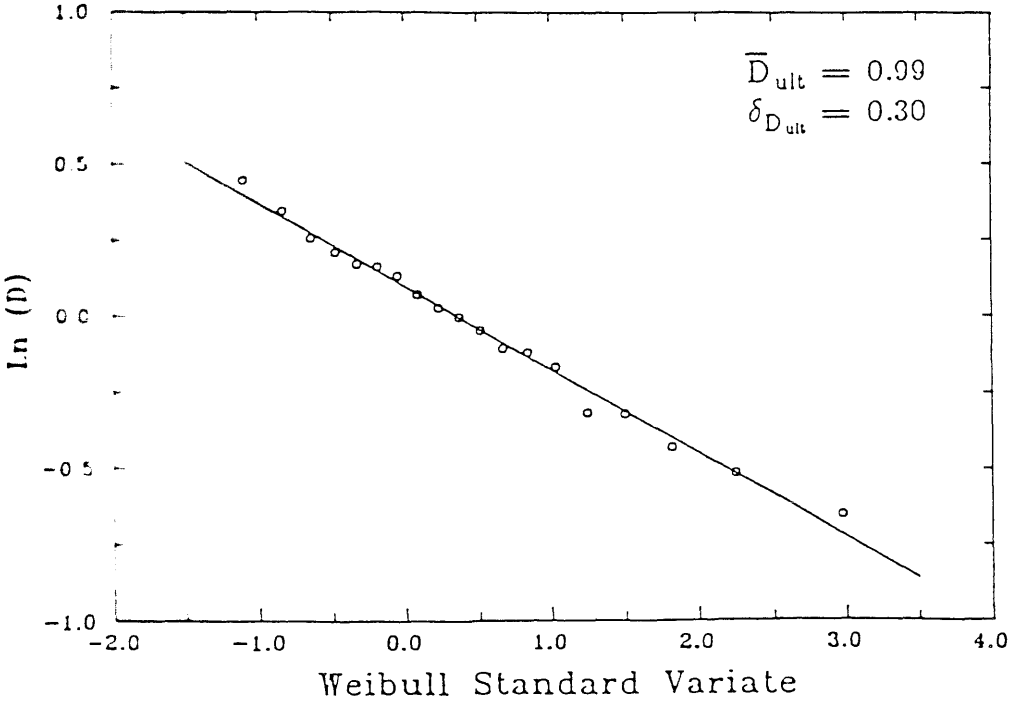

Fig. 2.4b Distribution of Ultimate Damage Index defined by Eq. 2.1b

CHAPTER 3

DAMAGE ANALYSIS OF MASONRY STRUCTURES

3.1 Introductory Remarks

The damage model developed in the previous chapter is the basis for a seismic damage assessment method for unreinforced masonry structures. The assessment method should be able to account for uncertainties in the structural capacity as well as in the loading and response predictions.

Since unreinforced masonry exhibits brittle load-deformation behavior and stiffness degradation when subjected to repeated loading, a material model reflecting such behavior is required. For this purpose, the nonlinear hysteretic restoring force model of Baber and Wen (1981) is adopted. Ground motion will be modeled as a nonstationary filtered shot noise, and the response statistics are obtained through a random vibration analysis using equivalent linearization of the nonlinear system (Atalik and Utku, 1976; Wen, 1980).

Since the maximum displacement and dissipated energy are the response quantities required in the damage assessment, methods suitable for obtaining the necessary response statistics are examined.

3.2 Damage Index Statistics

The structural capacity of a masonry component to resist damage is highly variable and may be modeled as a random variable. In order to incorporate the variability in the structural capacity with the uncertainty in the random response, the damage index of a masonry component i may be represented as,

$$D_i = \frac{D}{D_{ult}} \tag{3.1}$$

where: D = structural damage as defined by Eq. 2.1

D_{ult} = ultimate damage capacity with $\overline{D}_{ult} = 1.00$, $\sigma_{D_{ult}} = 0.31$.

When the structural damage D exceeds the damage capacity D_{ult}, the component damage index D_i exceeds one, indicating failure of the component.

Assuming no correlation between the maximum displacement and the dissipated energy, the mean and variance of D_i are obtained using a second-order approximation (Ang and Tang, 1975) as follows:

$$\overline{D}_i = (1 + \sigma^2_{D_{ult}})\,\overline{D} \tag{3.2}$$

and,

$$\mathrm{Var}[D_i] = \frac{1}{u_{fi}^2}\mathrm{Var}[u_{mi}] + \left(\frac{\epsilon}{q_{ui}u_{fi}}\right)^2 \mathrm{Var}[\int dE] + \sigma^2_{D_{ult}}\overline{D}^2 \tag{3.3}$$

where,

$$\overline{D} = \frac{\overline{u}_{mi}}{u_{fi}} + \frac{\epsilon}{q_{ui}u_{fi}}\mathrm{E}[\int dE] \tag{3.4}$$

The statistics of D_i are thus obtained in terms of the mean and variance of the response quantities u_m and $\int dE$.

3.2.1 Evaluation of Response Statistics

In order to obtain the statistics of the response quantities u_m and $\int dE$, the following are required: a restoring force model for masonry, a ground motion model, and a method for response analysis.

Restoring Force Model for Masonry -- A restoring force model describes the force-displacement relationship for a structural component under a given loading history. The monotonic load-displacement curve (or skeleton curve for cyclic loading) for a masonry wall is shown in Fig 3.1. Strength deterioration for displacements $u > u_u$ is highly variable, depending on the material properties, vertical compressive load, and amount of reinforcement. Masonry may have residual lateral load resistance due to friction (dashed line

of Fig. 3.1) but this cannot be relied upon. Hence, it will be assumed that for $u > u_u$, the resistance decreases with increasing displacement.

The restoring force model of Baber and Wen (1981) has been used to describe the behavior of ductile structural components (Sues, et al., 1983; Park, et al., 1984). Since masonry is a brittle material, a modification to the above restoring force model is necessary to describe the strength deterioration for $u > u_u$.

The force-displacement relationship is given by

$$q(u) = \alpha_1 q_u g(u) + \alpha_2 q_u z \tag{3.5}$$

in which,

$$g(u) = \left(1 - \left|1 - \frac{|u|}{a u_u}\right|^{\rho}\right) \frac{u}{|u|} \tag{3.6}$$

and,

$$\dot{z} = [\dot{u} - \nu(\beta|\dot{u}|z - \gamma\dot{u}|z|)]/(u_u\eta) \tag{3.7}$$

where α_1, α_2, a, ρ, γ, β, ν, and η are parameters.

The first term in Eq. 3.5 is the nonlinear, nonhysteretic component of the restoring force (see Fig. 3.2). Depending on the parameters α_1, a, and ρ, it governs the strength deterioration for $u > u_u$. The second term is the degrading hysteretic component with the loading and unloading characteristics controlled by γ and β, whereas the strength and stiffness degradations are controlled by ν and η.

The restoring force is maximum at u_u; thus, two conditions must be satisfied;

$$q_n = 1.0 \qquad \text{at } u_n = 1.0 \tag{3.8a}$$

and,

$$\frac{dq_n}{du_n} = 0.0 \qquad \text{at } u_n = 1.0 \tag{3.8b}$$

where $q_n = q/q_u$ and $u_n = u/u_u$. Hence, only six of the eight parameters in

Eqs. 3.5 through 3.7 are independent.

The parameters of the restoring force model can be obtained from results of cyclic load tests of masonry wall components. For this purpose it is convenient to rewrite the parameters as

$$\lambda,\ \alpha_2,\ a,\ \rho,\ (\gamma + \beta),\ (\gamma - \beta),\ \nu,\ \text{and}\ \eta\ .$$

The parameter λ is the ratio of the initial stiffness to the secant stiffness at ultimate load. It is used in place of α_1 because it can be more directly obtained from experimental results. Through Eq. 3.5, λ is related to the other parameters by,

$$\lambda = \frac{\alpha_1 \rho}{a} + \alpha_2 \tag{3.9}$$

The ratio of λ to λ_c is equal to the ratio of the actual to the computed initial stiffness (see Fig 3.3), i.e., the actual initial stiffness is given by,

$$k_i = \frac{\lambda}{\lambda_c} k_{ic} \tag{3.10}$$

The two hysteretic parameters are regrouped as $(\gamma + \beta)$ and $(\gamma - \beta)$ which then characterize the restoring force during loading and unloading, respectively. The influence of α_2, λ, and ρ on the restoring force is shown in Fig. 3.4.

The effect of α_2 on the restoring force is evident only under cyclic loading; in particular, pinching in the load-displacement curves becomes prominent when α_2 is small (see Fig. 3.4a). The contribution of the nonhysteretic component to the restoring force is large when α_2 is small. Therefore, as the displacement decreases when $u < au_u$, the decrease in the restoring force due to the nonhysteretic component causes pinching. Figure 3.4b indicates that although λ, being the ratio of the initial stiffness to the secant stiffness at ultimate load, is expected to affect the restoring force for $u < u_u$, it also has a significant effect on the post-ultimate load-displacement behavior. The parameter ρ, however, affects the load-displacement behavior only in the post-ultimate displacement range, $u > u_u$ (see Fig. 3.4c).

From Eq. 3.9, the parameter α_2 can be intepreted as the contribution from the hysteretic component to the initial stiffness. It is thus convenient to express α_2 as a fraction of λ. Pinching in the load-displacement curves results from the relative displacement between two parts of a masonry component caused by cracking. Hence, pinching is common in the load-displacement curves of reinforced walls failing in flexure. In this case, a value of $\alpha_2 = 0.6\lambda$ to 0.8λ is appropriate. For unreinforced masonry failing in shear, pinching is less common. Also, from Williams and Scrivener's (1973) experiments on reinforced masonry failing in shear, pinching which occurred during pseudo-static cyclic loading was less evident under dynamic cyclic loading. Hence, for masonry failing in shear, $\alpha_2 \geq 0.9\lambda$ appears appropriate.

Having determined α_2 in terms of λ, it is then possible, for a given λ, ρ, and $\nu = \eta = 1.0$, to solve for $(\gamma + \beta)$ and a using Eq. 3.8.

From Fig. 3.4c, it is observed that ρ has negligible influence on the restoring force for $u < u_u$. Therefore λ can be obtained by fitting the force-displacement relationships to experimental load-displacement points (for $u < u_u$) using an arbitrary ρ. For unreinforced masonry, the available data indicate that λ may vary between 3.0 and 6.0. Regression using load-displacement points from all test data yield a mean value of $\bar{\lambda} = 5.1$.

The parameter ρ controls the strength deterioration for $u > u_u$; a higher value of ρ represents more brittle behavior. Available load-displacement data for $u > u_u$ show wide variation in the post-ultimate behavior. Test data for unreinforced masonry indicate that ρ may be between 2.0 and 6.0 (see Fig 3.5). Regression using all data points gives a mean value of $\bar{\rho} = 3.3$.

The parameter $(\gamma - \beta)$ must be negative for the unloading stiffness to be positive. For the range of displacements of interest ($u < 2\ u_u$), unloading behavior is reasonably modeled by $(\gamma - \beta) = -5\rho$.

It is evident from all experimental load-displacement curves that stiffness degradation occurs with cyclic loading. The parameter η is the ratio of the initial to the degraded tangent stiffnesses at zero load of the hysteretic

component. Figure 3.6 shows η plotted against the normalized maximum displacement, indicating a linear relationship

$$\eta = 1.0 + 3.6\, u_{mn} \tag{3.11}$$

in which $u_{mn} = u_m / u_u$.

Since the parameters $(\gamma + \beta)$ and a were obtained for $\nu = \eta = 1.0$, Eq. 3.8 will no longer be satisfied with stiffness degradation. For most cases, this results in a maximum restoring force which is less than q_u as seen in Fig. 3.7 which shows an envelope curve and cyclic load-displacement curves with stiffness degradation. Thus it appears necessary to update $(\gamma + \beta)$ and a with each change in η. However, this is not desirable because changing a alters the restoring force characteristics beyond the ultimate displacement, whereas the actual post-ultimate behavior may not be similarly affected by stiffness degradation. Alternatively, the decrease in the maximum restoring force may be compensated through the parameter ν, which changes the magnitude of the hysteretic component. The value of ν depends on the degree of stiffness degradation, which according to Eq. 3.11, is dependent on u_{mn}. Thus ν can be given by

$$\nu = \begin{cases} \exp(-\delta_\nu u_{mn}) & u_{mn} \leq 1.0 \\ \exp(-\delta_\nu) & u_{mn} > 1.0 \end{cases} \tag{3.12}$$

in which

$$\delta_\nu = c_1(\lambda)^{-c_2}$$

For η given in Eq. 3.11, the constants may be approximated by

$$c_1 = \exp(7.73 - 2.90\sqrt{\rho} + 2.91 \ln \rho)$$

$$c_2 = 5.55 - 1.27\sqrt{\rho} + 1.12 \ln \rho$$

Hence for $\lambda = 5.1$ and $\rho = 3.3$, $\delta_\nu = 0.217$. When $u_m > u_u$, it is observed from experimental results that the restoring force, under repeated loading, is unable to reach q_u, i.e. there is deterioration in the maximum restoring force in the post-ultimate displacement range. Hence, it is not necessary to

compensate for strength deterioration when $u_{mn} > 1.0$.

Figure 3.8 shows a comparison between the observed load-displacement curves and those described by the restoring force model using appropriate parameters for two test specimens.

Ground Motion Model -- Ground motion is modeled as a zero-mean filtered Gaussian shot noise random process with a Kanai-Tajimi spectrum

$$S_{aa}(\omega) = s_0 \frac{1 + 4\zeta_g(\omega/\omega_g)^2}{[1-(\omega/\omega_g)^2]^2 + 4\zeta_g^2(\omega/\omega_g)^2} \tag{3.13}$$

where s_0 is the power spectral ordinate of the stationary unfiltered shot noise and ω is frequency. The filter parameters ω_g and ζ_g will generally depend on factors such as local site conditions, distance from the earthquake source, and earthquake magnitude.

To model the nonstationarity in the ground motion, its intensity is modulated by a time function given by

$$\psi(t) = \begin{cases} (t/t_1)^2 & 0 \le t \le t_1 \\ 1.0 & t_1 \le t \le t_2 \\ e^{-1.8(t-t_2)/t_d} & t_2 \le t \end{cases} \tag{3.14}$$

in which $t_1 = 0.15\,t_d$, $t_2 = 1.15\,t_d$ and t_d is the strong motion duration.

Random Vibration Response Analysis -- The equation of motion of a single-degree-of-freedom (SDF) system under ground excitation is given by

$$m\ddot{u} + c\dot{u} + q(u) = -m\ddot{x}_g \tag{3.15}$$

where m and c are the mass and damping, respectively, q(u) is the restoring force given by Eq. 3.5, and $\ddot{x}_g$ is the ground acceleration. Using an equivalent linearization procedure (Atalik and Utku, 1976; Wen, 1980), Eq. 3.6 can be written as

$$g(u) = k_{eu}\,u \tag{3.16}$$

in which the equivalent linearized stiffness

$$k_{eu} = \left(\frac{2}{\pi}\right)^{\frac{1}{2}} \frac{\rho}{\rho - 1} \frac{1}{\sigma_u} (I_1 - I_2) \tag{3.17}$$

where $\sigma_u = \sqrt{E[u^2]}$ and the integrals I_1 and I_2 are given in the Appendix. The variation of k_{eu} with σ_u is shown in the load-displacement curves of Fig. 3.9. As σ_u increases, the equivalent stiffness decreases and eventually becomes negative. The rate of decrease in the equivalent stiffness increases with ρ.

Similarly, Eq. 3.7 can be linearized as

$$\dot{z} = c_e \dot{u} + k_{ez} z \tag{3.18}$$

in which,

$$c_e = (1 - \left(\frac{2}{\pi}\right)^{\frac{1}{2}} \bar{\nu} \sigma_z (\beta \rho_{\dot{u}z} + \gamma)) / (u_u \bar{\eta}) \tag{3.19a}$$

and,

$$k_{ez} = - \left(\frac{2}{\pi}\right)^{\frac{1}{2}} \bar{\nu} \sigma_{\dot{u}} (\beta + \gamma \rho_{uz}) / (u_u \bar{\eta}) \tag{3.19b}$$

where $\sigma_z = \sqrt{E[z^2]}$ and $\rho_{\dot{u}z} = E[\dot{u}z] / \sqrt{E[\dot{u}^2] E[z^2]}$.
The resulting linearized equations of motion may be written in matrix form as

$$\dot{\mathbf{Y}} = \mathbf{G}\,\mathbf{Y} + \mathbf{F} \tag{3.20}$$

in which $\mathbf{Y} = \{ x_g, \dot{x}_g, u, \dot{u}, z \}^T$,

$$\mathbf{G} = \begin{bmatrix} 0 & 1 & 0 & 0 & 0 \\ -\omega_g^2 & -2\zeta_g\omega_g & 0 & 0 & 0 \\ 0 & 0 & 0 & 1 & 0 \\ \omega_g^2 & 2\zeta_g\omega_g & -\alpha_1 q_u k_{eu}/m & -c/m & -\alpha_2 q_u/m \\ 0 & 0 & 0 & c_e & k_{ez} \end{bmatrix},$$

and $\mathbf{F} = \{ 0, \ddot{\xi}_g, 0, 0, 0 \}^T$, where $\ddot{\xi}_g$ is the unfiltered ground acceleration. This leads to the equation (Lin, 1976)

$$\dot{\mathbf{S}} = \mathbf{G}\,\mathbf{S} + \mathbf{S}\,\mathbf{G}^T + \mathbf{B} \tag{3.21}$$

where $\mathbf{S} = E[\mathbf{Y}\mathbf{Y}^T]$ and $B_{ij} = 0$ except $B_{22} = 2\pi\psi(t)s_0$.

The zero-time lag covariance matrix $\mathbf{S}$ is obtained by integrating Eq. 3.21. Since the equivalent linearized quantities k_{eu}, c_e, and k_{ez} are functions of the response quantities in $\mathbf{S}$, these are updated at each integration time step. Extension of the above formulation to multi-degree-of-freedom (MDF) systems is straightforward (see Baber and Wen, 1980).

Since k_{eu} becomes negative when σ_u is large, $E[u^2]$ would eventually increase without bound. This is analogous to the situation in a deterministic analysis (i.e. a response-history analysis) where the displacement increases without bound when $u >> u_u$.

3.2.2 Response Statistics

Maximum Displacement Statistics -- The mean and variance of the maximum displacement, u_m, are required in estimating the statistics of the damage function in Eqs. 3.2 and 3.3. Yang and Liu (1981) and Park, et al. (1984) have separately proposed approximate methods to obtain the distribution of the displacement peaks over a given time period; by assuming independence between the peaks, the distribution of the maximum peak is also obtained. Because both these methods estimate the distribution of the peaks over the entire duration of interest, a decrease in the response (as, for example, following the strong motion phase of earthquake ground shaking) will cause the mean peak displacement to decrease. This in turn will result in a decrease in the calculated mean maximum displacement. However, by definition the maximum displacement cannot decrease. Therefore, in order to avoid this inconsistency, it is proposed that the distribution of peaks be obtained over several subintervals instead of over the entire duration of interest. Then the distribution of the maximum displacement, assuming independence between peaks, is

$$F_{u_m} = \prod_i [F^i_{u_p}]^{n_i} \tag{3.22}$$

where $F^i_{u_p}$ and n_i are the distribution and the number of peaks in the i-th subinterval. The number of peaks, n_i, can be approximated by the mean number of zero crossings of the displacement time history, i.e.,

$$E[n_i] = \frac{1}{\pi}\int \frac{\sigma_{\dot{u}}}{\sigma_u}(1 - \rho_{u\dot{u}})\ dt \tag{3.23}$$

where $\sigma_{\dot{u}} = \sqrt{E[\dot{u}^2]}$ and $\rho_{u\dot{u}} = E[u\dot{u}]/\sqrt{E[u^2]\,E[\dot{u}^2]}$. The distribution of the maximum displacement obtained from Eq. 3.22 will have a monotonically increasing mean. In order to establish the appropriate distribution for u_m, simulation was performed for two SDF systems with properties representing the wall sections of Fig 3.10. Wall 1 is relatively strong (q_u = 140kN), but brittle (ρ = 8.0), whereas Wall 2 is weak (q_u = 66kN), but relatively ductile (ρ = 2.0). The ground filter parameters are ω_g = 15.6 rad/s and ζ_g = 0.64. The root-mean-square (rms) acceleration is 0.3g. Monte Carlo simulations were performed for each wall using 150 trials.

From the simulation results, the maximum displacement within the time interval from 0 to t were plotted, for different t, on probability papers (as shown in Figs. 3.11 and 3.12) to ascertain the appropriate distribution for u_m. From Figs. 3.11 and 3.12, u_m is seen to have an extreme value Type I distribution for small σ_u (Figs. 3.11a and 3.12a), but as the response increases, u_m is better described by an extreme value Type II distribution (Figs. 3.11b and 3.12b). Yang and Liu (1981) have also shown through simulations that for a system with positive stiffness, u_m has an extreme value Type I distribution. However, for the masonry restoring force model, there is a tendency for the displacement to increase when $u > u_u$ because of decreasing stiffness. Hence, as u_m increases, the extreme value Type II distibution becomes more appropriate.

The distribution of the displacement peaks, u_p, for a narrow-band stationary Gaussian process is the Rayleigh distribution

$$F_{u_p} = 1 - \exp\left\{-\frac{1}{2}\left(\frac{u_p}{\sigma_u}\right)^2\right\} \tag{3.24}$$

In view of the simulation results, it is proposed that the tail of this distribution be modified to give a Pareto distribution as shown in Fig 3.13. Letting u_t be the peak displacement at which the distribution changes form, the probability density function for $u > u_t$ is

$$f_{u_p} = c \frac{k}{u_p} \left(\frac{u_t}{u_p} \right)^k \tag{3.25}$$

where c and k are the parameters. The requirement that the density function is continuous at $u = u_t$ gives

$$c = \exp(-0.5\, k^2) \tag{3.26a}$$

and,

$$k = \left(\frac{u_t}{\sigma_u} \right)^2 \tag{3.26b}$$

From the simulation results, the peak displacement u_t may be assumed to be the value of σ_u at which the equivalent linearized stiffness, k_{eu}, is zero. From Eq. 3.17, $k_{eu} = 0$ implies $I_1 = I_2$. The values of σ_u satisfying this condition were obtained for different ρ, and regression gives

$$u_t = a u_u (1.47 - 0.33 \ln \rho) \tag{3.27}$$

Hence, when σ_u is small, the peak distribution is essentially Rayleigh and Eq. 3.22 yields the extreme value Type I distribution for F_{u_m}. As σ_u increases, the Pareto tail of F_{u_p} causes F_{u_m} to approach the extreme value Type II distribution.

Analytical estimates of the maximum displacement statistics were obtained using the method of Yang and Liu (1981) and the method proposed here. Figure 3.14 shows the mean maximum displacement over time and Fig. 3.15 shows the distribution of u_m just before the analytical solution becomes unstable (due to negative k_{eu}). The method by Yang and Liu gives good estimates of the mean maximum displacement but the extreme value Type I distribution is inappropriate, resulting in an underestimation of the variance of the maximum displacement as shown in Fig. 3.15.

Hysteretic Energy Statistics -- The covariance matrix S does not yield statistics for the hysteretic energy. Since

$$dE = \alpha_2 q_u z\, du = \alpha_2 q_u z \dot{u}\, dt \tag{3.28}$$

an additional equation (for each degree of freedom)

$$\dot{E}[\int dE] = \alpha_2 q_u E[z\dot{u}] \tag{3.29}$$

is integrated along with Eq. 3.21 to give the mean of $\int dE$.

To obtain the variance of the hysteretic energy, σ_E^2, at time t, a double integration of certain elements of the two-time covariance matrix S(s,v), where s, v $\leq$ t, is required (Pires, et al., 1983). For this integral to be accurately evaluated, S(s,v) must be computed for sufficently small time intervals ds and dv. Hence, in the response analysis, about 80 to 90 percent of the computation involves the evaluation of σ_E^2. Figure 3.16 shows the contribution of the variance in the hysteretic energy to the total variance of the damage index for different system periods T. It can be seen that this contribution is small (less than 2% in most cases); hence σ_E^2 may be approximated or even neglected. Figure 3.17 shows the variation over time of the cov of the hysteretic energy, δ_E, for several systems. It appears that σ_E^2 decreases with time, and increases with the period of the system. It is also fairly constant for all degrees of freedom in MDF systems. Regression gives the empirical relation

$$\delta_E = 1.7\, T^{2.3}\, t^{-1/2} \tag{3.30}$$

where t is time in seconds, and T is the system period. Using this approximation to obtain σ_E^2 reduces the computing time substantially with negligible error in the variance of the damage index.

3.3 Overall Damage Assessment

In a multistory structure, it is desirable to have an overall indicator of damage. This overall damage index should reflect the effect of a story's damage on the total damage of a structure and the distribution of damage among

the stories of a building. Assuming that the story damage distribution would be proportional to the distribution of the potential energy, an overall structural damage index can be defined as the sum of the story damage indices, each weighted by the maximum potential energy of the story, i.e.,

$$D_s = \sum_i w_i D_i \tag{3.31}$$

in which $w_i = e_{pi} / \sum_j e_{pj}$, where e_{pi} is the mean maximum potential energy of the i-th story. Observe that in a multistory building, w_i will generally be greater for the lower stories because of higher lateral loads, unless there is damage concentration in a particular story.

The mean maximum potential energy is obtained by integrating the first term in Eq. 3.5, giving

$$e_p = \begin{cases} \alpha_1 q_u \left(E[u_m] + \dfrac{a u_u}{\rho + 1} \left(|1-x|^{\rho}(1-x) - 1 \right) \right) ; & x < 2.0 \\ 2\alpha_1 q_u a u_u \left(1 - \dfrac{1}{\rho + 1} \right) ; & x \geq 2.0 \end{cases} \tag{3.32}$$

in which $x = \dfrac{E[u_m]}{a u_u}$.

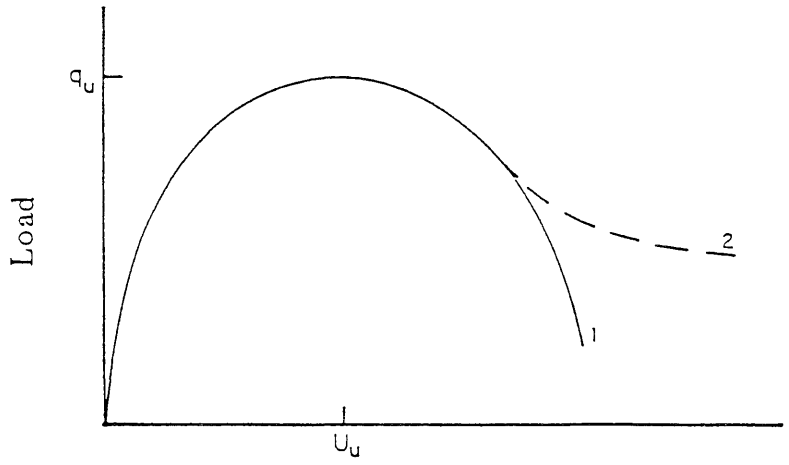

Fig. 3.1 Monotonic Load-Displacement Curve for Masonry

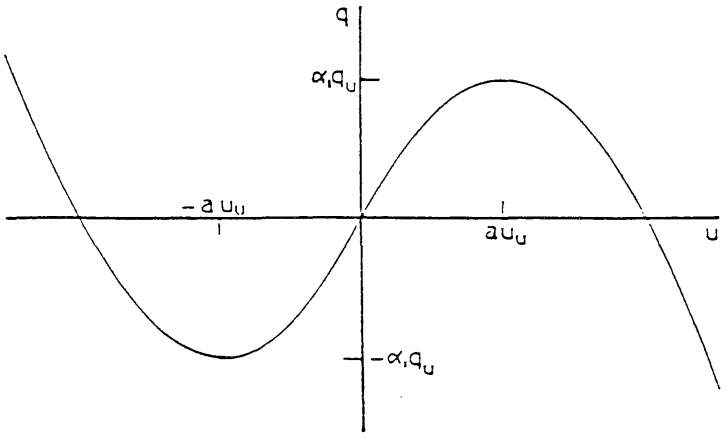

Fig. 3.2 Nonhysteretic Component of Restoring Force

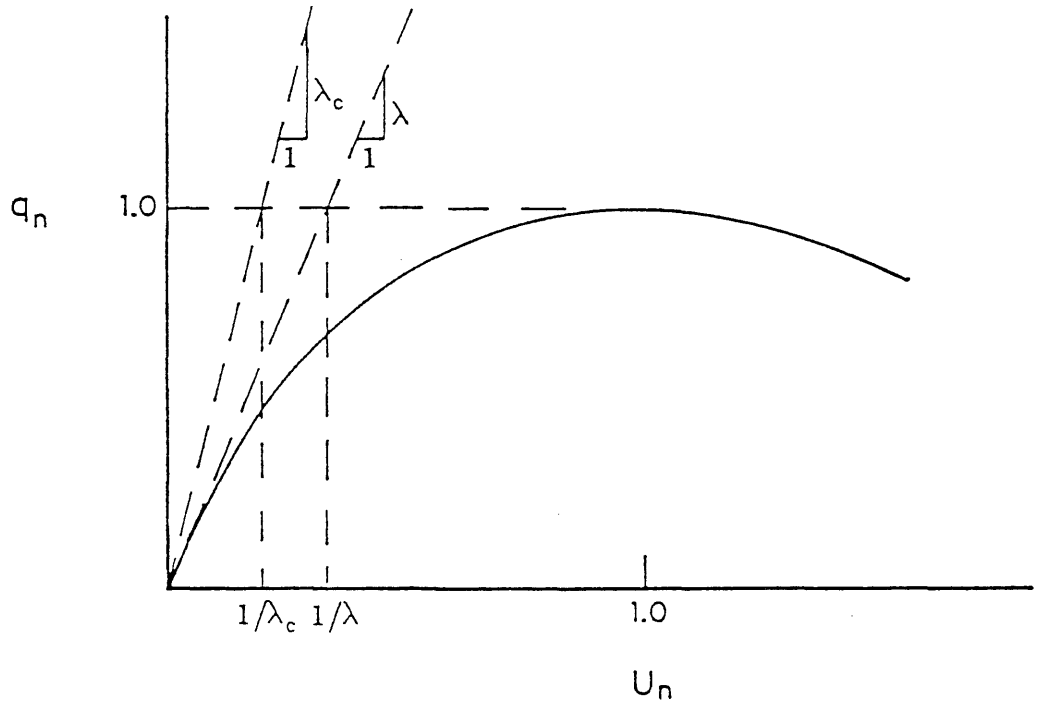

Fig. 3.3 Definition of λ and λ_c

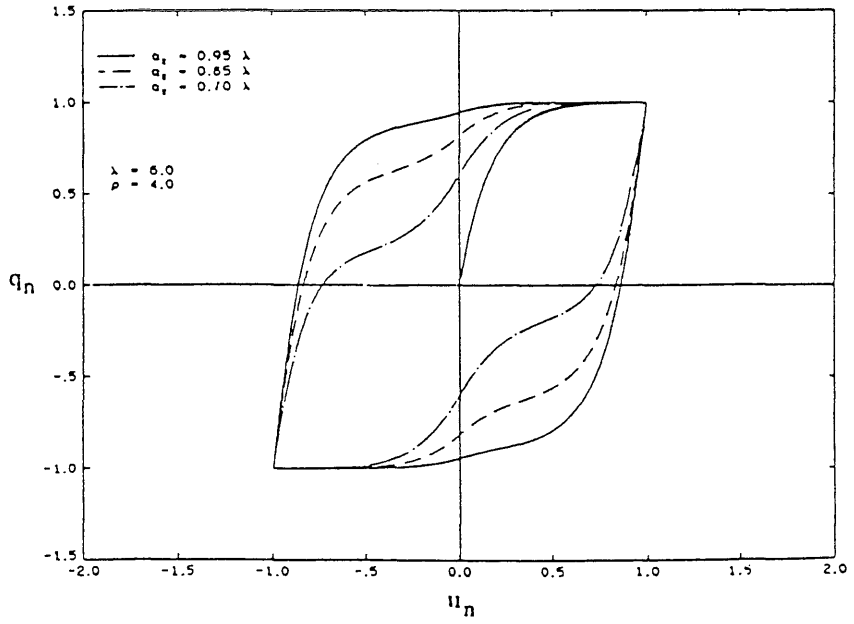

Fig. 3.4a Influence of α_2 on Restoring Force

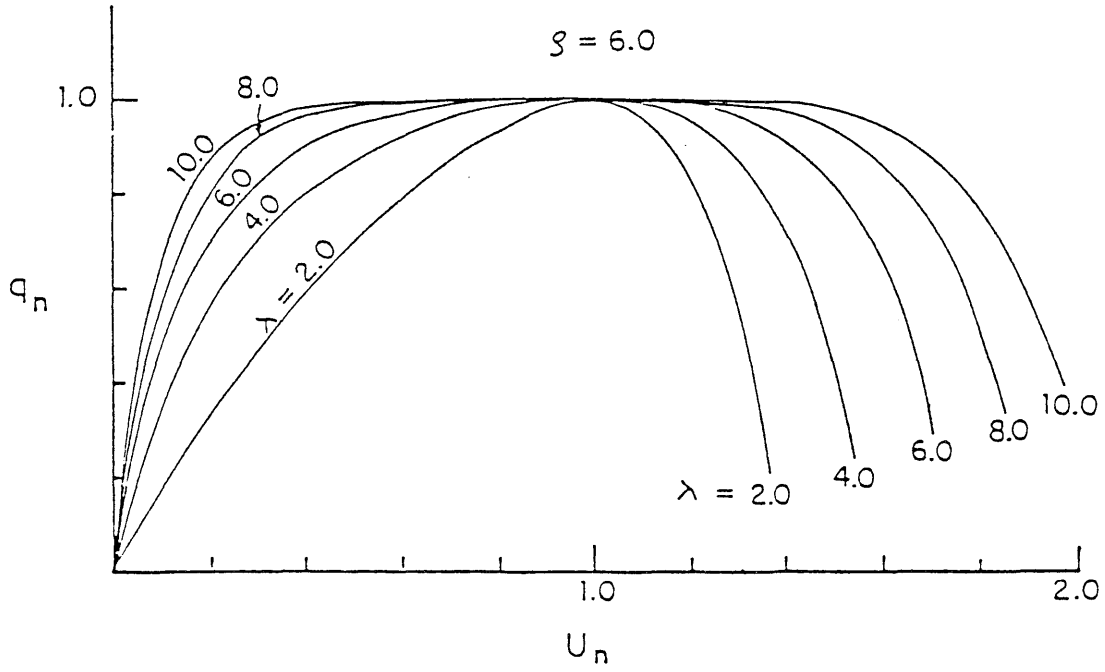

Fig. 3.4b Influence of λ on Restoring Force

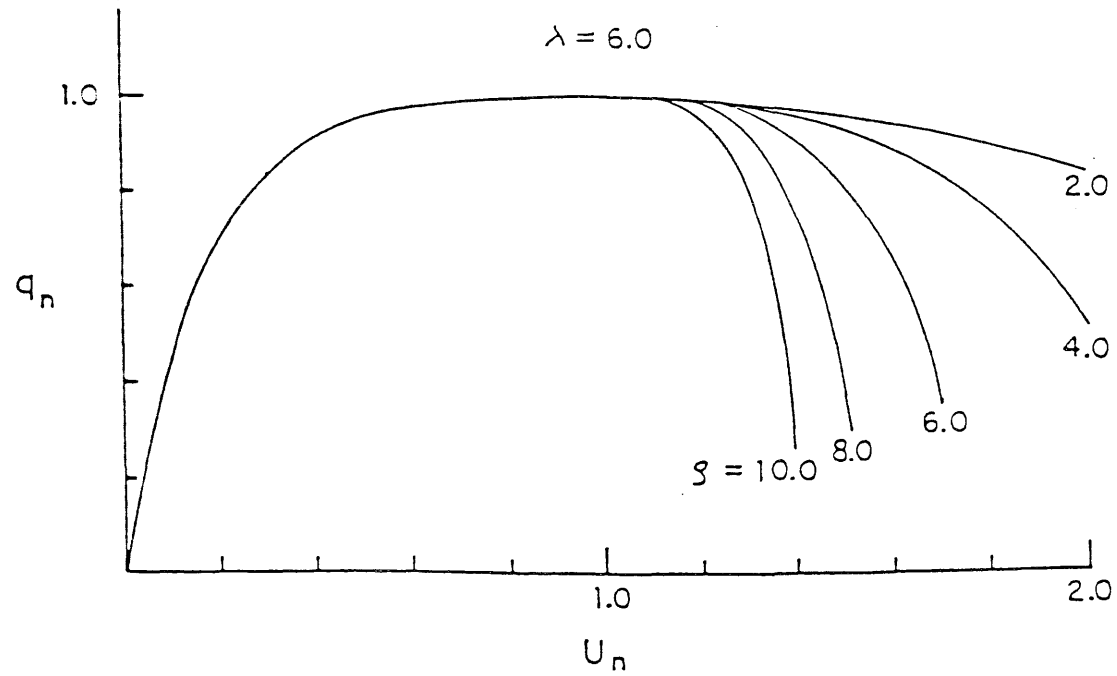

Fig. 3.4c Influence of ρ on Restoring Force

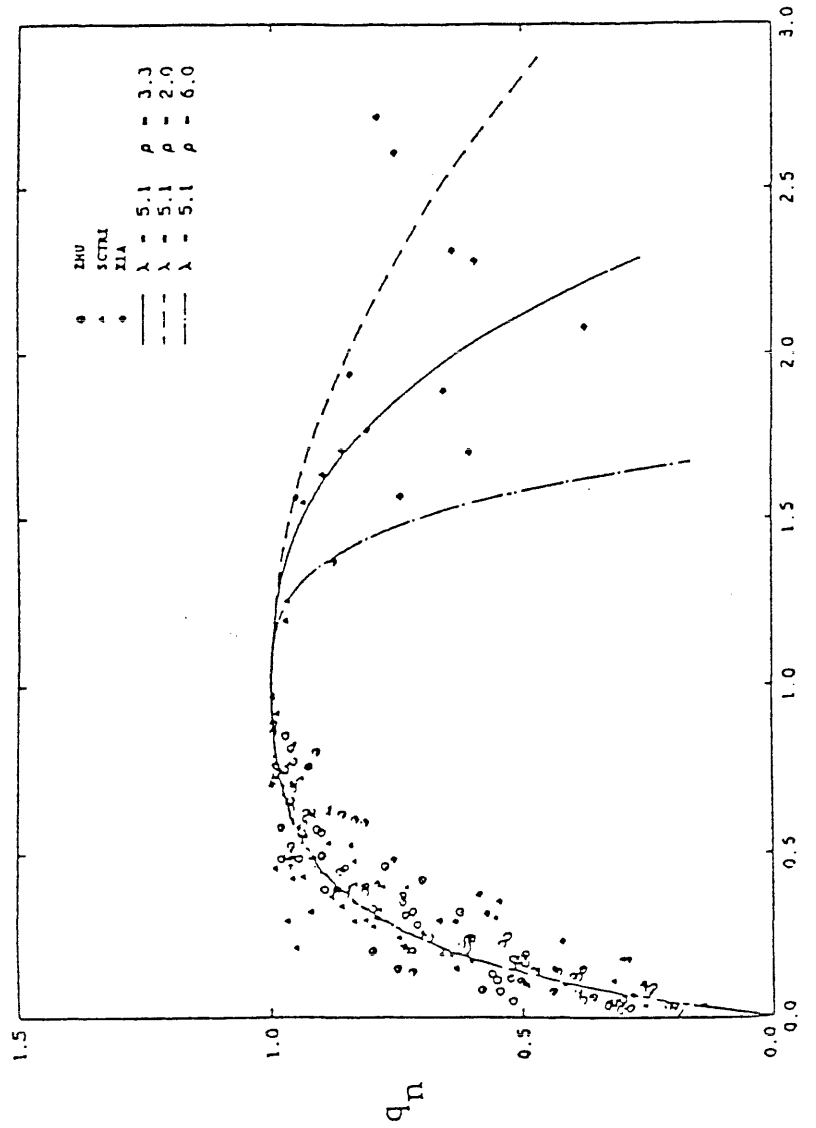

Fig. 3.5 Regression for ρ

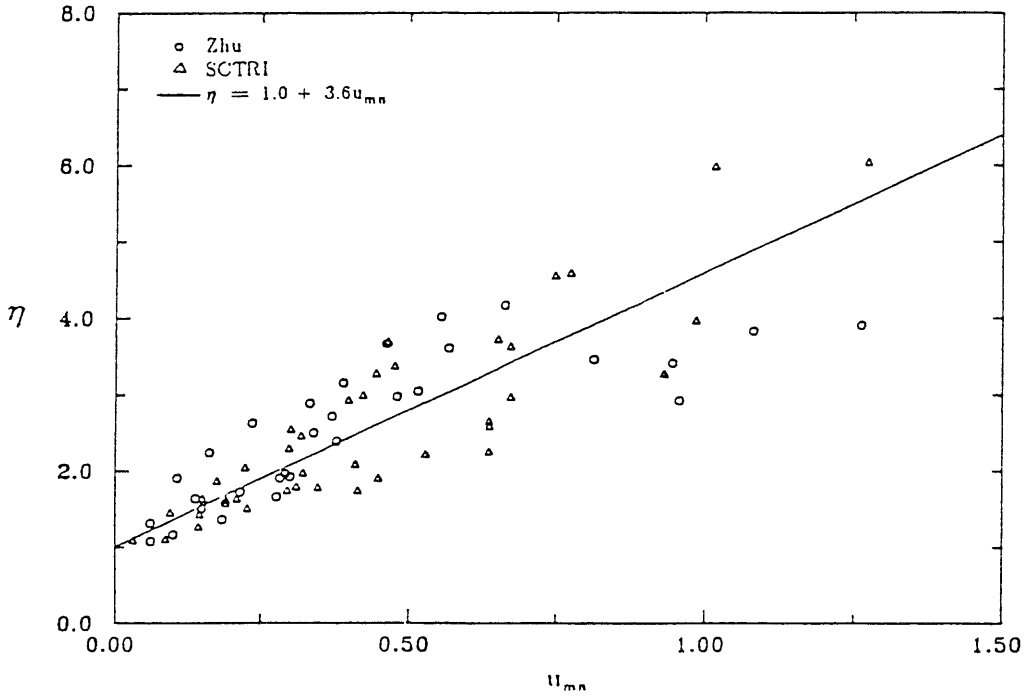

Fig. 3.6 Regression for η

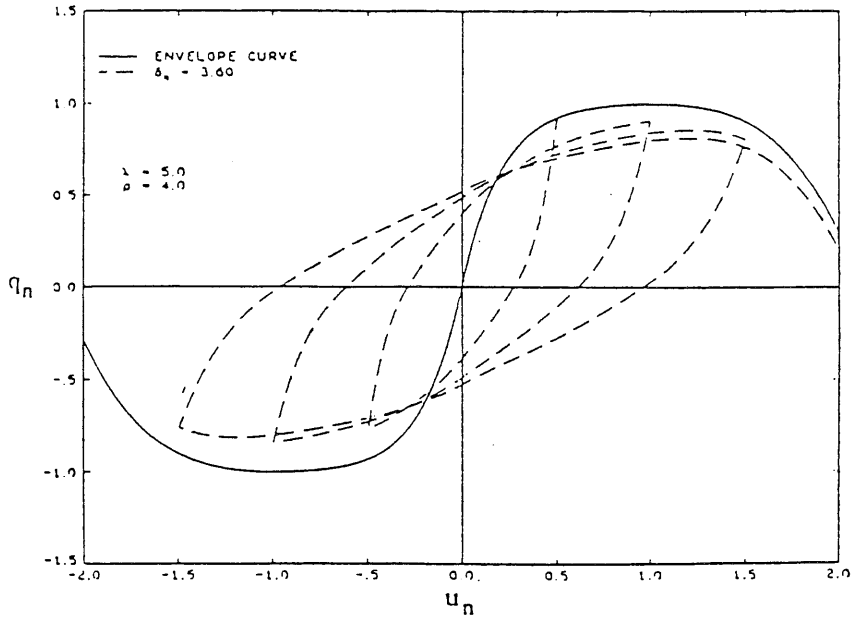

Fig. 3.7 Influence of Stiffness Degradation on Restoring Force

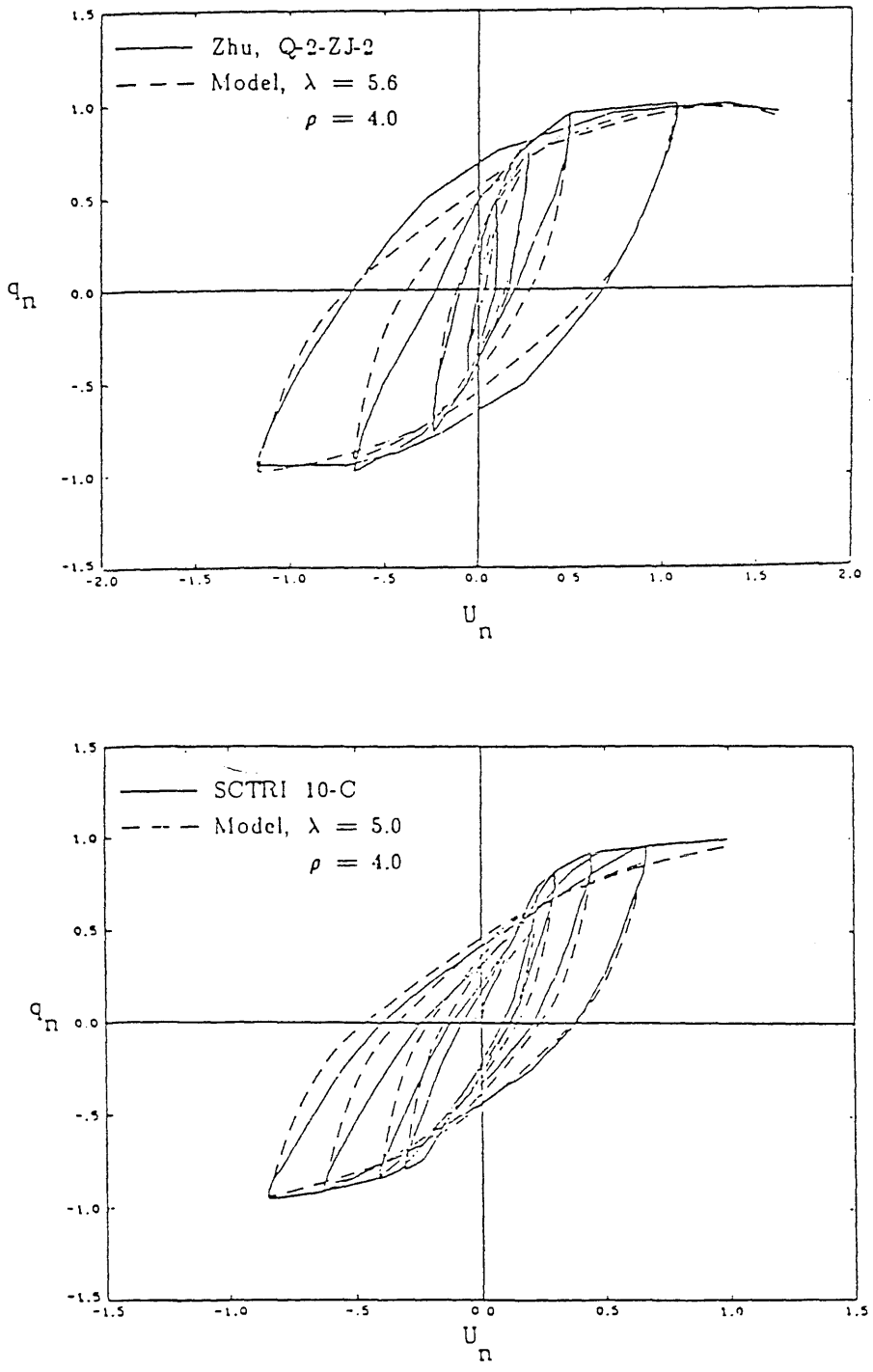

Fig. 3.8 Comparison of Observed and Model Load-Displacement Curves

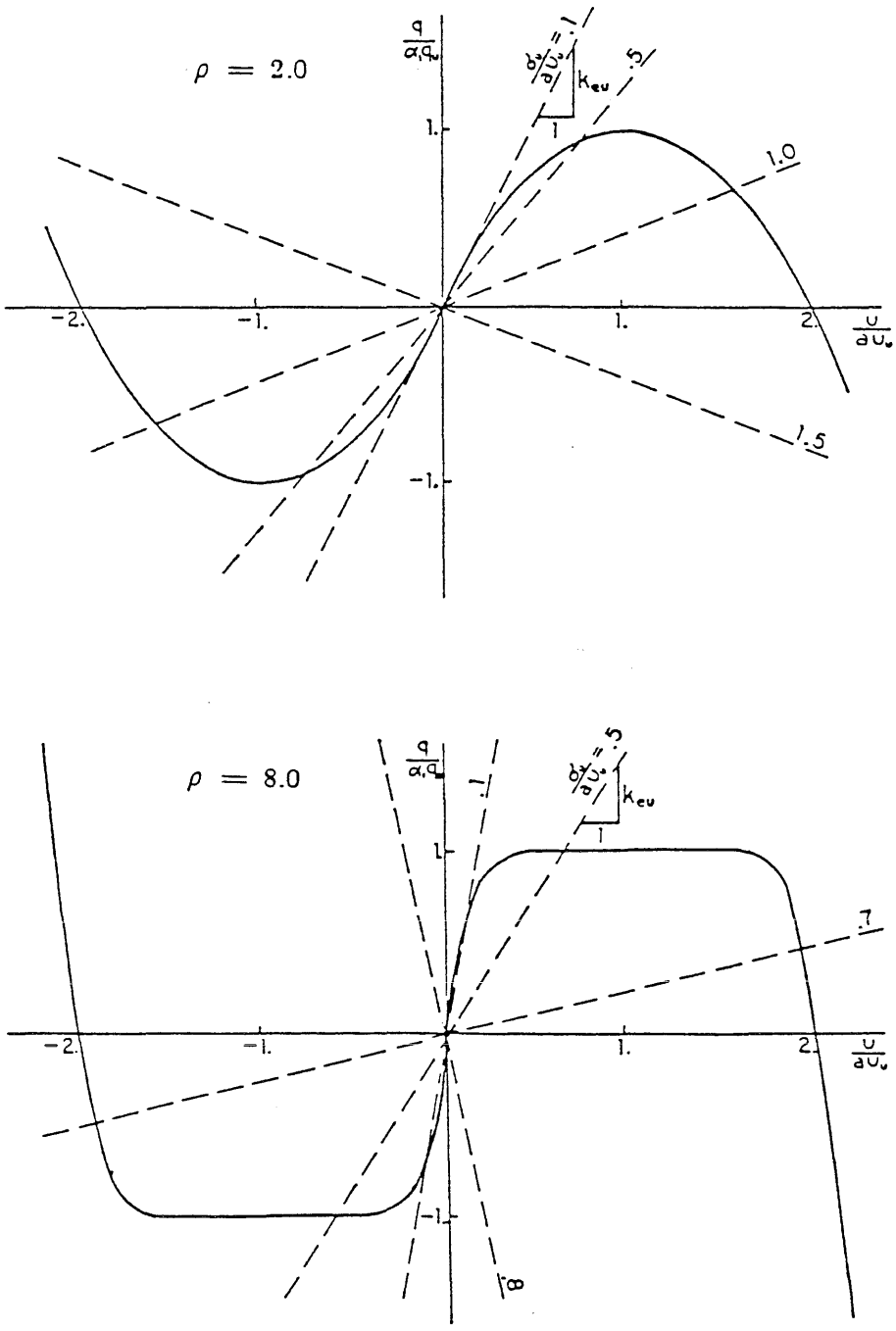

Fig. 3.9 Variation of k_{eu} with σ_u

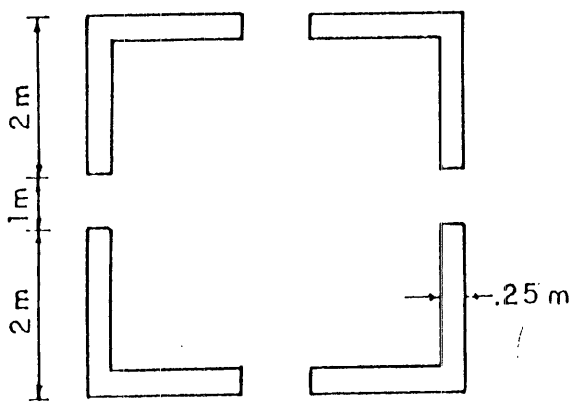

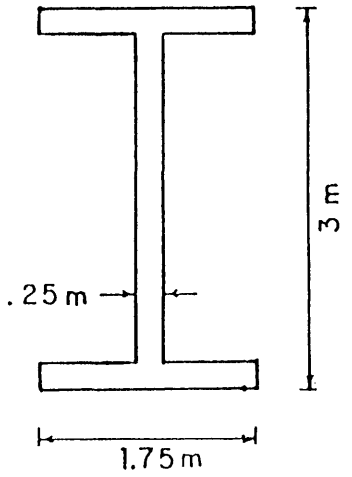

WALL 1

Height = 3.0 m
Mass = 23.0 t
q_u = 140. kN
u_u = 7.16 mm

WALL 2

Height = 3.0 m
Mass = 14.8 t
q_u = 66.4 kN
u_u = 4.83 mm

Fig. 3.10 Sections and Properties of Walls Used in Simulations

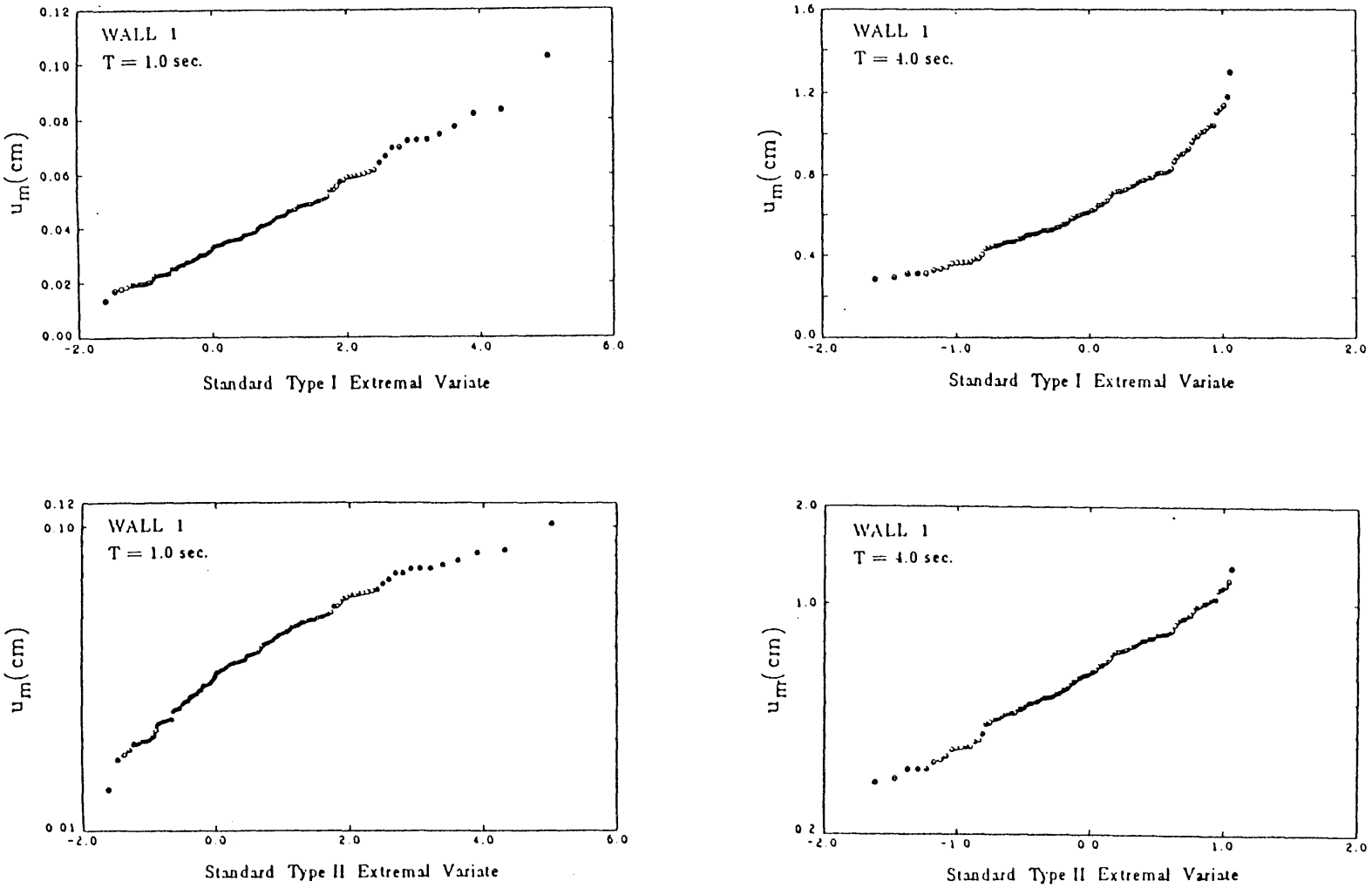

(a) (b)

Fig. 3.11 Distribution of Maximum Displacement for Wall 1

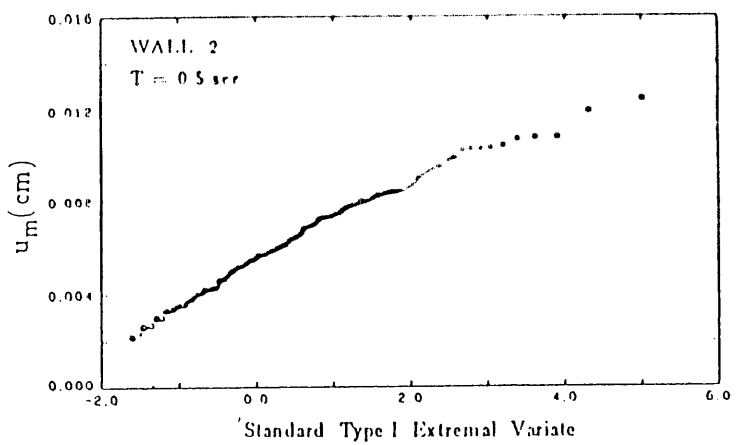

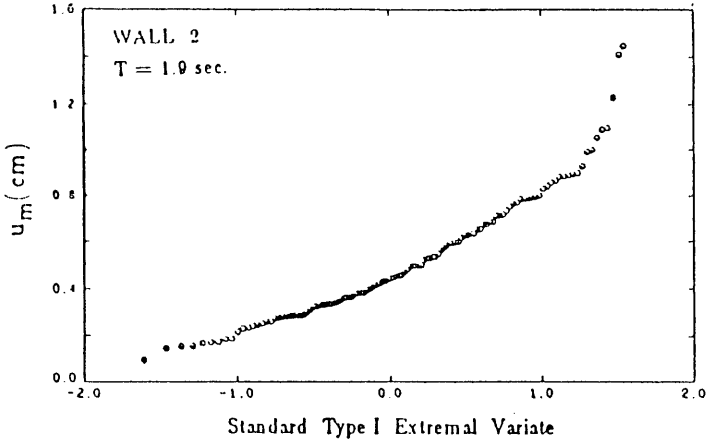

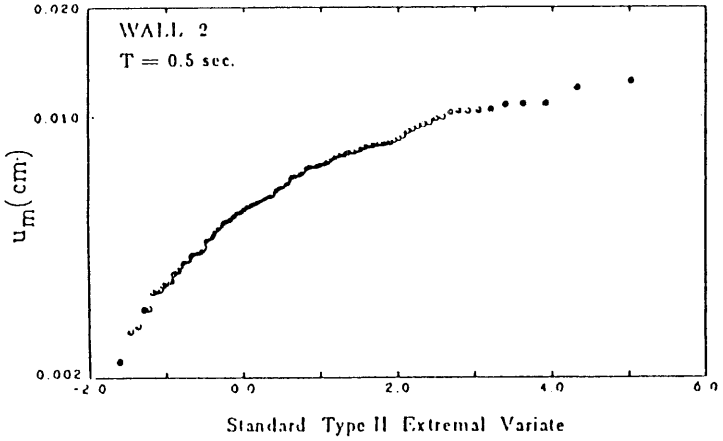

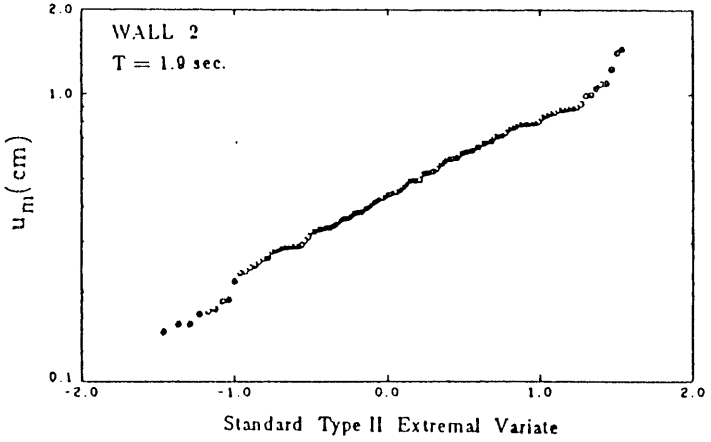

(a) (b)

Fig. 3.12 Distribution of Maximum Displacement for Wall 2

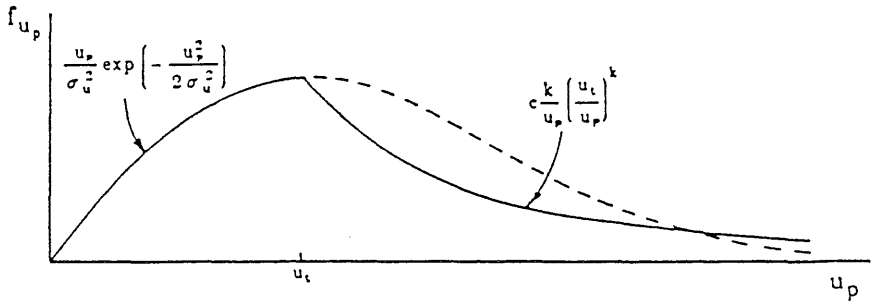

Fig. 3.13 Proposed Distribution of Peak Displacements

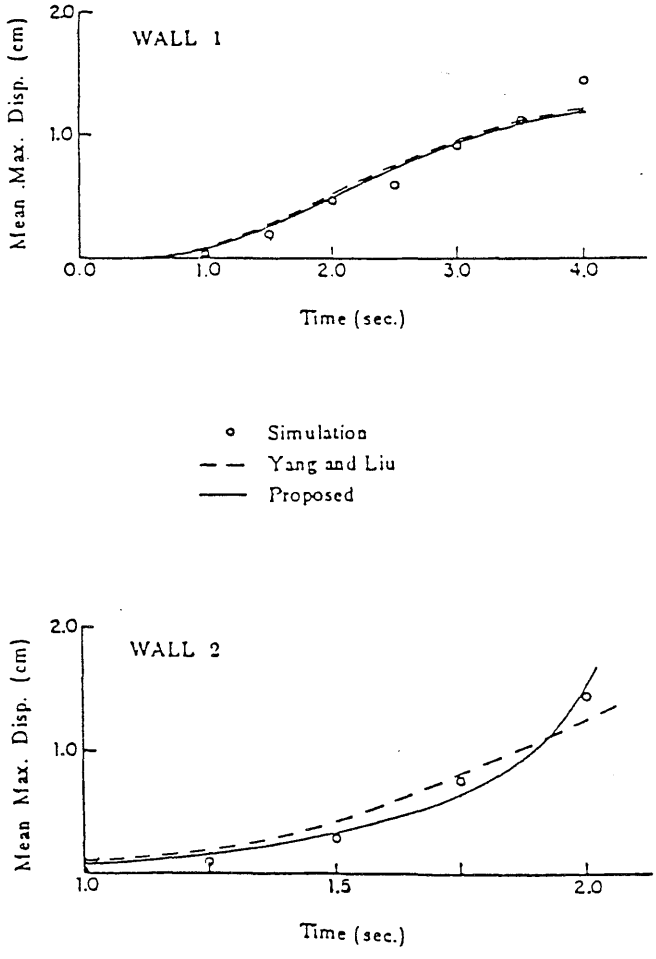

Fig. 3.14 Variation of Maximum Displacement with Time

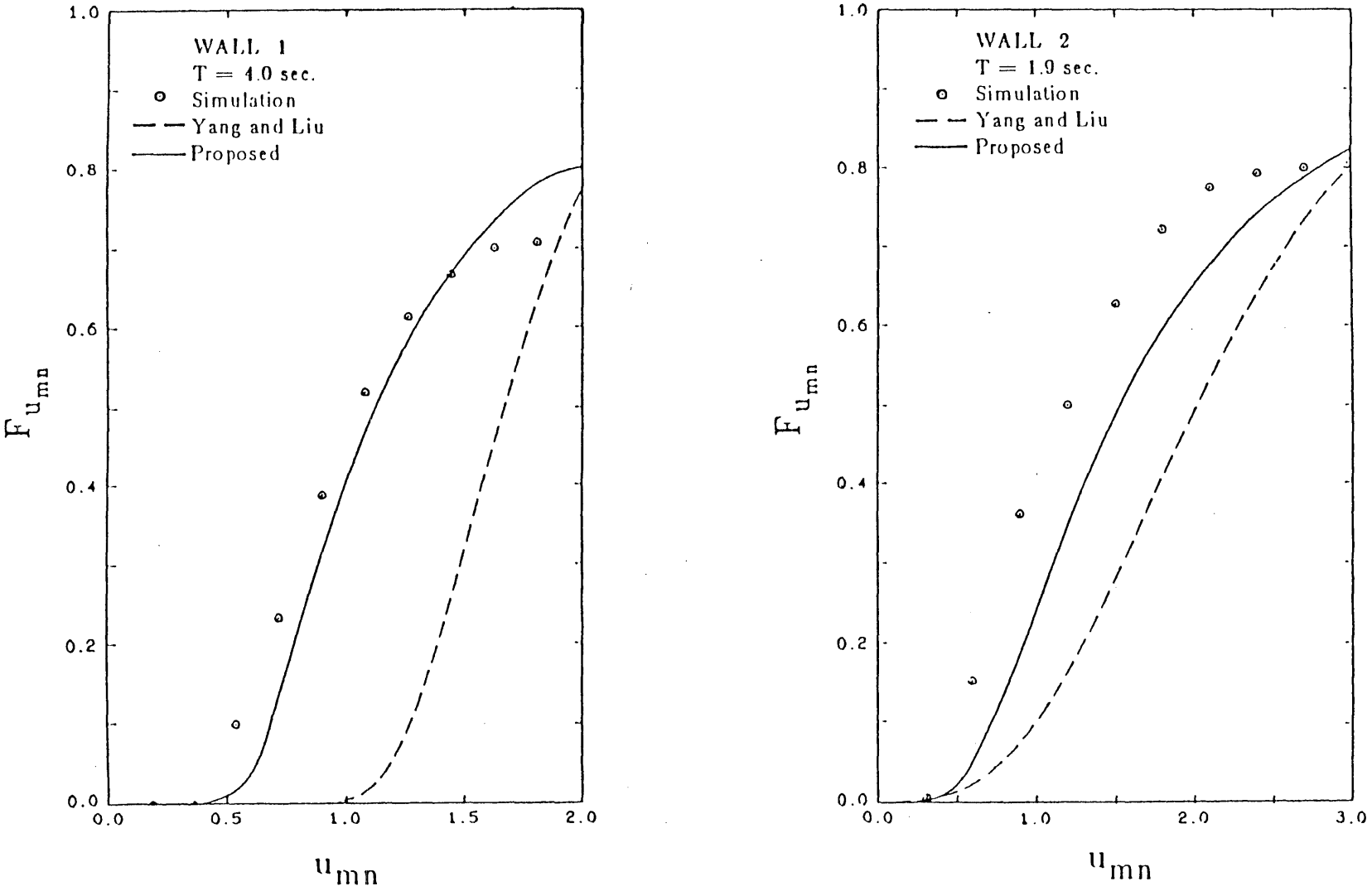

Fig. 3.15 CDF of Maximum Displacement

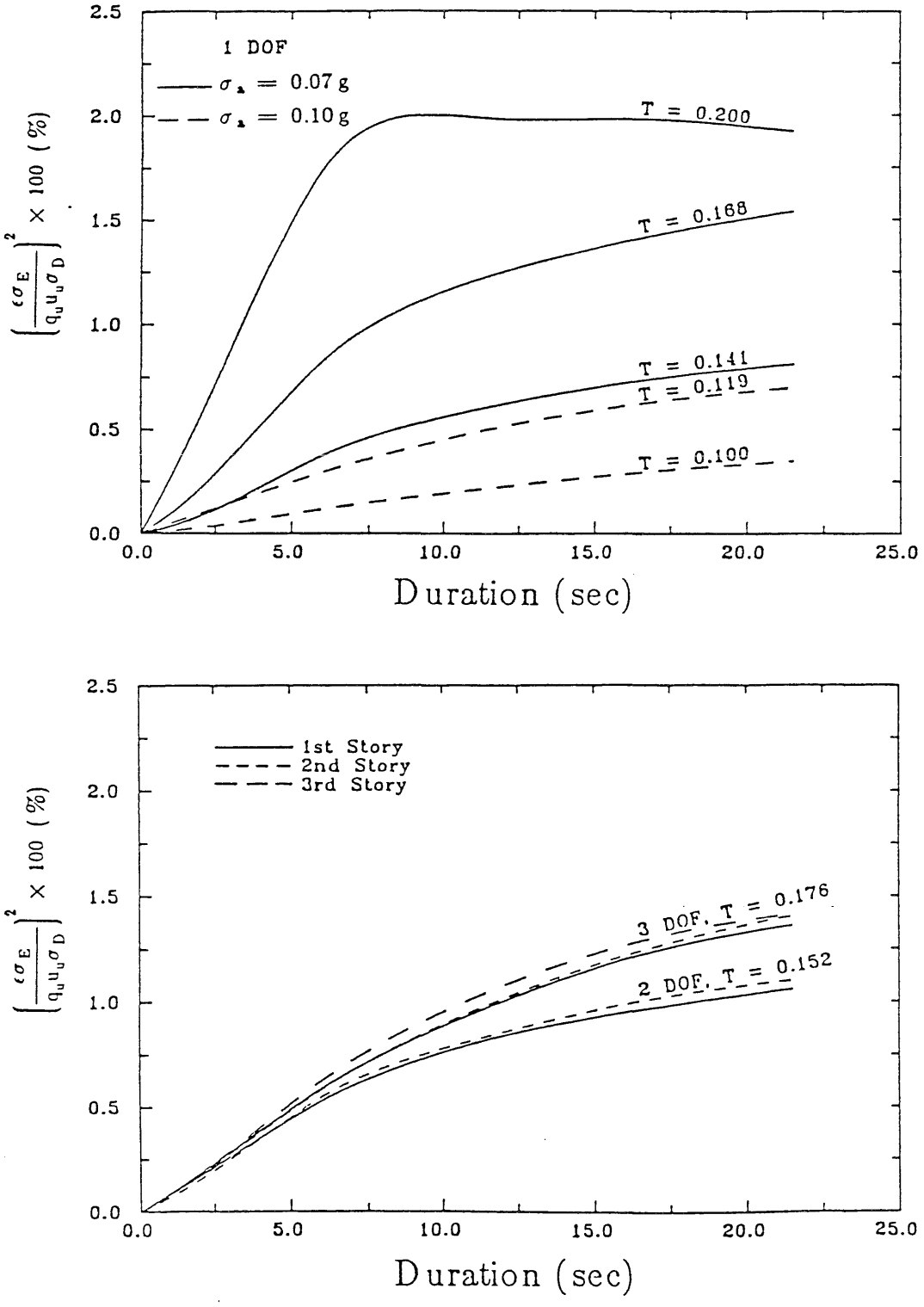

Fig. 3.16 Contribution of Variance of Hysteretic Energy to Variance of Damage Index

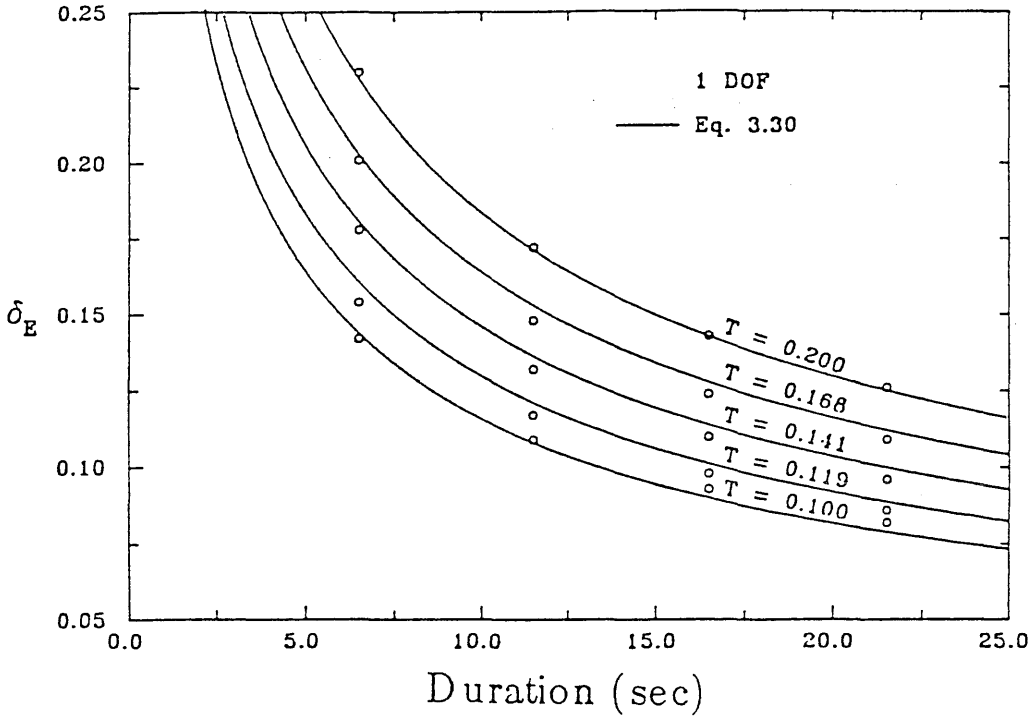

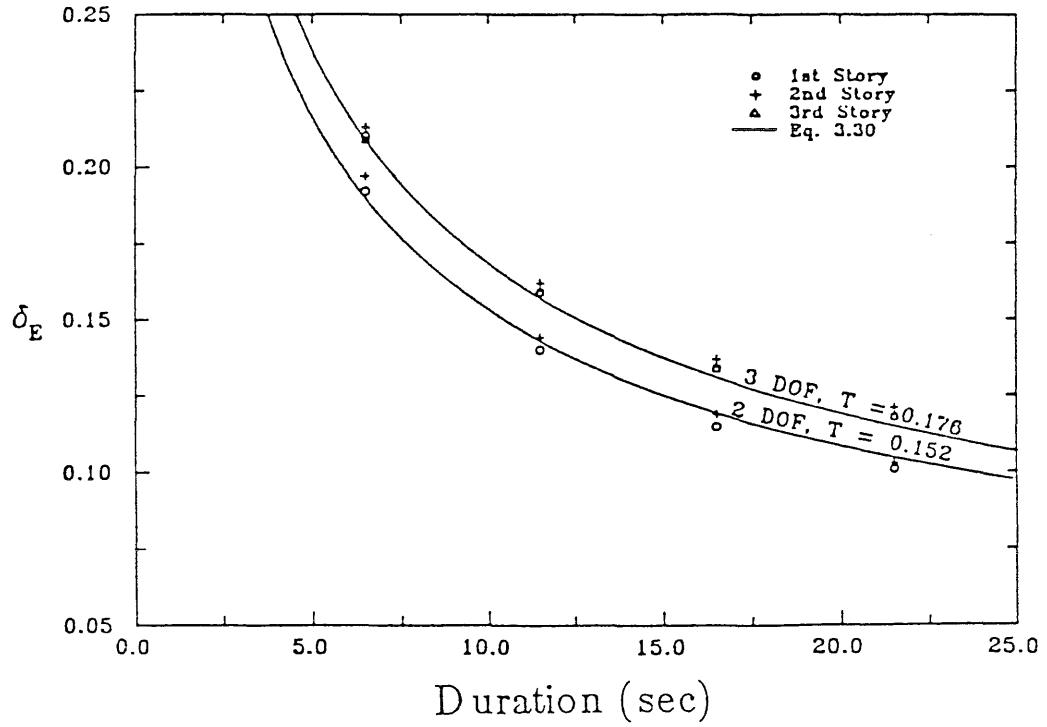

Fig. 3.17 Variation of COV of Hysteretic Energy with Earthquake Duration

CHAPTER 4

CALIBRATION OF THE DAMAGE INDEX

4.1 Purpose of Calibration

The damage index for masonry has been defined such that $D \geq 1.0$ represents failure, i.e., total loss of structural integrity, whereas $D = 0.0$ represents no damage. However, for practical purposes, intermediate values of the damage index must be related to actual levels of damage. For this purpose, it is necessary to calibrate the damage index with observed damage from past earthquakes. Forty five low-rise unreinforced brick masonry buildings damaged during five recent earthquakes in the PRC are used in this calibration process.

4.2 Building Damage Data

The buildings selected for the calibration of the damage index are those whose damage can be attributed primarily to ground motion. Buildings that were damaged by ground subsidence or pounding from adjacent buildings were excluded. Also, buildings with irregular floor plans such that torsional effects could be significant were also not considered. From about 90 buildings whose structural details and damages are documented, 45 were selected for the calibration. The list of these buildings with a brief description of the respective type and degree of damage is given in Table 4.1.

The selected buildings are unreinforced brick masonry structures damaged during the 1965 Wulumuqi earthquake, the 1966 Dongchuan earthquake, the 1969 Yangjiang earthquake, the 1970 Tonghai earthquake, and the 1975 Haicheng earthquake in the PRC. Structural details and results of damage surveys are available in Yang, et al. (1981), and in Ref. 26.

The 1965 Wulumuqi earthquake, with a Richter magnitude of 6.7 and a

focal depth of between 40 to 50 km, occurred about 20 km east of Wulumuqi city in Xinjiang Province. Situated in the river valley of the Wulumuqi River, the city rests on about 10 m of clay or sandy clay overlying cobble or gravel. Most masonry structures in the city were 2 to 3-story residential buildings, schools, or offices. Some were designed for ground motion equivalent to (Chinese) intensity 7, which was the maximum ground motion intensity experienced during this earthquake. Fifteen buildings that were damaged during this earthquake were analysed.

The 1966 Dongchuan earthquake, with a magnitude of 6.5 and a focal depth of 10 km, occurred 13 km north of Dongchuan city in Yunnan Province. Most masonry buildings in this area were 2 to 4 stories, and were not designed for earthquake resistance. A distinguishing feature of the damage to masonry buildings in this area is that greater damage is observed in the upper stories of some buildings. Two buildings damaged during this earthquake were analysed.

The 1969 Yangjiang earthquake, of magnitude 6.4 and a focal depth of 5 km, occurred about 20 km south-west of Yangjiang city in Guangdong Province. The ground motion was primarily in the north-south direction. Most masonry buildings in Yangjiang were 2 to 3 stories with solid or cavity walls and floors of reinforced concrete or timber overlaid with masonry slabs. An exterior corridor supported by masonry columns is common in most buildings. Seven buildings, most of which experienced only minor damage, were analysed.

The 1970 Tonghai earthquake in Yunnan Province, having a magnitude of 7.7 and a focal depth of 13 km, occurred along a fault break roughly corresponding to a section of the Qu river. Masonry buildings in the area affected by the earthquake were few. Three severely damaged or collapsed buildings in Eshan city (intensity 9) were analysed. Damage to these buildings can be attributed to low mortar strength.

The 1975 Haicheng earthquake in Liaoning Province, having a magnitude of 7.3 and a focal depth of 16 km, occurred near a densely populated and

heavily industrialized area. The masonry buildings in the areas affected by the ground motion were not designed for earthquake resistance. In Haicheng city (intensity 8 to 9) the most common damage to masonry buildings were diagonal tension cracks in the walls, separation and displacement of cracked wall segments, and partial collapse of walls. Eighteen buildings in the cities of Haicheng, Yinkou, Pailou, and Huaji were analysed.

4.2.1 Structural and Ground Motion Parameters

The main lateral load resisting components of the masonry buildings selected for analysis are unreinforced masonry shear walls. Wall thickness is governed by the size of the brick units and are usually 37 cm for exterior walls and 24 cm for interior walls. The strength of brick units in most parts of the PRC is 100 kg/cm^2 and this was assumed in the analysis unless indicated otherwise by the damage data. Mortar strength estimated during site damage surveys, ranging from 10 to 50 kg/cm^2, were used in the analysis. In estimating the stiffnesses of walls, the effect of openings was considered, assuming windows to be 1.4 m high, positioned at 1.0 m above the floor level, and doors are assumed to be 2.0 m high.

The dead loads are estimated assuming 2.4 t/m^3 for concrete, 1.8 t/m^3 for brick masonry, and 0.8 t/m^3 for timber. Live loads are assumed to be one half the nominal values which are 0.1 t/m^2 for roofs, 0.2 t/m^2 for residential buildings, schools, and hospitals, 0.25 t/m^2 for offices, 0.375 t/m^2 for shops, and 0.5 t/m^2 for assembly areas. The structural damping is assumed to be 4 percent of critical.

Since recorded ground motion is not available, it is estimated from observed intensity. Reference 8 gives the following relation between mean peak acceleration, $a_p\,(\mathrm{cm/s^2})$, and intensity, I,

$$\log_{10} a_p = 0.3\,I \tag{4.1}$$

This equation is based mostly on data for $I \leq 7$, with limited data for intensity

8. Therefore, extrapolation to higher intensities can be erroneous. For example, it would indicate a mean peak acceleration of 4.1 g for intensity 12, which is not realistic. Therefore, Eq. 4.1 should be limited to $I \leq 7$; for $I > 7$ the

$$\log_{10} a_p = 2.1 + 0.2(I - 7) \qquad (I \geq 7) \qquad (4.2)$$

Equation 4.2 would give $a_p = 1.3\,g$ for $I = 12$. Assuming that the ratio of peak ground acceleration to rms acceleration, σ_a, is 3.0 (Sues, et al., 1983), the shot noise power spectral ordinate, s_0, can be obtained from

$$\sigma_a^2 = s_0 \frac{\pi \omega_g}{2 \zeta_g}(1 + 4 \zeta_g^2) \qquad (4.3)$$

The predominent period of the ground motion, from which ω_g is computed, and the duration of the strong motion phase are obtained from Hu (1984) and summarized in Table 4.2. The parameter ζ_g is assumed to be 0.60.

For buildings with cast-in-place reinforced concrete floor slabs, all structural walls in a story are assumed to have the same displacement; whereas for buildings with precast reinforced concrete floor slabs or timber floors, individual walls are assumed to respond independently of each other.

Where the direction of ground motion is known, or where the damage is primarily in walls in one direction, the building was analysed in that direction only. However, in those cases in which damage was equally evident in both directions, or where the ground motion direction cannot be ascertained, the building was analysed for both principal building directions. Interaction between walls perpendicular to each other was not considered.

The damage index for each building was evaluated at time t_d beyond the end of the strong motion phase, i.e. at time 2.15 t_d (see Fig. 4.1). The increase in the damage index beyond this point should be negligible because of the decrease in the ground motion intensity. In general, the damage index at time 2.15 t_d is about 5 to 20 percent higher than that at the end of the strong motion phase.

The uncertainty in the damage index is due to the ground motion (as reflected in the variance of the maximun displacement and the dissipated energy) and the structural capacity. Since material and workmanship between stories may be assumed to be highly correlated, the story damage indices should also be highly correlated. Hence, the variance of the overall damage index is obtained by assuming perfect correlation between the story damage indices.

4.3 Results of Damage Analysis

The overall damage indices for the buildings analysed are given in Table 4.3 together with the corresponding observed degree of damage. Figure 4.2 shows the story damage indices for a few typical buildings.

In general, the distribution of damage among the stories in a building is not uniform. For a building with a fairly uniform distribution of stiffness and mass, the lower stories tend to sustain greater damage. This is to be expected as there are higher lateral loads and hence greater displacements and dissipated energy in the lower stories. Accordingly, higher damage indices are also indicated for the lower stories (Figs. 4.2a through 4.2e). However, the damage data indicate that a number of buildings were more severely damaged in the higher stories. This may be attributed to two main reasons: (i) When a story is structurally weak, damage will be concentrated in that story as observed in Buildings W9, W14, D5, HP25, and HP27. For Building W9, some interior transverse walls on the upper stories were only half as thick (12 cm) as the same walls on the first story. For Buildings W14, D5, and HP27, the upper stories had lower mortar strengths than the lower stories, and for Building HP25, the mortar strength was high (50 kg/cm^2) but it was observed that the bond between brick and mortar on the second story was poor, perhaps due to poor workmanship. In the analysis of these buildings, a smaller wall area or a lower mortar strength resulted in lower stiffness and ultimate strength, and hence a higher damage index (Figs. 4.2f, 4.2h and 4.2i). (ii) A large mass on

the top story. For most structures, the mass of the top story is smaller than the masses of the other stories because of lower live load and in some cases a thinner slab. However, buildings in the areas affected by the Wulumuqi and Haicheng earthquake have a thick layer of insulation (20 to 25 cm of coke or foam concrete) on the roof. This increases the inertial lateral load and results occasionally in a more uniform distribution of damage; whereas in other instances, results in greater damage to the top story. This is observed in Buildings W3 and W11 (Fig. 4.2g); also the higher damages on the upper stories of Buildings W9, W14, HP25 and HP27 are due in part to this factor.

It is worth observing that buildings with a distribution of stiffness and mass that corresponds to an approximately linear mode shape tend to have a fairly uniform distribution of damage among the stories (see Figs. 4.2j and 4.2k). This is expected since damage to masonry is governed mainly by the maximum displacement, and for low-rise structures, which respond mainly in the fundamental vibration mode, a linear mode shape would indicate uniform interstory displacements. In addition, uniform distribution of damage also requires the ratio of story strength to stiffness to be fairly constant so that damage does not concentrate in a weak story.

When the damage index, D, is less than unity, the variance in D is due mainly to the variance of the structural capacity (cov = 0.31). Hence, the cov of D, and the cov of D_s, δ_{D_s}, does not vary much; having values between 0.30 and 0.35 (see Table 4.3). However, as the maximum displacement, u_m, increases, the variance of u_m increases and contributes more to the variance of the damage index. Since the distribution of u_m is Type II extreme, its variance can, with increasing u_m, eventually become indeterminate. This is observed in one of the interior longitudinal walls of Building HP27 where u_m for the second story exceeds u_u, and the variances of u_m and D for this story are indeterminate.

The results summarized in Table 4.3 is also shown graphically in Fig. 4.3. The damage index is seen to increase with the severity of the observed

damage. This is also evident from Fig. 4.4 which shows the mean and standard deviation of the damage indices for various degrees of damage. However, for a given degree of damage, buildings located in a low intensity area tend to have smaller damage indices. For example, for moderately damaged buildings, all buildings with $D_s < 0.2$ are in areas with intensity 7 (Wulumuqi or Yangjiang), whereas the two buildings in an intensity 9 area (Huajī) have higher damage indices. The damage index for a given degree of damage should, however, be independent of the ground motion intensity. This dependence of D_s on the intensity may be caused by estimating the rms acceleration for response analysis from intensity, which is a measure of the severity of ground motion based on the overall observed damage in an area, but does not represent actual ground motion at a building site. For example, in a low intensity area, where most buildings have only minor damage, some buildings may be severely damaged from ground motion that is more severe than in the rest of the area. Response analysis for these severely damaged buildings, using rms acceleration estimated for the low intensity area, would underestimate the damage index. Therefore, in intepreting the results in Table 4.3 and Fig. 4.3, it would be more meaningful to consider only buildings with severe damage in the higher intensity areas and buildings with minor damage in the lower intensity areas.

Figure 4.5 plots the cumulative distribution function (CDF) of D_s for severely damaged buildings in areas with intensity $\geq$ 8. From Figs. 4.4 and 4.5, an overall damage index of $D_s \leq 0.25$ may be considered to represent repairable damage, whereas $D_s > 0.25$ represents severe, irrepairable damage. Figure 4.5 indicate that for severe damage, the probability of $D_s > 0.25$ is about 80 percent.

Table 4.1 Building Damage Description

Building Designation	No. of Stories	Brief Description of Damage
W1	2	Diagonal tension cracks in interior transverse walls; cracks more severe in first story; maximum crack width about 8mm. Diagonal tension cracks in longitudinal walls; horizontal cracks above doors in interior longitudinal walls
W2	2	Diagonal tension cracks in east end wall. Inclined or vertical cracks in interior longitudinal walls.
W3	2	Horizontal cracks in exterior longitudinal walls; diagonal tension cracks in most transverse walls on second story. Minor damage on first story.
W4	2	Longitudinal walls undamaged. Diagonal tension cracks in end walls on first story.
W7	4	No observed damage.
W8	3	No observed damage.
W9	3	Shear cracks in most transverse walls in lower stories; second story more severely damaged; maximum cracks width about 3 cm. V-shaped cracks around windows in exterior longitudinal walls; diagonal tension cracks in longitudinal walls on lower stories.
W10	3	No observed damage.
W11	2	Diagonal tension cracks in most transverse walls; damage more severe in second story. Separation at joint between longitudinal walls and some transverse walls on second story.
W12	2	Diagonal tension cracks in transverse walls; cracks more severe on first story and at ends of building. Horizontal cracks in end walls below roof level.
W13	3	Prominent cracks in end walls and transverse walls at staircase. Hairline cracks in other walls.
W14	3	Diagonal tension cracks in most transverse walls on lower stories; damage more severe on second story.
W15	3	Hairline cracks in all walls.
W17	3	No observed damage.

Table 4.1 (contd.)

Building Designation	No. of Stories	Brief Description of Damage
W18	3	No observed damage.
D2	2	Horizontal cracks above openings in corridor longitudinal walls on second story.
D5	4	Damage more severe on upper stories and at ends of building. Diagonal tension cracks in transverse walls on upper stories. Separation between transverse and longitudinal walls at joint. Horizontal cracks around openings in longitudinal walls.
Y6	2	No observed damage.
Y7	2	Curved cracks at top of all transverse walls, especially in end walls.
Y10	2	Short hairline cracks around most openings, mostly on the first story.
Y18	3	Diagonal tension cracks in longitudinal wall piers between openings. Inclined or vertical cracks below windows at both ends of longitudinal walls on all stories. Curved cracks at top of end walls.
Y19	2	Hairline cracks in end walls.
Y21	2	Horizontal cracks in front longitudinal walls on second story; V-shaped cracks in upper corners of openings. Severe crack between back wall and canopy.
Y24	2	(6 buildings with the same floor plan) Vertical or inclined cracks around openings in front walls. In two buildings, exterior corridor wall inclining outwards; splitting cracks at arches and in west end wall on first story.
T5	2	Collapse of portions of north-west corner walls and front wall on second story; exterior walls buldging outwards by 40 cm; diagonal tension cracks in all transverse walls in lower story; severe cracks in all other walls. Cracks observed on ground; crack width up to 5 cm.
T6	2	Collapse of west half of building and east end exterior longitudinal walls. Displacement of south-west corner of wall foundation. Severe diagonal tension cracks in transverse walls. Separation and displacement of cracked wall segments.

Table 4.1 (contd.)

Building Designation	No. of Stories	Brief Description of Damage
T7	2	Collapse of all walls except end walls of first story.
HHC2	3	Diagonal tension cracks in all walls. West end wall on the verge of collapse; separation and displacement of cracked transverse walls; less severe damage in upper stories; longitudinal walls inclined outwards due to displacement of transverse walls.
HHC3	2	Diagonal tension cracks in all transverse walls on bottom story; large separation and displacement of cracked wall segments; horizontal or inclined cracks at corners of openings in interior longitudinal walls. Less severe damage on second story.
HHC8	2	Severe diagonal tension cracks in all transverse walls on first story and in interior longitudinal walls. Less severe damage on second story.
HHC11	2	Minor diagonal tension cracks in interior longitudinal walls. No damage on second story and in first story interior transverse walls.
HHC13	2	Hairline cracks under a few windows and in corner rooms on second story.
HHC14	2	Short hairline cracks at openings.
HY16	3	Crack at top of third story wall in west unit of building.
HY19	3	Horizontal and diagonal tension cracks in transverse walls in lower stories. Diagonal tension cracks in end wall of conference room on third floor. Most longitudinal walls were undamaged.
HY23	2	Hairline cracks above a few openings.
HP25	2	Diagonal tension cracks in some longitudinal walls. Severe diagonal tension cracks in all transverse walls; separation and displacement of cracked wall segments; portion of walls falling apart. Longitudinal wall inclined outwards with break in wall below window level on second story due to displacement of transverse walls. Partial collapse of corner walls. Damage more severe in second story.
HP26	2	Diagonal tension cracks in first story longitudinal walls and in transverse walls; Almost no damage on second story.

Table 4.1 (contd.)

Building Designation	No. of Stories	Brief Description of Damage
HP27	3	Diagonal tension cracks in wall piers between windows on lower stories and in end walls; diagonal tension and horizontal cracks in interior longitudinal and transverse walls; damage more severe in second story. Almost no damage on third story.
HP28	3	Diagonal tension cracks in longitudinal walls and corridor walls in central portion of first story.
HHJ29	2	Hairline inclined cracks in walls on first story; diagonal tension cracks in end walls. No damage on second story.
HHJ30	3	(Same floor plan as HHJ29) Severe diagonal tension cracks in all first story walls. Minor damage in upper stories.
HHJ31	2	(15 buildings with the same floor plan) Diagonal tension cracks in all walls. Prominent separation and displacement of cracked walls segments. Some wall corners falling apart. Some longitudinal walls inclined from the vertical by 4 cm.
HHJ32	2	(6 buildings with the same floor plan) Minor horizontal and V-shaped cracks at corners of openings in exterior longitudinal walls. Diagonal tension cracks in end walls, some transverse walls and corridor walls.
HHJ33	2	Severe diagonal tension cracks in first story exterior longitudinal walls and one end wall. No damage on second story.

Table 4.2 Ground Motion Parameters

EARTHQUAKE City	Intensity (Chinese Scale)	Epicentral Distance (km)	Predominent Period (sec)	Strong Motion Duration (sec)
WULUMUQI				
Wulumuqi	7	50	0.15 - 0.3	10
DONGCHUAN				
Dongchuan	8	13	0.15 - 0.2	5
YANGJIANG				
Yangjiang	7	20	0.15 - 0.2	5
TONGHAI				
Eshan	9	45	0.15 - 0.3	12
HAICHENG				
Haicheng	8 - 9	17	0.3 - 0.7	10
Yinkou	7	43	0.4 - 0.7	15
Pailou	9	5	0.2 - 0.5	7
Huaji	9	5	0.2 - 0.5	7

Table 4.3 Degree of Damage and D_s

Building Designation*	Degree of Damage**	Longitudinal		Transverse	
		$\overline{D}_s$	δ_{D_s}	$\overline{D}_s$	δ_{D_s}
W1	Severe	0.129	0.299	0.286	0.298
W2	Moderate			0.185	0.304
W3	Moderate	0.166	0.302	0.156	0.303
W4	Moderate			0.155	0.302
W7	Slight			0.067	0.311
W8	Slight	0.105	0.305		
W9	Severe	0.173	0.306	0.183	0.302
W10	Slight	0.104	0.299		
W11	Moderate			0.189	0.308
W12	Severe			0.277	0.301
W13	Moderate			0.158	0.308
W14	Severe			0.189	0.306
W15	Moderate	0.131	0.301	0.095	0.304
W17	Slight			0.085	0.313
W18	Slight			0.100	0.303
D2	Minor	0.154	0.308		
D5	Severe	0.220	0.315	0.138	0.310
Y6	Slight			0.063	0.314
Y7	Minor			0.064	0.317
Y10	Minor	0.047	0.305		
Y18	Minor	0.108	0.305		
Y19	Minor			0.136	0.312
Y21	Minor	0.107	0.309		
Y24	Minor to Severe	0.139	0.317	0.098	0.318
T5	Severe	0.680	0.306	0.597	0.302
T6	Partial Collapse	0.691	0.307	0.623	0.306
T7	Collapse	0.823	0.311		
HHC2	Severe	0.407	0.304	0.360	0.299
HHC3	Severe			0.585	0.340
HHC8	Severe	0.293	0.300	0.154	0.310

Table 4.3 (contd.)

Building Designation*	Degree of Damage**	Longitudinal		Transverse	
		$\overline{D}_s$	δ_{D_s}	$\overline{D}_s$	δ_{D_s}
HHC11	Minor	0.291	0.305		
HHC13	Slight			0.181	0.299
HHC14	Slight			0.110	0.305
HY16	Minor	0.103	0.300	0.072	0.311
HY19	Moderate			0.389	0.297
HY23	Slight	0.101	0.300		
HP25	Severe			0.601	0.344
HP26	Severe	0.324	0.303	0.368	0.308
HP27	Severe	0.963	-	0.450	0.329
HP28	Minor	0.288	0.306		
HHJ29	Minor	0.397	0.313	0.241	0.306
HHJ30	Severe	0.480	0.328	0.301	0.306
HHJ31	Severe	0.318	0.298	0.378	0.306
HHJ32	Minor to Moderate	0.344	0.300	0.303	0.309
HHJ33	Moderate	0.364	0.302	0.244	0.302

* Building Designation

Prefix	Earthquake	City
W	Wulumuqi	Wulumuqi
D	Dongchuan	Dongchuan
Y	Yangjiang	Yangjiang
T	Tonghai	Eshan
HHC	Haicheng	Haicheng
HY	Haicheng	Yinkou
HP	Haicheng	Pailou
HHJ	Haicheng	Huaji

Number corresponds to building number in Yang et al., (1981)

Table 4.3 (contd.)

** Degree of Damage (From Yang, et al., 1981)

Degree of Damage	Damage Description
Collapse	Complete collapse of building; complete collapse of some upper storys; collapse of more than 75 percent of building.
Partial Collapse	Complete collapse of exterior longitudinal walls; collapse of top story of buildings with timber floors; collapse of more than 25 percent of building.
Severe	Severe cracks in walls; prominent separation and displacement of cracked wall segments; portions of floors may have fallen apart; building may have to be demolished or requires extensive repairs to be serviceable again.
Moderate	Cracks in main structural components at joints; severe damage or collapse of nonstructural walls or secondary structures; damage is repairable.
Minor	Main structural components are essentially undamaged; hairline cracks in walls or floors; damage to parts of secondary structures; damage has little effect on normal functioning of building; requires only minor repairs.
Slight	Essentially no damage to structural or nonstructural components; minor cracks at openings, wall corners, architectural components etc.; cracking of plaster.

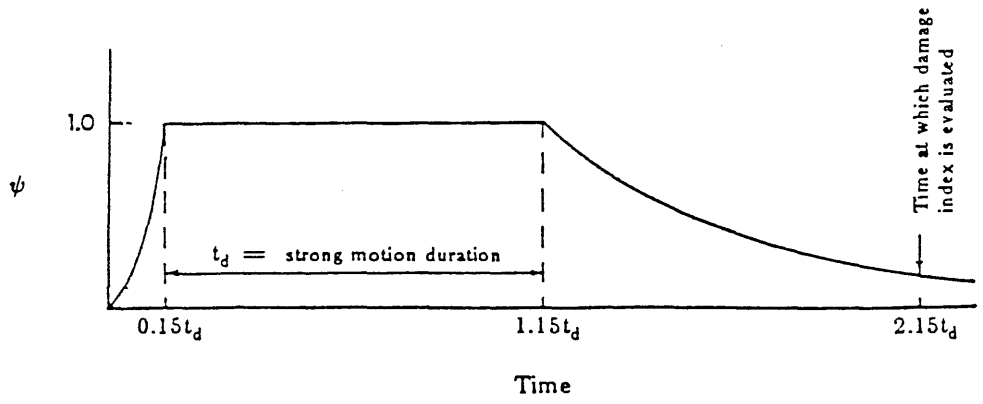

Fig. 4.1 Intensity Time Function

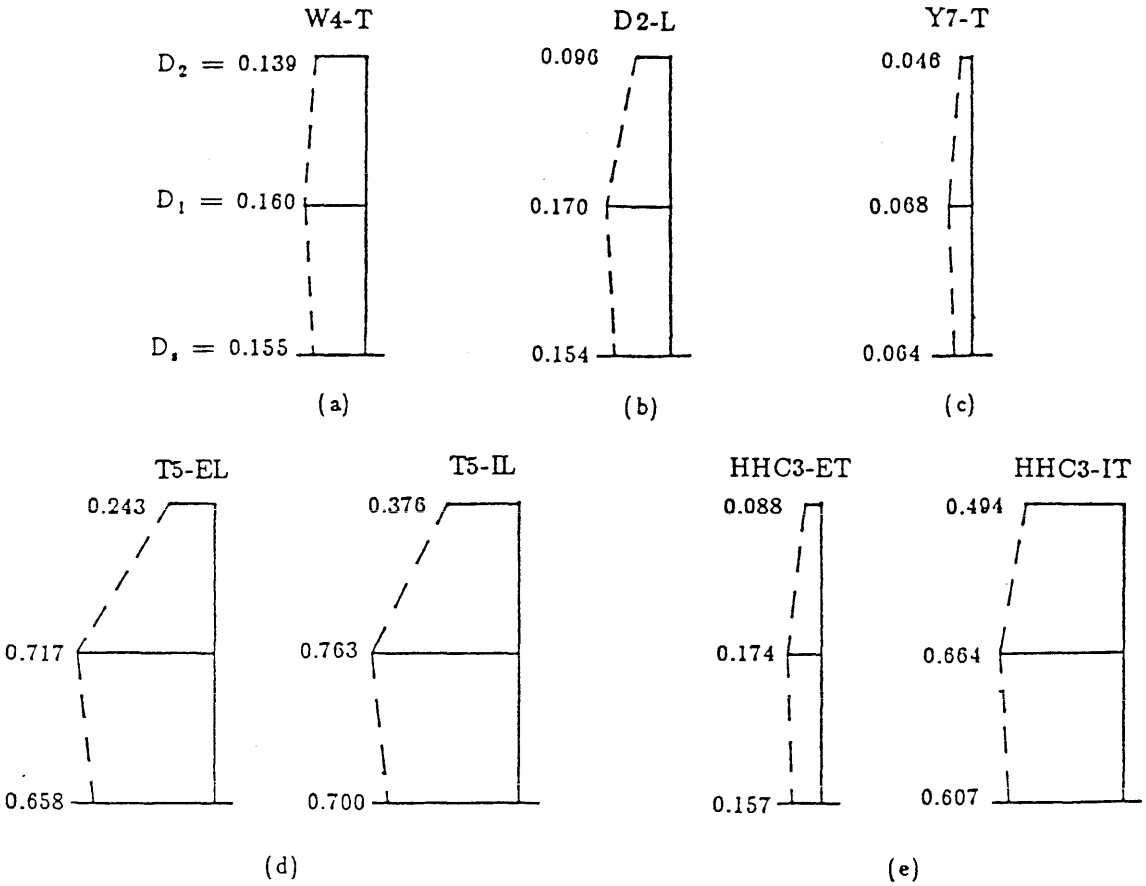

Fig. 4.2 Damage Indices for Typical Buildings

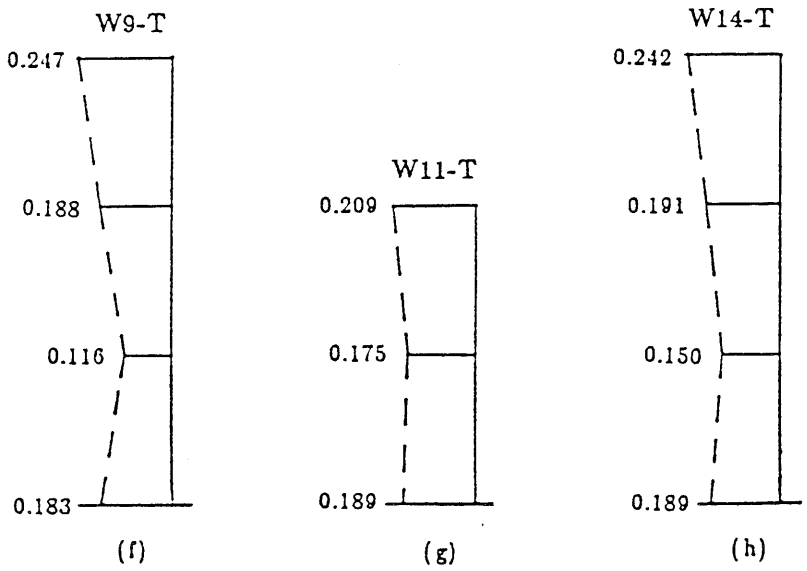
W9-T
0.247
0.188
0.116
0.183
(f)
W11-T
0.209
0.175
0.189
(g)
W14-T
0.242
0.191
0.150
0.189
(h)

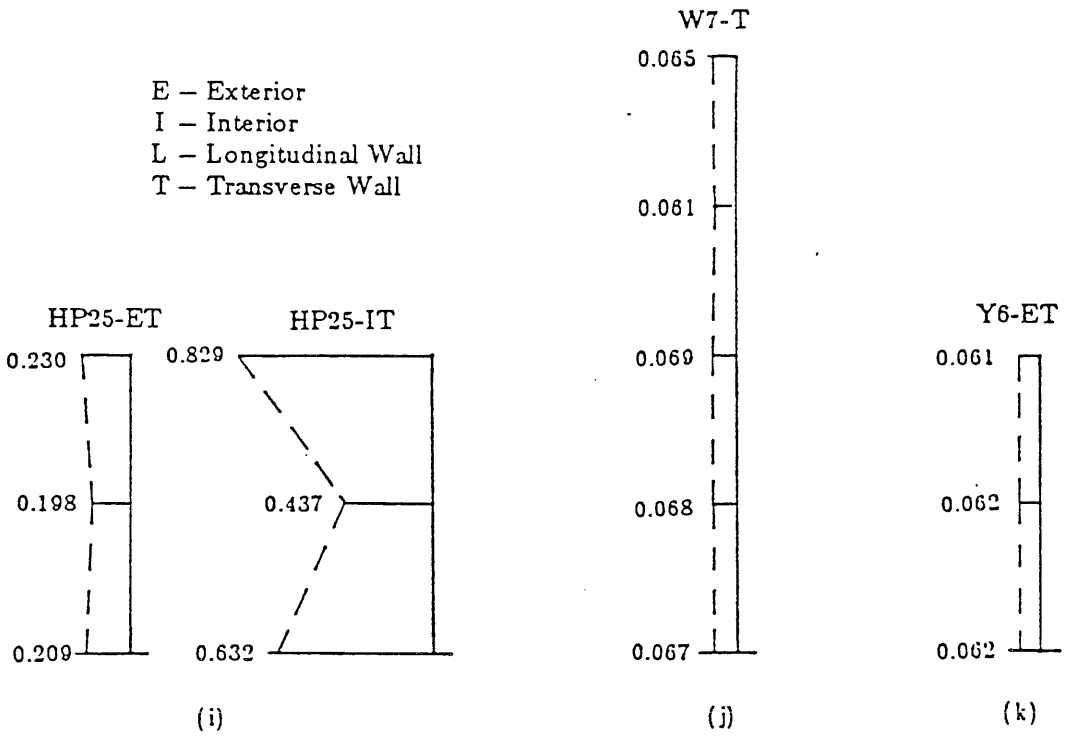
E – Exterior
I – Interior
L – Longitudinal Wall
T – Transverse Wall
HP25-ET
0.230
0.198
0.209
HP25-IT
0.829
0.437
0.632
(i)
W7-T
0.065
0.061
0.069
0.068
0.067
(j)
Y6-ET
0.061
0.062
0.062
(k)

Fig. 4.2 (contd.)

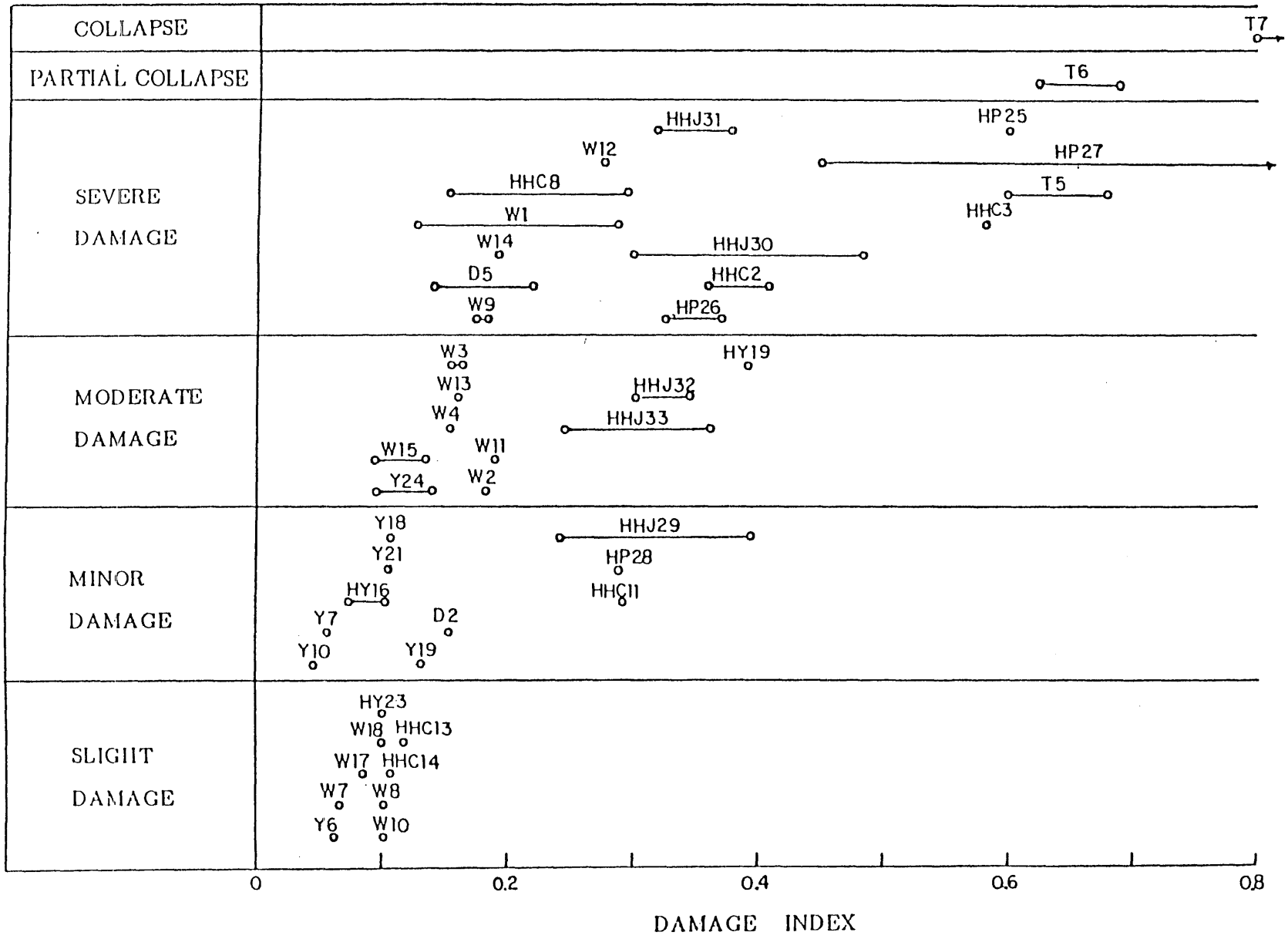

Fig. 4.3 Observed Damage and Calculated Damage Indices

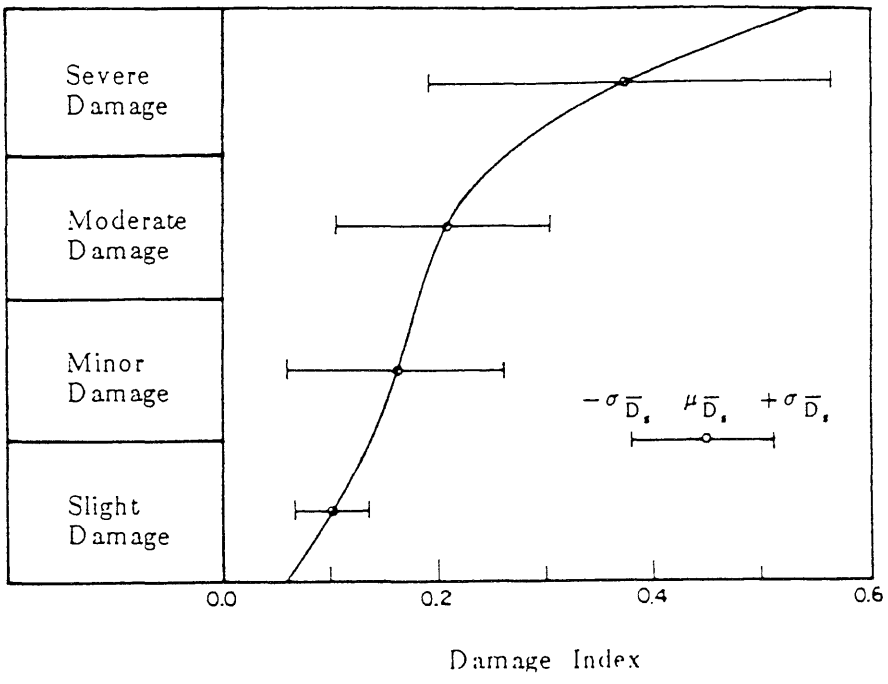

Fig. 4.4 Mean and Standard Deviation of Mean Damage Index

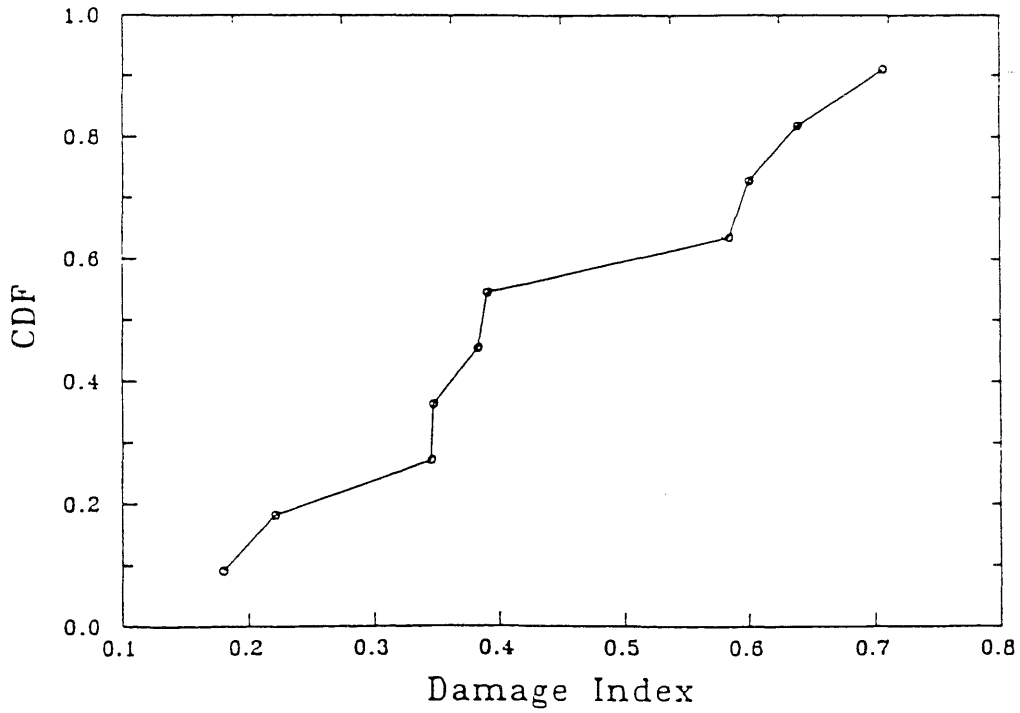

Fig. 4.5 CDF of Damage Index for Severe Damage

CHAPTER 5

DAMAGE-LIMITING DESIGN OF MASONRY BUILDINGS

5.1 Introduction

The aim of aseismic design is to prevent catastrophic collapse of a structure during a severe earthquake, but to allow some level of damage; otherwise construction cost will be prohibitively high. For masonry structures, severe damage to a lower story will render the higher stories unserviceable, even though the higher stories may not have suffered much damage. Therefore, it is also desirable that damage should not be concentrated in any particular story, but should be uniformly distributed among the various stories.

For design purposes, a simpler method (than that involving nonlinear random vibration) is proposed to estimate the story and overall damage indices of a structure. In this latter method, the damage index is obtained as a function of the seismic load and the structural resistance. The seismic load is expressed in terms of the rms acceleration, the strong motion duration, and the predominant period of the ground motion, whereas the structural resistance is expressed in terms of the strength and stiffness of the structure.

To limit the damage and to prevent damage concentration, a modification to the equivalent lateral load procedure, currently used in many building codes, is proposed. In particular, this modification involves the determination of the base shear coefficient as a function of the limiting damage level. The potential damage to a given design is evaluated using the proposed method for estimating the overall damage index to ensure that it is less than the tolerable damage level.

5.2 Simplified Procedure for Estimating Damage Index

5.2.1 Distribution of Damage

The damage index as defined by Eq. 2.1 consists of two terms: D_u, a function of the maximum displacement, and D_e, a function of the hysteretic energy. If the ratio of D_u to D_e is constant for all stories, the damage distribution vector ϕ_D will have elements given by

$$\phi_{Di} = \frac{D_i}{\sum_{j=1}^{N} D_j} = \frac{D_{ui}}{\sum_{j=1}^{N} D_{uj}} = \frac{u_{mi}/u_{ui}}{\sum_{j=1}^{N} u_{mj}/u_{uj}} \tag{5.1}$$

where N is the number of stories. Since the response of a low-rise multistory building is dominated by the first mode of vibration, the vector of story maximum displacements can be expected to be proportional to the interstory first mode displacement vector ϕ', i.e.,

$$u_{mi} = c\,\phi_i' = c\,(\phi_i - \phi_{i-1}) \qquad \text{for } i = 1, \ldots, N \tag{5.2}$$

where c is a constant, and ϕ_i is the first mode displacement of the i-th story. Therefore, the story damage index, D_i, is a function of ϕ_i' and u_{ui}. From the damage index distribution of two to five-story structures, D_i is observed to be approximately proportional to the square of the ratio of ϕ_i' to u_{ui}, i.e.,

$$D_i = c \left(\frac{\phi_i'}{u_{ui}} \right)^2 \tag{5.3}$$

Equation 5.3 implies that a building with constant story height and linear mode shape (ϕ_i' = constant) will have uniform distribution of damage, provided u_u is constant (i.e., the ratio of the ultimate strength to the story stiffness is constant) for all stories. Figure 5.1 indicates that the damage distribution of structures with a linear mode shape and constant u_u for all stories is fairly uniform, with slightly higher damage indices in the lower stories. If a more accurate estimate of the story damage index is desired, Eq. 5.3 can be modified to give

$$D_i = c \frac{(\phi_i')^{n_{\phi i}}}{u_{ui}^2} \tag{5.4}$$

where $n_{\phi i}$ is given in Table 5.1. The damage distribution vector ϕ_D is then

$$\phi_{Di} = \frac{(\phi_i'/u_{ui})^2}{\sum_{j=1}^{N}(\phi_j'/u_{uj})^2} \tag{5.5a}$$

or

$$\phi_{Di} = \frac{(\phi_i')^{n_{\phi i}}/u_{ui}^2}{\sum_{j=1}^{N}(\phi_j')^{n_{\phi j}}/u_{uj}^2} \tag{5.5b}$$

Figure 5.2 compares the damage distribution obtained through the random vibration method and Eq. 5.5 when u_{u1} is varied, indicating that Eq. 5.5 is reasonably accurate for practical purposes.

5.2.2 Estimation of Damage Index

Seismic damage to a structure is a function of the seismic load and the resistance of the structure. Therefore, the damage index can be expressed as a ratio of the seismic load to the structural resistance. The seismic load may be described by the intensity of the ground motion, its duration and frequency content, whereas the structural resistance may be described by the strength and stiffness of the structure.

The intensity may be specified by the rms acceleration, σ_a, during the strong motion phase. The duration of the ground motion can be represented by the duration of the strong motion phase, t_d, and the frequency content can be characterized by the predominant period, T_g, of the ground motion relative to the structural period, T, of the structure.

The stiffness of the structure can be described by its fundamental period. For a SDF system, its strength can be described by its ultimate strength, q_u, or by its ultimate displacement, u_u, since the two are related by $u_u = \lambda q_u/k_i$.

Therefore, the damage index of a SDF system can be written as

$$D = \frac{L(\sigma_a, t_d, T/T_g)}{R(T, u_u)} \tag{5.6}$$

in which L and R are load and resistance functions. Figure 5.3 show the variation of D with σ_a, t_d, T, and u_u for a SDF system. This figure indicates that the load and resistance functions can be given by

$$L = c_l f_{T_g} (\sigma_a)^{n_I} (t_d)^{n_t} \tag{5.7a}$$

$$R = c_r (T)^{n_T} (u_u)^{n_u} \tag{5.7b}$$

where c_l and c_r are constants, f_{T_g} is a function of T/T_g, and n_I, n_t, n_T and n_u are exponents to be determined. Since the damage index is dimensionless and the four variables σ_a, t_d, T and u_u have units of length and time, the following relations between the exponents should be satisfied:

$$2n_I = n_t - n_T \tag{5.8a}$$

$$n_I = n_u \tag{5.8b}$$

For a SDF system, the exponents $n_I = 1.825$, $n_t = 0.35$, $n_T = -3.3$, and $n_u = 1.825$ are appropriate. Similar results were obtained by Park, et al., (1984) for reinforced concrete, in which $n_I = 1.5$ and $n_t = 0.5$.

The above method for estimating the damage index for a SDF system can be readily extended to MDF systems by assuming that a relation similar to Eqs. 5.6 through 5.8 applies to the sum of the story damage indices, i.e.,

$$S_D = \sum_{i=1}^{N} D_i = c_N f_{T_g} \frac{(\sigma_a)^{n_I} (t_d)^{n_t}}{(T)^{n_T} (u_{ue})^{n_I}} \tag{5.9}$$

in which c_N is a constant and u_{ue} is an equivalent ultimate displacement. From the observed variation of S_D with u_{ui}, the equivalent ultimate displacement can be obtained as the sum of the story ultimate displacements, each weighted by the corresponding element in the damage distribution vector, i.e.,

$$u_{ue} = \sum_{i=1}^{N} u_{ui} \phi_{Di} \tag{5.10}$$

From a study of the variation of S_D for one to five-D OF systems, the appropriate exponents for N-story buildings are

$$n_t = 0.35 \tag{5.11a}$$

$$n_T = -3.40 + 0.10N \tag{5.11b}$$

and

$$c_N = 0.057\, N^{-0.2} \tag{5.11c}$$

assuming $f_{T_g} = 1.0$. Equations 5.9 through 5.11 apply for the following ranges of the load and resistance parameters:

$$0.035\,g \leq \sigma_a \leq 0.14\,g$$
$$\tfrac{1}{3}T_L \leq T \leq T_L$$
$$5.0\,\text{sec} \leq t_d \leq 20.0\,\text{sec}$$
$$0.35\,\text{cm} \leq u_u \leq 1.4\,\text{cm}$$

in which $T_L = 0.04(4 + N)$ sec In addition, S_D obtained using Eqs. 5.9 and 5.11 is accurate only when none of the damage indices exceed 0.7; otherwise S_D will be underestimated. This is because as the story damage index increases, and the story stiffness decreases, the damage index increases at an increasing rate.

Figure 5.4 show the variation of the damage index with T/T_g, for several systems. For each system, T_g is varied between 0.2 sec to 0.8 sec, covering the range of predominant periods for ground motions between rock and soil sites. The damage index increases to a maximum at about $T/T_g = 0.55$ and then decreases as T/T_g increases further. The maximum damage index is not obtained when T/T_g is equal to 1.0 because T is only the initial structural period. As the damage index increases and the stiffness decreases, the structural period increases. Therefore, a structure with T equal to T_g will be past the point of resonance, and its response will decrease, as its period increases. On the other hand, a structure with $T < T_g$ will approach resonance as its period increases. Since Eq. 5.11 is obtained for T/T_g ranging from 0.20 to 0.73 and the damage index is not much affected by T_g over this range, the function f_{T_g} can be given by

$$f_{T_g} = \begin{cases} 1.0 & ; \quad T/T_g \leq 0.70 \\ 1./(0.80(T/T_g) + 0.44) & ; \quad T/T_g > 0.70 \end{cases} \tag{5.12}$$

The function f_{T_g} is also plotted in Fig. 5.4. Figure 5.5 shows the results for S_D obtained using Eqs. 5.9 to 5.12 versus those obtained through the random vibration method for several one to five-DOF systems.

Once S_D and ϕ_D are known, the story damage indices are obtained as

$$D_i = \phi_{Di} S_D \tag{5.13}$$

To obtain the overall damage index, it is necessary to determine the maximum story potential energy, e_{pi}, which is a function of the maximum story displacement given by

$$u_{mi} = \left(\frac{D_i}{1 + \sigma^2_{D_{ult}}} - D_{ei} \right) \alpha u_{ui} \tag{5.14}$$

It is proposed, however, that the maximum story displacement be approximated by

$$u_{mi} = D_i u_{ui} \tag{5.15}$$

This approximation tends to overestimate u_{mi} for large D_i (by about 15 percent for $D_i \approx 0.5$) because the contribution of the energy term D_{ei} to D_i increases with D_i, and neglecting it overestimates u_{mi}. On the other hand, u_{mi} is underestimated for small D_i (by about 20 percent when $D_i \approx 0.05$). However, the effect of this approximation on the overall damage index is small when the story damage indices are fairly uniform.

Figure 5.6 plots the overall damage indices obtained through Eqs. 5.9 to 5.15 against those obtained with the random vibration method for the structures used in the calibration of the damage index. The proposed method gives very good estimates of the overall damage index for $D_s \leq 0.5$, beyond which D_s tends to be underestimated because S_D is underestimated by Eqs. 5.9 through 5.12 when the story damage indices are large.

The proposed simplified procedure for estimating the damage indices of a structure can be summarized as follows:

1.a. Determine the seismic load on the structure in terms of σ_a, t_d, and T_g.

b. Determine the period of the structure, T, and the ultimate displacement, u_u, for each story.

2. Obtain the damage distribution vector, ϕ_D, using Eq. 5.5.

3.a. Determine the equivalent ultimate displacement, u_{ue}, using Eq. 5.10.

b. Compute the sum of the story damage indices, S_D, using Eqs. 5.9, 5.11 and 5.12.

c. Compute the individual story damage indices using Eq. 5.13.

4. Compute the overall damage index according to Eq. 3.31, using Eq. 5.15 to estimate the maximum story displacements and Eq. 3.32 to obtain the interstory potential energies.

The proposed simplified method has been used to obtain the damage indices of six and seven-story structures and found to give good estimates relative to those obtained through nonlinear random vibration analysis; however, its accuracy can be expected to deteriorate for higher structures.

5.3 Damage-Limiting Design

The previous section describes a simplified procedure for estimating the damage index of a given structure. The simplified procedure can be used as the basis for developing designs with a permissible level of potential damage when subjected to a specified ground motion.

The resulting design procedure is a modification of the equivalent lateral load method currently used in many seismic building codes. The dynamic lateral forces are also replaced by equivalent static forces, which are determined from an estimate of the base shear of the structure. However, the base shear coefficient is determined as a function of the tolerable damage level.

Consider a multistory building whose overall damage index is to be limited to a maximum value D_L. To avoid damage concentration in any story, the story damage indices should also be close to or less than D_L. The sum of the damage indices should therefore be limited to ND_L. Then Eq. 5.9 can be rewritten as

$$(u_{ue})^{n_I} \geq \frac{c_N f_{T_g} (\sigma_a)^{n_I} (t_d)^{n_t}}{ND_L (T)^{n_T}} \tag{5.16}$$

from which u_{ue} is computed given σ_a, t_d, T, and T_g.

It has been noted earlier that a building with constant ϕ_i' and u_{ui} will have a fairly uniform distribution of damage. Constant ϕ_i' is obtained when the story stiffness distribution is proportional to the distribution of the story shears. For a building with constant story mass, height, and ϕ_i', equating the maximum potential and kinetic energies give

$$\sum_{i=1}^{N} k_i(\phi_i')^2 = m\omega_1^2 \sum_{i=1}^{N} (i\phi_i')^2 \tag{5.17}$$

in which

$$k_i = k_1 \frac{\sum_{j=i}^{N} j}{\sum_{j=1}^{N} j} \tag{5.18}$$

where m and k are the story mass and stiffness, respectively, and ω_1 is the first natural frequency. From Eqs. 5.17 and 5.18, it can be shown that

$$\omega_1^2 = \frac{k_1}{m} \frac{2}{N(N+1)} \tag{5.19}$$

The required strength in the first story is

$$\begin{aligned} q_{u1} &= k_1 u_{u1}/\lambda \\ &= \frac{2}{g} \left(\frac{\pi}{T} \right)^2 (N+1) \frac{u_{u1}}{\lambda} W \end{aligned} \tag{5.20}$$

where W is the total weight of the structure. The design base shear can thus be written as

$$V = C_s W \tag{5.21}$$

in which

$$C_s = \frac{2}{g}\left(\frac{\pi}{T}\right)^2 (N+1)\frac{u_{ue}}{\lambda} \tag{5.22}$$

where u_{ue} is given by Eq. 5.16. Observe that the base shear coefficient is explicitly a function of the limiting damage level, as u_{ue} is a function of D_L.

The equivalent lateral forces may then be obtained from the base shear according to

$$F_i = \frac{w_i h_i}{\sum_{j=1}^{N} w_j h_j} V \tag{5.23}$$

where F_i, w_i, and h_i are the lateral force, story weight, and height above the ground, respectively, of the i-story. The design equation to be satisfied for shear is, therefore,

$$V_i = \sum_{j=i}^{N} F_j \leq A_i \tau_i \tag{5.24}$$

where V_i, A_i, and τ_i denote the shear force, shear area, and shear strength, respectively, of the i-th story.

In satisfying Eq. 5.24, the designer is often under some constraints. The length and spacing of the walls in a building are often governed by architectural requirements, and the wall thickness is dependent on the size of masonry units available. It is possible to vary the shear strength by varying the mortar strength, but it is not good construction practice to use several mortar strengths in one building.

After designing the walls, the design has to be checked to ensure that its overall damage index is less than the limiting value, and also that no story damage index exceeds the same limiting value. For this purpose, the simplified

method described in Sect. 5.2 can be used. If necessary, the design process can be repeated, using updated values of the structural period and story masses, until an adequate design is achieved.

Comparison of the proposed base shear coefficient with those of current building codes is not straight-forward, because of different load and resistance factors or allowable stresses specified by different building codes. Therefore, for comparison purposes, consider an adjusted base shear coefficient, C_s', obtained as follows: let the design equation for shear be written as

$$\gamma V_i \leq \phi A_i \tau_{all} \tag{5.25}$$

where γ and ϕ are load and resistance factors, and τ_{all} is the allowable shear stress. From Eqs. 5.23 and 5.24, the story shear, V_i, is given by

$$V_i = f_i C_s W \tag{5.26}$$

where $f_i = \sum_{j=i}^{N}(w_j h_j / \sum_k w_k h_k)$. Therefore, Eq. 5.25 may be rewritten as

$$C_{si}' f_i W \leq A_i \tau_i \tag{5.27}$$

in which

$$C_s' = \frac{\gamma}{\phi}\frac{\tau}{\tau_{all}} C_s \tag{5.28}$$

where the shear strength, τ, is given by Eqs. 2.3 and 2.5 with $\mu = 0.5$.

Figure 5.7 shows the plot of the proposed C_s' versus the structural period for $\sigma_a = 0.033\,g$ and $0.067\,g$, and $t_d = 10$ sec Since the proposed C_s is a function of N, it is assumed, for the purpose of Fig. 5.7, that $T = 0.05N$. Also shown in Fig. 5.7 is the C_s' of ATC-3-06 (1978), the Uniform Building Code (1985), and the PRC's Aseismic Design Code for Industrial and Civil Buildings (TJ 11-78).

For ATC-3-06, C_s' is computed using the following: $R = 1.25$, $S = 1.2$, and $A_a = A_v = 0.1$ and 0.2 for $\sigma_a = 0.033\,g$ and $0.067\,g$, respectively. The ratio, $\gamma/\phi = 1.00/(2.5 \times 0.40) = 1.00$, and τ and τ_{all} are obtained for a

masonry unit strength of $f_{mu} = 100\,kg/cm^2$; type N mortar for $\sigma_a = 0.033\,g$, type S mortar for $\sigma_a = 0.067\,g$; and vertical compressive stress, $\sigma_c = 3.0\,kg/cm^2$, representing approximately the compressive stress at the bottom story of a three-story building.

For the UBC, C_s' is computed using K = 1.33, I = 1.0, CS = 0.14 and Z = 3/4 and 3/8 for $\sigma_a = 0.033\,g$ and $0.067\,g$, respectively. The ratio, $\gamma/\phi = 1.0/1.33 = 0.75$ for $\sigma_a = 0.033\,g$, and $\gamma/\phi = 1.5/1.33 = 1.13$ for $\sigma_a = 0.067\,g$. The allowable shear stress is obtained for a masonry strength of $f_m' = 55$ and $75\ kg/cm^2$ for $\sigma_a = 0.033\,g$ and $0.067\,g$, respectively.

For the PRC's TJ 11-78 Code, C_s' is computed using C = 0.45, and $\alpha_{max} = 0.45$ and 0.23 for $\sigma_a = 0.033\,g$ and $0.067\,g$, respectively. The ratio, $\gamma/\phi = 2.0 \times 1.2 = 2.4$ and τ_{all} is obtained using a mortar strength of $f_{mo} = 50\,kg/cm^2$ for $\sigma_a = 0.033\,g$, and $f_{mo} = 75\,kg/cm^2$ for $\sigma_a = 0.067\,g$.

Table 5.2 summarizes the computation of the adjusted base shear coefficients. From Fig. 5.7, the C_s' of ATC-3-06, corresponding to $D_L < 0.10$, is much higher than the proposed C_s' and those of the UBC and TJ 11-78. Also, the C_s' of TJ 11-78 corresponds approximately to $D_L = 0.40$.

5.4 Design Examples

Two buildings are designed to illustrate the proposed damage-limiting design procedure. Both buildings have a common floor plan as shown in Fig. 5.8; one with three stories and the other with five stories. The story height is assumed to be three meters for all stories. Floors are to be constructed using precast concrete slabs. Live load is assumed to be $0.1\ t/m^2$ for the roof and $0.2\ t/m^2$ for the other floors. The strength of the masonry units is assumed to be $100\ kg/cm^2$.

The predominant period of the ground motion is assumed to be 0.4 sec ($\omega_g = 5\pi$) with $\zeta_g = 0.6$, which corresponds to firm ground condition.

5.4.1 Design of Three-Story Building

The building is assumed to be located in an area where the seismic load may be characterized by $\sigma_a = 0.067\,g$, corresponding approximately to a peak acceleration of 0.2 g, with a strong-phase duration of $t_d = 10\,sec$. It is assumed that the walls in the building vibrate independently of each other.

The story masses are computed assuming a floor dead load of 0.36 t/m^2 and the permanent live load (such as partitions) to be half of the total live load. Let the wall thickness be 24 cm for the transverse walls and 36 cm for the longitudinal walls. For an interior transverse wall, the tributary floor mass is $28(0.36 + 0.10) + (0.36\times5.67 + 0.24\times5.64)(3\times1.8) = 31.2\,t$ for the first and second stories and 20.7 t for the top story. Assuming a structural period of 0.15 sec, $C_s = 0.478$ is obtained for a tolerable damage of $D_L = 0.25$, giving a base shear of $0.478(31.2\times2 + 20.7) = 39.7\,t$. Similarly, for an interior longitudinal wall, the tributary floor mass is 79.3 t for the first two stories and 52.6 t for the top story, giving a base shear of 101.0 t. The equivalent lateral forces, F, inter-story shears, V, and overturning moments, M, are as follows:

Story	Transverse Wall			Longitudinal Wall		
	F (t)	V (t)	M (tm)	F (t)	V (t)	M (tm)
3	15.8	15.8	47.4	40.3	40.3	120.9
2	15.9	31.7	142.5	40.5	80.8	363.3
1	8.0	39.7	261.6	20.2	101.0	666.3

For the transverse wall, the wall area is $A_w = 0.24\times5.64 + 0.36\times4.0 = 2.79\ m^2$, and the shear area (area of web of I wall section) is $A_v = 0.24\times6.36 = 1.53\ m^2$; whereas for the longitudinal wall, the corresponding values are 7.87 m^2 and 4.41 m^2, respectively. Assuming that the masonry shear strength, τ, is given by Eqs. 2.3 and 2.5 with $\mu = 0.5$, the vertical compressive stress, σ_c, and the required mortar strength for shear, f_{mo}, are:

Story	Transverse Wall		Longitudinal Wall	
	σ_c (kg/cm^2)	f_{mo} (kg/cm^2)	σ_c (kg/cm^2)	f_{mo} (kg/cm^2)
3	0.74	22	0.67	19
2	1.86	43	1.68	36
1	2.98	42	2.68	34

The overturning moments are resisted by vertical loads. The moment of inertia is $I = 0.24\times5.64^3/12 + 0.36\times2\times3.0^2\times2 = 16.55$ m^4 for the transverse wall and 157.4 m^4 for the longitudinal wall. The vertical loads, P, and the flexural stresses induced by the overturning moment, f_b, are as follows:

Story	Transverse Wall		Longitudinal Wall	
	P (t)	f_b (kg/cm^2)	P (t)	f_b (kg/cm^2)
3	29.8	0.16	75.7	0.34
2	61.0	-0.55	155.0	0.10
1	92.2	-1.72	234.3	-0.46

in which $f_b = \frac{P}{A_w} - \frac{Mc}{I}$, where c = 3.18 m and 8.12 m for the transverse and longitudinal walls, respectively. The permissible tensile stress for walls in flexure is 1.90 kg/cm^2 for Type N mortar (UBC, 1985) which has $f_{mo} \approx$ 35 to 70 kg/cm^2 (Sahlin, 1971). Therefore, assuming the mortar strength to be 50 kg/cm^2 for the first and second stories and 25 kg/cm^2 for the top story, the story ultimate shear capacity, $q_u = A_v\tau$, would be as given below:

Story	Ultimate Shear Capacity, q_u (t)	
	Transverse Wall	Longitudinal Wall
3	16.9	47.2
2	33.8	93.4
1	42.4	115.7

The simplified procedure is used to evaluate the potential damage to the above design. The initial story stiffness, k_i, and the ultimate displacement, u_u,

for the transverse wall are computed as follows:

Story	k_{ic} (t/cm)	λ_c	k_i (t/cm)	u_u (cm)
3	486	14.43	172	0.502
2	764	12.54	311	0.555
1	764	10.38	375	0.576

where $k_{ic} = E_m/(\frac{h^3}{12I} + \frac{h}{0.4A_v})$, $E_m = 700 f'_m$, and h is the story height. The masonry compressive strength, f_m, is assumed to be 35 and 55 kg/cm^2 for $f_{mo} =$ 25 and 50 kg/cm^2, respectively. The factor λ_c is given by Eq. 2.10 and $k_i = \lambda k_{ic}/\lambda_c$ with $\lambda = 5.1$. Similarly, the story stiffnesses and ultimate displacements for the longitudinal wall are:

Story	k_{ic} (t/cm)	λ_c	k_i (t/cm)	u_u (cm)
3	1560	14.78	538	0.447
2	2440	12.99	958	0.497
1	2440	10.87	1145	0.515

where $k_{ic} = E_m/(\frac{h^3}{12I} + \sum_{i=1}^{2}\frac{h_i}{0.4A_{vi}})$, with $h_1 = 2\,m$ (assumed height of doors), $A_{v1} = 4.41\,m^2$, $h_2 = 1\,m$ and $A_{v2} = 5.85\,m^2$. The structural period is $T = 0.1256$ sec, and the first mode shape is $\phi^T = \{0.357 \quad 0.699 \quad 1.000\}$ for the transverse wall. For the longitudinal wall, $T = 0.1143$ sec with $\phi^T = \{0.362 \quad 0.704 \quad 1.000\}$. The damage distribution vector is computed using Eq. 5.5b, yielding the following:

Story	Transverse Wall			Longitudinal Wall		
	ϕ'	$\frac{\phi'^{n_\phi}}{u_u^2}$	ϕ_D	ϕ'	$\frac{\phi'^{n_\phi}}{u_u^2}$	ϕ_D
3	0.301	0.319	0.283	0.296	0.386	0.274
2	0.342	0.360	0.319	0.342	0.449	0.318
1	0.357	0.449	0.398	0.362	0.576	0.408

For the transverse wall, the sum of the story damage indices, from Eq. 5.9, is

$$S_D = 0.0458 \frac{(65.4)^{1.725}(10)^{0.35}}{(0.1256)^{-3.10}(0.548)^{1.725}} = 0.631$$

For the longitudinal wall, the corresponding sum of the story damage indices is

$$S_D = 0.0458 \frac{(65.4)^{1.725}(10)^{0.35}}{(0.1143)^{-3.10}(0.491)^{1.725}} = 0.670$$

Using Eqs. 5.13 and 3.31, the story damage indices, D, maximum displacement, u_m, and the overall damage index, D_s, can be summarized as follows:

Story	Transverse Wall			Longitudinal Wall		
	D	u_m (cm)	wD	D	u_m (cm)	wD
3	0.178	0.089	0.020	0.156	0.070	0.016
2	0.201	0.112	0.061	0.181	0.090	0.054
1	0.251	0.145	0.147	0.232	0.120	0.139
		D_s =	0.228		D_s =	0.209

The potential damage to the design is also examined using the random vibration method. The story damage indices and the overall damage index are shown in Fig. 5.9a; the corresponding damage indices obtained with the simplified method are shown in parentheses. Observe that the overall damage index obtained by either method is less than the tolerable damage of $D_L = 0.25$; also Fig. 5.9a shows that the damage distribution is fairly uniform among the different stories. The above results show that the simplified method gives reliable overall damage indices.

For comparision, the same building is also designed with the UBC and TJ 11-78. This building cannot be designed as an unreinforced masonry structure using the ATC-3-06 because it would fall under Seismic Performance Category C, which requires all structural components to be of reinforced masonry.

According to the UBC, the base shear coefficient is C_s = ZIKCS = 0.14 (with Z = 3/4 for Seismic Zone No. 3, I = 1.0, K = 1.33, and CS = 0.14), giving a base shear of 0.14× 83.1 = 11.6t for the transverse wall and 0.14×

211.2 = 29.6 t for the longitudinal wall. The story shears, overturning moments, and flexural stresses would be as follows:

Story	Transverse Wall			Longitudinal Wall		
	V (t)	M (tm)	f_b (kg/cm^2)	V (t)	M (tm)	f_b (kg/cm^2)
3	4.6	13.8	0.80	11.8	35.4	0.78
2	9.3	41.7	1.39	23.7	106.5	1.42
1	11.6	76.5	1.83	29.6	195.3	1.97

There are no tensile stresses caused by overturning moments. For Seismic Zone No. 3, the UBC requires that the shear walls be designed to resist 1.5 times the above shear forces. Using type S mortar (f_{mo} = 75 kg/cm^2, f'_m = 75 kg/cm^2), the design shear forces, vertical compressive stresses, allowable story shears, and ultimate shear capacities, are as follows:

Story	Transverse Wall				Longitudinal Wall			
	1.5 V (t)	σ_c (kg/cm^2)	V_{all} (t)	q_u (t)	1.5 V (t)	σ_c (kg/cm^2)	V_{all} (t)	q_u (t)
3	6.9	0.74	17.1	32.8	17.7	0.67	48.3	92.9
2	14.0	1.86	21.6	41.3	35.6	1.68	60.2	115.1
1	17.4	2.98	26.2	49.9	44.4	2.68	71.9	137.2

where $V_{all} = 1.33 A_v(F_v + 0.2\sigma_c)$, A_v = 1.53 m^2 and 4.41 m^2 for the transverse and longitudinal walls, respectively, and F_v = 6.9 t/m^2 for f'_m = 75 kg/cm^2. Since the allowable story shears are much higher than the design shear forces, the wall thickness can be reduced to 18 cm for the transverse wall and 24 cm for the longitudinal wall. Repeating the design calculations, the following are obtained:

Story	Transverse Wall				Longitudinal Wall			
	1.5 V (t)	σ_c (kg/cm^2)	V_{all} (t)	q_u (t)	1.5 V (t)	σ_c (kg/cm^2)	V_{all} (t)	q_u (t)
3	6.0	0.90	13.0	24.9	15.3	0.82	33.2	63.7
2	11.7	2.19	16.8	32.1	29.9	2.00	42.3	80.9
1	14.6	3.48	20.6	39.3	37.2	3.17	51.4	98.0

The damage indices for this design, obtained by the random vibration method and the simplified method, are shown in Fig. 5.9b.

Observe that for this three-story building, the story damage indices are less uniform than those of the proposed method. In particular, the lower stories tend to have higher damage indices.

According to the TJ 11-78, $C_s = C\alpha = 0.203$ for $C = 0.45$ and $\alpha = 0.45$. The story shears, overturning moments, and flexural stresses are as follows:

Story	Transverse Wall			Longitudinal Wall		
	V (t)	M (tm)	f_b (kg/cm^2)	V (t)	M (tm)	f_b (kg/cm^2)
3	6.7	20.1	0.68	17.1	51.3	0.70
2	13.5	60.6	1.03	34.3	154.2	1.17
1	16.9	111.3	1.16	42.9	282.9	1.52

Using a mortar strength of 25 kg/cm^2, the σ_c, V_{all}, and q_u are as follows:

Story	Transverse Wall			Longitudinal Wall		
	σ_c (kg/cm^2)	V_{all} (t)	q_u (t)	σ_c (kg/cm^2)	V_{all} (t)	q_u (t)
3	0.74	14.9	16.9	0.67	42.4	47.2
2	1.86	17.7	25.5	1.68	49.8	69.5
1	2.98	20.1	34.0	2.68	56.2	91.5

where $V_{all} = A_v R_r / K\xi$, $R_r = R_j\sqrt{1 + \sigma_c/R_j}$, in which $R_j = 2.0$ kg/cm^2 for $f_{mo} = 25$ kg/cm^2, $K = 2.0$, and $\xi = 1.2$. The damage indices for this design is shown in Fig. 5.9c.

The damage indices are higher than those of the building designed with the proposed method or with the UBC; this is the result of using lower strength mortar for the lower stories.

5.4.2 Design of Five-Story Building

For this structure, the seismic load is assumed to be $\sigma_a = 0.033$ g, corresponding approximately to a peak acceleration of 0.1 g, with $t_d = 10$ sec. Let the walls be 18 cm thick. The tributary floor mass for an interior transverse wall is 17.1 t for the top story and 24.0 t for all the other stories. For a longitudinal wall, the floor mass is 43.6 t for the top story and 61.3 t for the other stories. Assuming a structural period of 0.20 sec, $C_s = 0.221$ is obtained for a tolerable damage of $D_L = 0.25$. The equivalent lateral forces, story shears, and overturning moments are:

Story	Transverse Wall			Longitudinal Wall		
	F (t)	V (t)	M (tm)	F (t)	V (t)	M (tm)
5	6.6	6.6	19.8	16.8	16.8	50.4
4	7.4	14.0	61.8	18.8	35.6	157.2
3	5.5	19.5	120.3	14.1	49.7	306.3
2	3.7	23.2	189.9	9.4	59.1	483.6
1	1.8	25.0	264.9	4.7	63.8	675.0

For the transverse wall, $A_w = 1.77$ m^2, $A_v = 1.11$ m^2, and $I = 9.44$ m^4; whereas for the longitudinal wall, the corresponding values are 4.89 m^2, 2.19 m^2, and 81.5 m^4, respectively. The mortar strengths required for shear and the flexural stresses caused by overturning moment are:

Story	Transverse Wall		Longitudinal Wall	
	f_{mo} (kg/cm^2)	f_b (kg/cm^2)	f_{mo} (kg/cm^2)	f_b (kg/cm^2)
5	2	0.63	9	0.68
4	2	0.62	17	0.88
3	-	0.07	18	0.65
2	-	-0.85	11	0.14
1	-	-1.95	-	-0.50

Since f_b for the first story of the transverse wall exceeds the allowable tensile stress of 1.90 kg/cm^2 for $f_{mo} = 50\ kg/cm^2$, the wall thickness for the first story is increased to 24 cm. Recalculating the required mortar strengths and flexural stresses gives:

Story	Transverse Wall		Longitudinal Wall	
	f_{mo} (kg/cm^2)	f_b (kg/cm^2)	f_{mo} (kg/cm^2)	f_b (kg/cm^2)
5	2	0.63	9	0.68
4	2	0.60	18	0.86
3	-	0.03	19	0.62
2	-	-0.91	12	0.09
1	-	-1.47	-	0.32

Because overturning moments result in tensile stresses in the first two stories and only a small compressive stress in the third story, a mortar strength of 50 kg/cm^2 is used for the lower three stories and 25 kg/cm^2 for the upper two stories. The damage indices will be higher for the longitudinal wall because the required mortar strengths are higher for this wall. Therefore, it is only necessary to check for damage in the longitudinal wall. The ultimate shear capacities, story stiffnesses, and ultimate displacements for the longitudinal wall are:

Story	q_u (t)	k_i (t/cm)	u_u (cm)
5	25.9	286	0.461
4	39.6	402	0.503
3	65.3	634	0.526
2	79.0	749	0.538
1	104.2	993	0.535

The structural period, $T = 0.1961$ sec with $\phi^T = \{0.173 \quad 0.386 \quad 0.600 \quad 0.844 \quad 1.000\}$, and the damage distribution vector, $\phi_D^T = \{0.161 \quad 0.221 \quad 0.199 \quad 0.284 \quad 0.136\}$, giving $u_{ue} = 0.515$ cm. The sum of the story damage indices is

$$S_D = 0.0413 \frac{(32.7)^{1.625}(10)^{0.35}}{(0.1961)^{-2.90}(0.515)^{1.625}} = 0.698$$

Therefore, the story damage indices are:

Story	1	2	3	4	5
D	0.113	0.154	0.139	0.198	0.095

and the overall damage index is 0.150. Damage indices calculated with the random vibration method is shown in Fig. 5.10a. Again, the proposed simplified method yields good estimates of the story and overall damage indices (shown in parentheses in Fig. 5.10a). Observe that the change in the mortar strength from 50 kg/cm^2 to 25 kg/cm^2 between the third and the fourth stories results in some damage concentration in the fourth story.

Designing the same building based on the UBC, the base shear coefficient, $C_s = 0.07$ (with $Z = 3/8$ for Seismic Zone No. 2). Using a wall thickness of 24 cm for the first story and 18 cm for the upper stories, the story shears, flexural stresses, vertical compressive stresses, and allowable story shears are as follows:

Story	V (t)	f_b (kg/cm^2)	σ_c (kg/cm^2)	V_{all} (t)
5	5.4	1.02	0.89	22.4
4	11.4	1.93	2.15	29.7
3	15.9	2.71	3.40	37.0
2	18.9	3.40	4.65	44.3
1	20.5	3.40	4.53	58.5

where V_{all} is computed assuming Type N mortar ($f_{mo} = 50\ kg/cm^2$) is used for all the stories. The damage indices for this wall is shown in Fig. 5.10b.

Based on the TJ 11-78, $C_s = 0.104$ ($\alpha = 0.23$). Using a wall thickness of 24 cm for the first story and 18 cm for the upper stories, and a mortar strength of 25 kg/cm^2 for all the stories, the following are obtained:

Story	V (t)	σ_c (kg/cm^2)	V_{all} (t)	q_u (t)
5	8.0	0.89	21.9	25.9
4	16.9	2.15	26.3	39.6
3	23.6	3.40	30.0	53.3
2	28.1	4.65	33.3	67.0
1	30.5	4.53	44.2	88.2

The corresponding damage indices for the longitudinal wall is shown in Fig. 5.10c. Again, higher damages are observed than those of the design obtained with the proposed method or the UBC because of the use of lower strength mortar in the lower stories.

The above two examples show that the proposed design method can yield structures with fairly uniform distribution of damage among the different stories of a masonry building; this should improve the seismic resistance as all the stories are participating equally in resisting the lateral forces.

5.5 Reliability of Proposed Design Method

In the proposed design method, potential damage to a building subjected to the design earthquake is limited to a tolerable damage level, $D_L = 0.25$ to prevent severe, irrepairable damage. However, because ground motion and structural capacity are highly variable, there is always the probability that the building will suffer severe damage or collapse, $(D \geq 1.0)$, even when subjected to the design earthquake. In additional to the uncertainties in the ground motion and the structural capacity, there are also uncertainties in the model parameters such as the story mass, ultimate strength, and stiffness. These uncertainties can be attributed to the inherent variabilities of the parameters and to the errors in modeling the parameters. Because of these model parameter uncertainties, the failure probability is a random variable, since it is a function of the distribution of the damage index, which in turn depends on the model parameters. It is necessary to account for all these uncertainties in evaluating the reliability of the proposed design method.

It was observed in Chap. 4 that the uncertainty in the damage index is due mainly to the uncertainty in the structural capacity, represented by the ultimate damage index D_{ult}. Since D_{ult} has a Weibull distribution, the damage index can be expected to have an extreme value Type II distribution. The failure probability may then be given by

$$p_f = 1 - \exp\{-(v_D)^{k_D}\} \tag{5.29}$$

where v_D and k_D are the distribution parameters. This failure probability is conditional on the mean damage index, $\overline{D}$, which is a random variable because of the uncertainties in the model parameters. If q is the probability that p_f will be less than the value $(p_f)_q$, i.e.,

$$P[1 - \exp\{-(v_D)^{k_D}\} \leq (p_f)_q] = q \tag{5.30}$$

then assuming that $\overline{D}$ is lognormally distributed, with parameters λ_D and ζ_D, it can be shown that

$$(p_f)_q = 1 - \exp\left\{ - \left[\frac{\exp\{\lambda_D + \zeta_D \Phi^{-1}(q)\}}{\Gamma(1 - 1/k_D)} \right]^{k_D} \right\} \tag{5.31}$$

where $\Phi^{-1}(.)$ is the inverse normal distribution function and $\Gamma(.)$ is the gamma function.

In Chap. 4, it was observed that the cov of D, δ_D, varies between 0.30 and 0.35. Using $\delta_D = 0.35$, the distribution parameter $k_D = 4.603$.

To evaluate λ_D and ζ_D, the mean and variance of $\overline{D}$ are required. The variance of $\overline{D}$ is obtained using a first-order approximation (Ang and Tang, 1975):

$$\sigma_{\overline{D}}^2 = \sum_i \sum_j c_i c_j \sigma_{pi} \sigma_{pj} \rho_{ij} \tag{5.32}$$

where c_i = the partial derivative of $\overline{D}$ with respect to the model parameter p_i, evaluated at the mean values of the model parameters; σ_{pi} = the standard deviation of p_i; and ρ_{ij} = the coefficient of correlation between the parameters p_i and p_j. To evaluate $\sigma_{\overline{D}}^2$ the uncertainties in the model parameters are required.

5.5.1 Uncertainties in Model Parameters

From the study by Portillo and Ang (1976), the variability in the mass of a building may be represented by a cov of 0.12.

The uncertainties in the ultimate strength and the stiffness consist of the inherent variabilities and the modeling errors. From the limited experimental data available, it is not possible to determine the inherent variabilities in the strength and stiffness. Therefore, these will be assumed to be represented by a cov of 0.30 for both strength and stiffness. Using the methods in Chap. 2 to evaluate the ultimate strengths and stiffnesses of the wall test specimens used by Zhu (1980), Ref. 27, and Xia (1986), modeling errors of 0.11 for strength and 0.36 for stiffness are obtained. Hence the total uncertainty is expressed by a cov of $\Omega_q = \sqrt{0.30^2 + 0.11^2} = 0.32$ for strength, and a cov of

$\Omega_k = \sqrt{0.30^2 + 0.36^2} = 0.47$ for stiffness. Figure 5.11 show that strength and stiffness are correlated, with a correlation coefficient of 0.89. This is to be expected because both strength and stiffness depend on the wall section and masonry properties.

The structural damping coefficients of 14 unreinforced masonry buildings are reported in Yang, et al., (1981). From these data, the cov of the structural damping coefficient is 0.42.

Lai (1982) evaluated the Kanai-Tajimi parameters ω_g and ζ_g for 140 ground motions records, obtaining a cov of 0.44 for ω_g and a cov of 0.42 for ζ_g.

There are also uncertainties associated with the restoring force model parameters. However, except for the parameter ρ, these are small and do not significantly affect the uncertainty in $\overline{D}$. For the parameter ρ, the experimental data indicate a range of 2.0 to 6.0 with a mean value of 3.3. Therefore, assuming a lower triangular distribution for ρ gives a cov of 0.28.

Using the cov's for the various model parameters determined above, the variance of $\overline{D}$ is evaluated for three SDF systems with structural periods of $T = 0.1$, 0.2, and 0.3 sec, using $\zeta = 0.04$, $\omega_g = 5\pi$, $\zeta_g = 0.60$, and $t_d = 10$ sec The intensity of the ground motion is varied to give different values of the mean damage index.

Figure 5.12 shows the contribution to the total variance of $\overline{D}$ from the uncertainties of the model parameters for the system with $T = 0.2$ sec, indicating that the uncertainties in the strength and stiffness have the greatest contribution to the total uncertainty in $\overline{D}$.

Figure 5.13 plots the cov of $\overline{D}$, $\delta_{\overline{D}}$, for the above three SDF systems. It is observed that $\delta_{\overline{D}} = 0.5$ to 0.6 for small $\overline{D}$ ($\overline{D}<0.3$), but increases substantially as $\overline{D}$ approaches 1.0. Hence, the cov of $\overline{D}$ can be conservatively assumed to be 0.6 for $\overline{D} \leq 0.25$, and increases linearly to 1.2 for $\overline{D} = 0.75$, as shown by the dotted line in Fig. 5.13.

5.5.2 Failure Probability

The probability of failure, $p_f = P(D \geq 1.0)$, is evaluated for different values of $\overline{D}$ and corresponding error bounds using Eq. 5.31. The results are plotted against $\overline{D}$ and the ratio $L_s/L_{s,des}$ in Fig. 5.14. L_s is a seismic load defined by

$$L_s = f_{T_g}(\sigma_a)^{n_I}(t_d)^{n_t} \tag{5.33}$$

where n_I and n_t are given by Eqs. 5.8 and 5.11, and $L_{s,des}$ is the design seismic load. The damage index is a linear function of L_s, and for Fig. 5.14, it is assumed that the proposed design method is used for a tolerable damage of $D_L = 0.25$. Observe that the 80% confidence interval for p_f widens as $\overline{D}$ increases, because $\delta_{\overline{D}}$ increases with increasing $\overline{D}$. Specifically, for a mean damage index of 0.25, there is 90 percent probability that p_f is less than 0.01.

Table 5.1 Values of n_ϕ

Story	Number of Storys					
	2	3	4	5	6	7
1	1.85	1.85	1.90	1.90	1.90	1.90
2	2.15	2.05	2.00	1.95	1.95	1.95
3		2.10	2.05	2.05	2.00	2.00
4			2.05	2.05	2.05	2.05
5				2.05	2.05	2.05
6					2.05	2.05
7						2.05

Table 5.2a Computation of Adjusted Base Shear Coefficient, C_s', for $\sigma_a = 0.033\,g$

	f_v (kg/cm^2)	$\frac{\tau}{f_v}$	$\frac{\gamma}{\phi}$	C_s	C_s'
ATC-3-06	1.05	2.65	1.00	0.200	0.530
UBC	1.19	2.34	0.75	0.070	0.123
TJ 11-78	4.24	0.66	2.40	0.104	0.165

$\tau = 2.78\ kg/cm^2$

Table 5.2b Computation of Adjusted Base Shear Coefficient, C_s', for $\sigma_a = 0.067\,g$

	f_v (kg/cm^2)	$\frac{\tau}{f_v}$	$\frac{\gamma}{\phi}$	C_s	C_s'
ATC-3-06	1.41	2.32	1.00	0.400	0.928
UBC	1.29	2.53	1.13	0.140	0.400
TJ 11-78	4.77	0.69	2.40	0.203	0.336

$\tau = 3.27\ kg/cm^2$

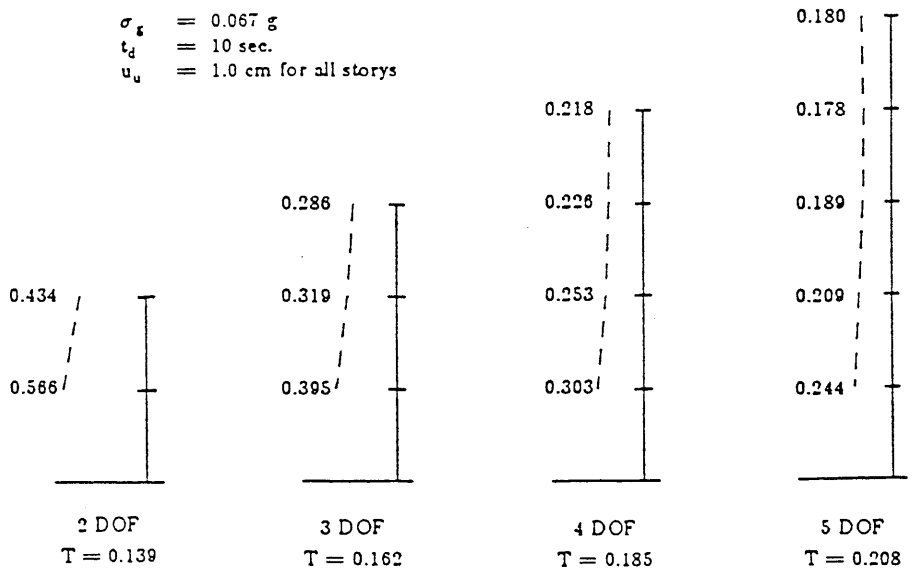

Fig. 5.1 Damage Distribution for Systems with Linear Mode Shapes

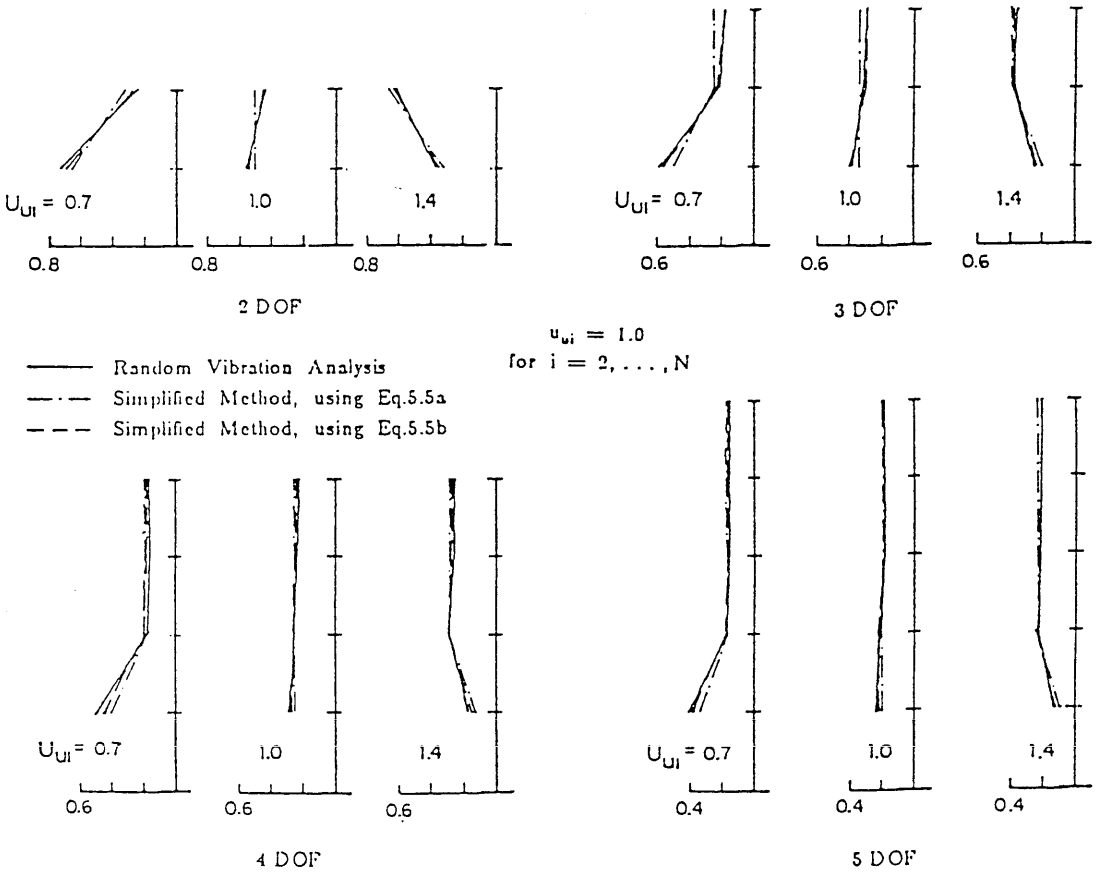

Fig. 5.2 Influence of u_{u1} on Damage Distribution

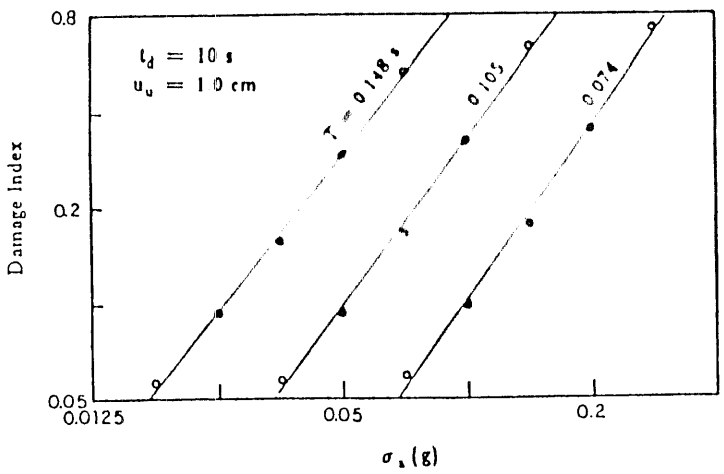

Fig. 5.3a Variation of Damage Index with σ_a

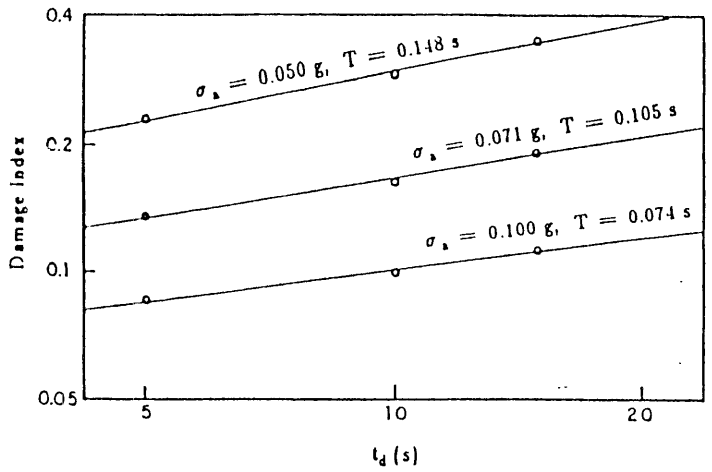

Fig. 5.3b Variation of Damage Index with t_d

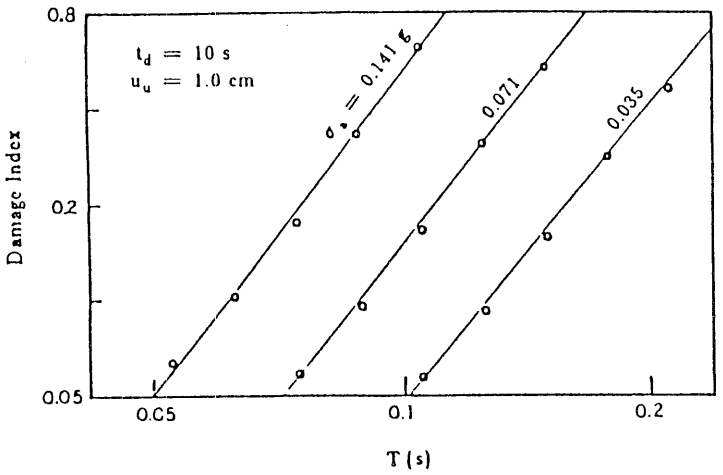

Fig. 5.3c Variation of Damage Index with T

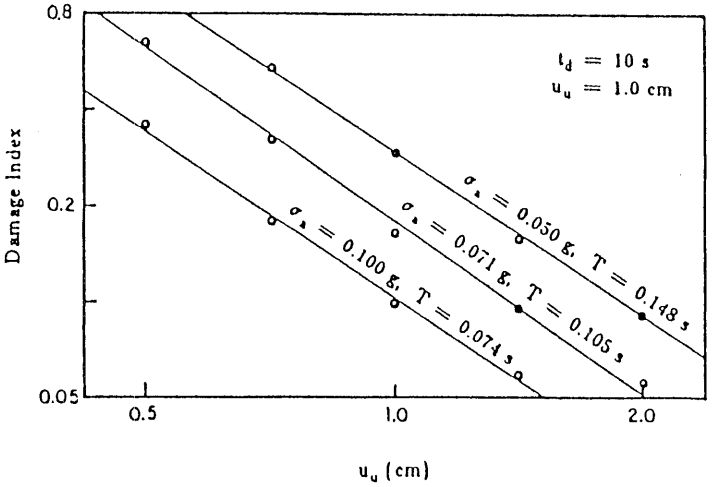

Fig. 5.3d Variation of Damage Index with u_u

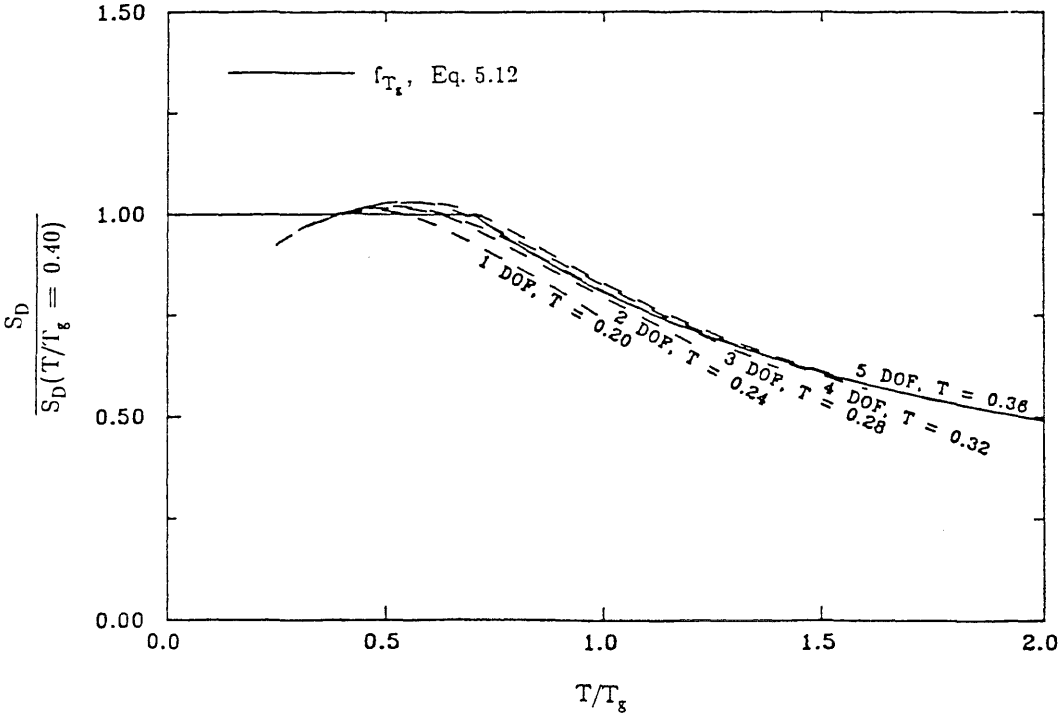

Fig. 5.4 Variation of S_D with T/T_g

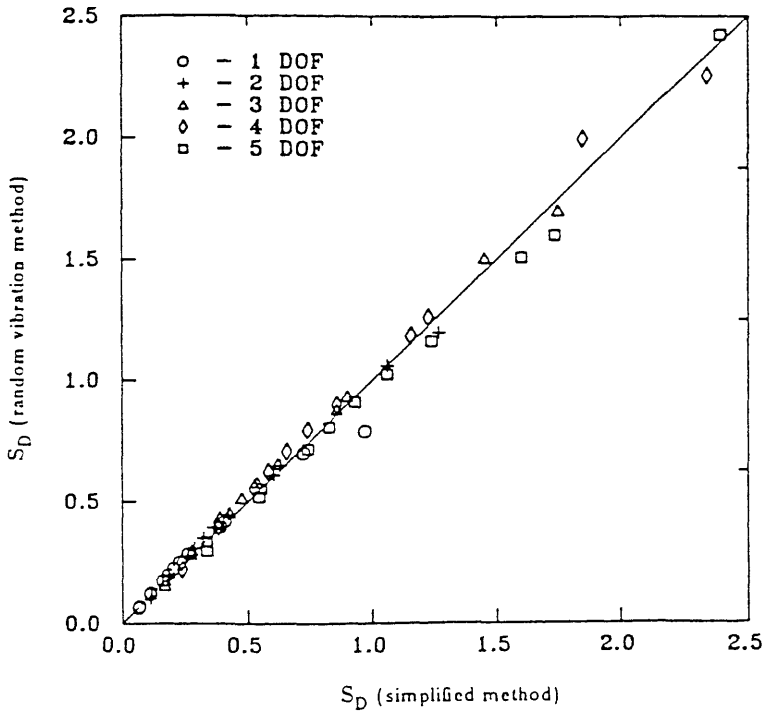

Fig. 5.5 S_D Obtained Using the Random Vibration Method and the Simplified Method

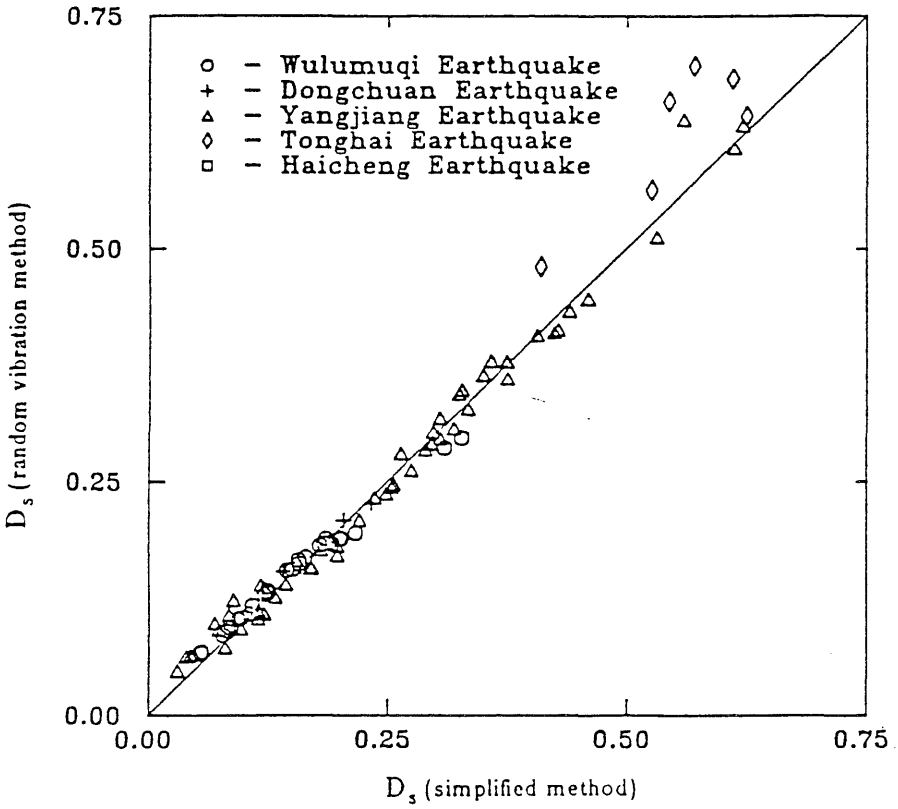

Fig. 5.6 D_s Obtained Using the Random Vibration Method and the Simplified Method

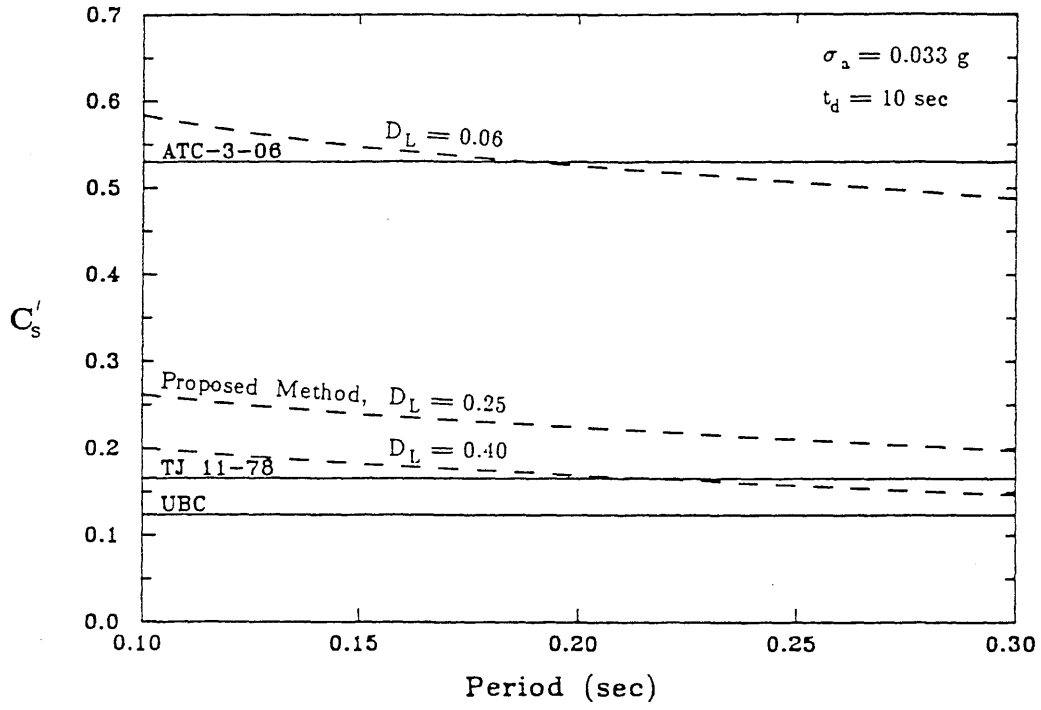

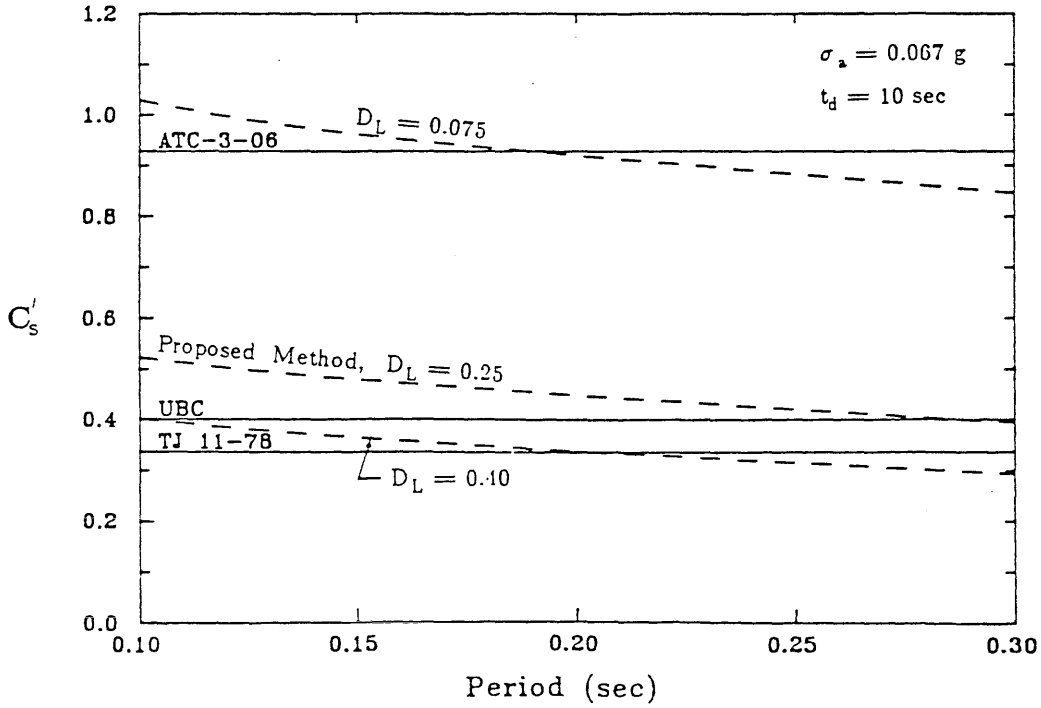

Fig. 5.7 Comparison of C_s'

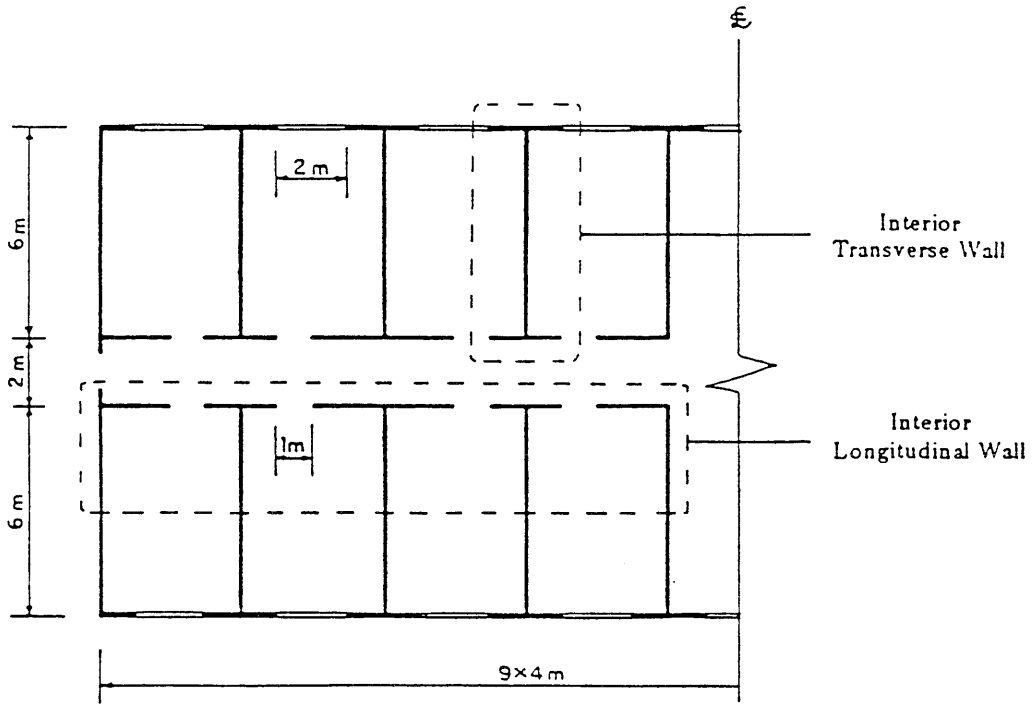

Floor Plan

Fig. 5.8 Floor Plan of Building

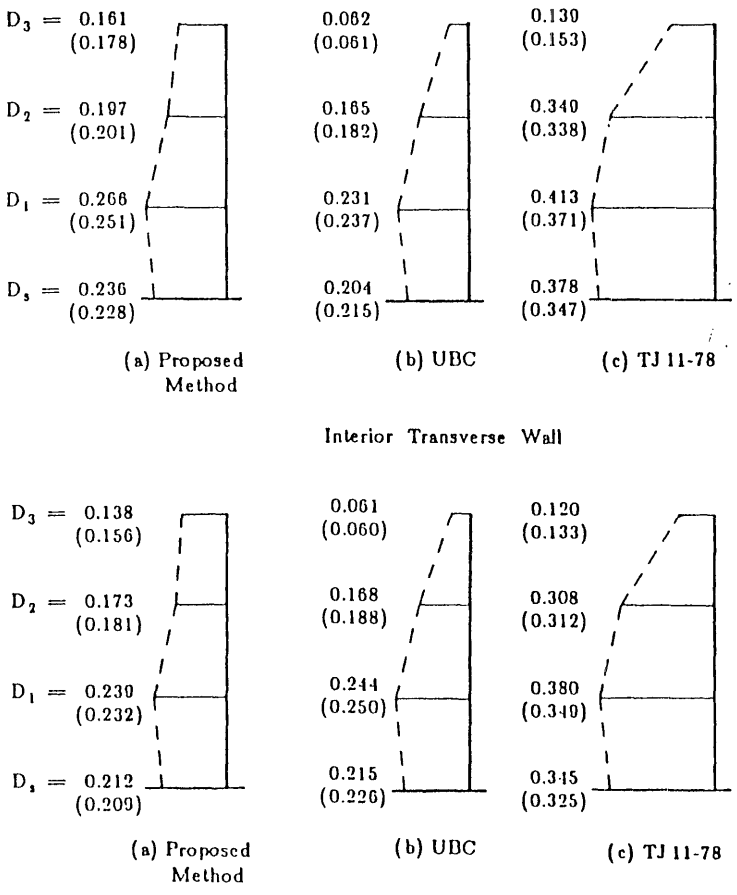

Fig. 5.9 Interstory Damage Indices of Walls in 3-Story Building

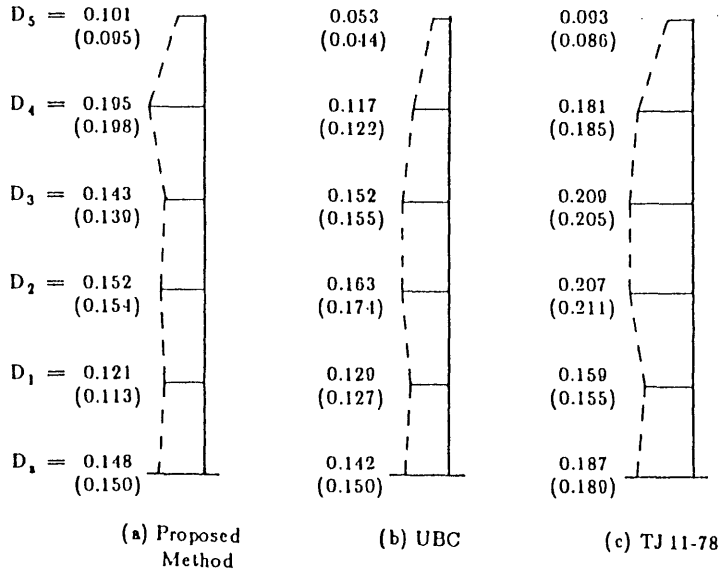

Fig. 5.10 Interstory Damage Indices of Walls in 5-Story Building

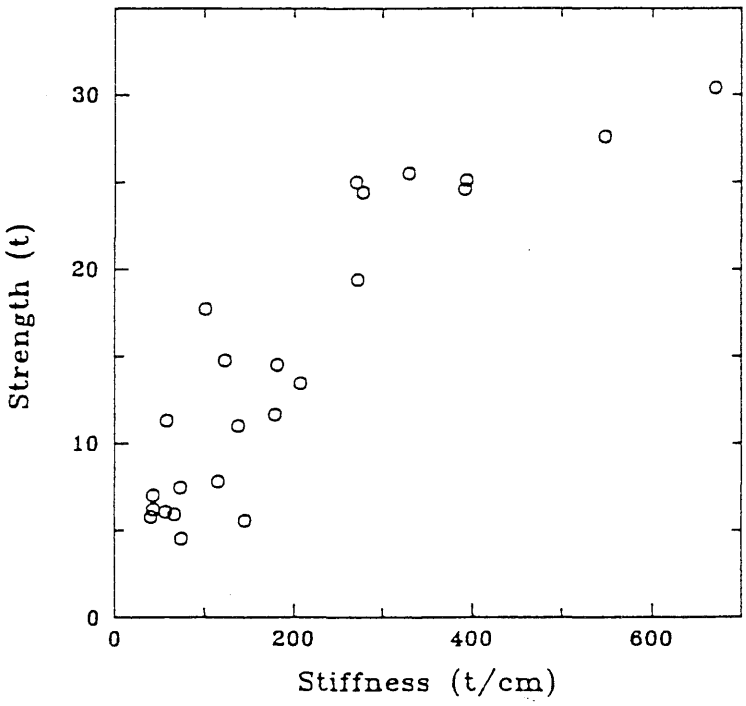

Fig. 5.11 Correlation between Strength and Stiffness

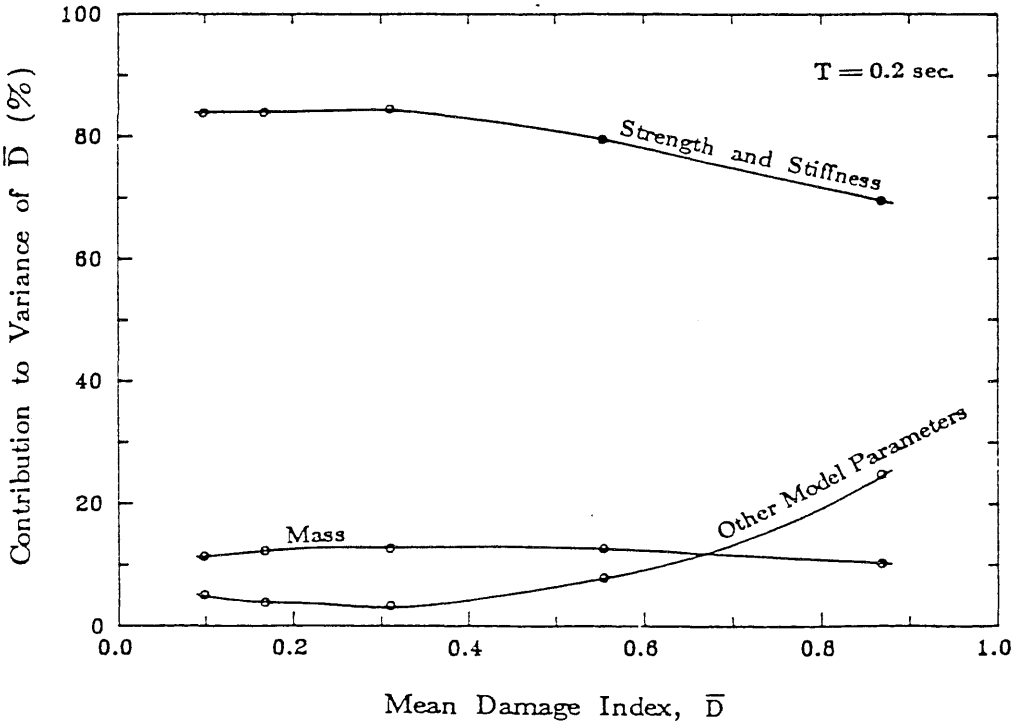

Fig. 5.12 Contribution to Variance of $\bar{D}$ from Uncertainties in Model Parameters

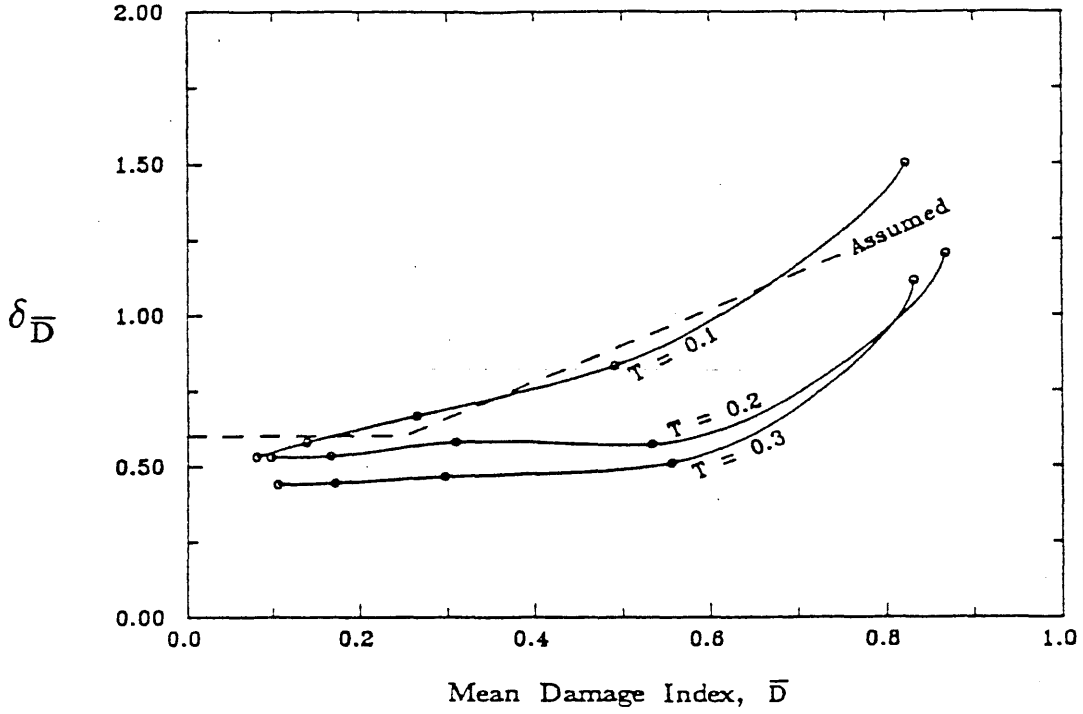

Fig. 5.13 COV of Mean Damage Index, $\overline{D}$

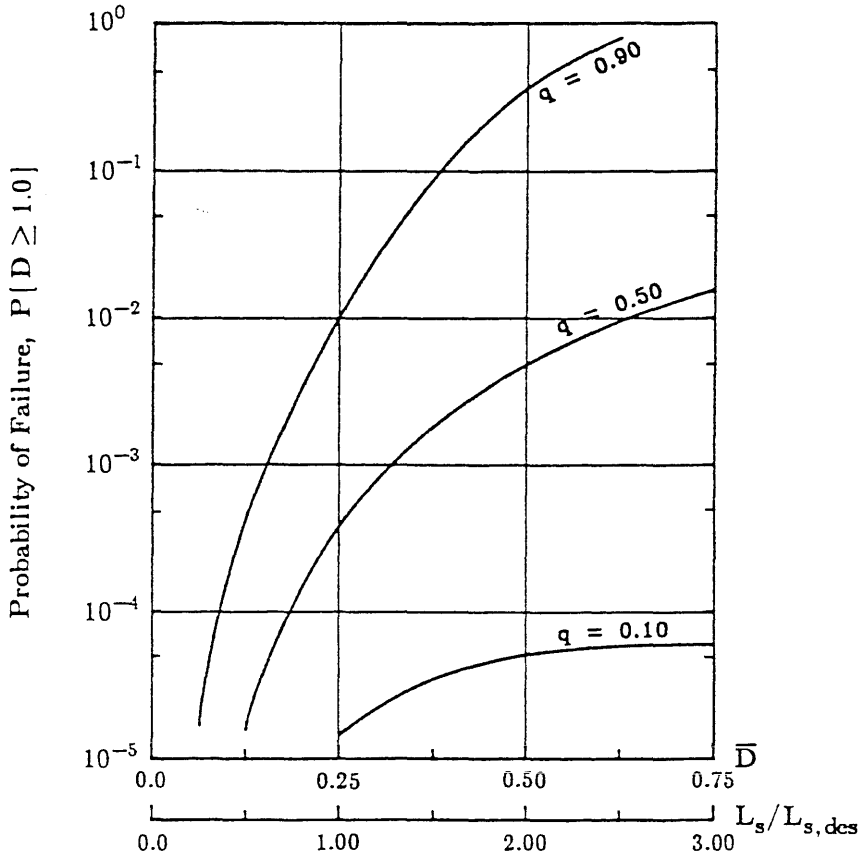

Fig. 5.14 Probability of Failure

CHAPTER 6

SUMMARY AND CONCLUSIONS

A seismic damage model for masonry structures is developed. Damage is measured by a damage index, which is a function of the maximum deformation and the absorbed hysteretic energy. The parameters for the damage index are evaluated using results from cyclic load tests on unreinforced brick masonry shear walls. The ultimate damage index, representing the structural capacity to resist damage, is shown to be described by a Weibull distribution with a mean value of 0.99 and a cov of 0.31.

A restoring force model was developed to model the nonlinear, stiffness and strength degrading characteristics of masonry. The model parameters were determined for unreinforced brick masonry. A random vibration approach was adopted to determine the response statistics of the maximum displacement and absorbed energy. It is shown that the contribution of the uncertainty in the absorbed energy to the total uncertainty in the damage index is small.

The damage indices for forty five unreinforced brick masonry buildings from five earthquakes in the PRC were evaluated. Correlating the calculated damage indices with observed damage suggests that to avoid severe (irrepairable) damage, the damage index should not exceed 0.25. Collapse is expected when the damage index approaches 1.0. Damage in a masonry building is usually higher in the lower stories because the maximum displacement and absorbed energy is greater in the lower stories. However, fairly uniform distribution of damage is observed in buildings with a linear mode shape and constant ratio of strength to stiffness. It is also observed that when the damage index is less than one, its uncertainty is due mainly to the uncertainty in the structural capacity. Therefore, the cov of the damage index is fairly contant - having values between 0.30 and 0.35.

An alternate method for evaluating the damage index is also developed. Damage is expressed as a ratio of the seismic load to the structural capacity. The seismic load is represented by the rms acceleration, the strong motion duration, and the predominant period of the ground motion. The structural capacity is expressed in terms of the structural period and the ultimate deformation capacity. This simplified method is shown to give good estimates of the damage index.

A modification to the equivalent lateral load procedure is proposed for the design of low-rise unreinforced masonry structures. The base shear coefficient is derived as an explicit function of the limiting damage level. Uniform distribution of damage is achieved through the appropriate selection of wall stiffness and strength. It is shown that the base shear coefficients of the ATC-3-06 is high for unreinforced masonry construction, whereas the base shear coefficients of the UBC and TJ 11-78 correspond to a limiting damage index of about 0.40. Two design examples show that unreinforced masonry buildings can be designed with an explicit measure of tolerable damage; moreover, fairly uniform distribution of damage can also be achieved. The reliability of the proposed design method was evaluated taking into consideration uncertainties in the model parameters in addition to the uncertainties in the seismic loading and the structural capacity. When subjected to the design earthquake, the probability of failure of a building designed according to the proposed method is less than 0.01 with a 90 percent confidence.

APPENDIX

The integrals I_1 and I_2 in Eq. 3.17 are

$$I_1 = \int_0^1 z^{1/(\rho-1)} \exp\left(-x^2(1-z^{1/(\rho-1)})^2\right) dz \qquad (A.1)$$

$$I_2 = \int_0^\infty z^{1/(\rho-1)} \exp\left(-x^2(1+z^{1/(\rho-1)})^2\right) dz \qquad (A.2)$$

where $x = \frac{1}{\sqrt{2}} \frac{au_u}{\sigma_u}$. In general, numerical evaluation of these integrals is necessary. However, if ρ is an integer, it can be shown that Eq. 3.17 may be rewritten as

$$k_{eu} = \frac{\rho}{au_u} \frac{1}{\sqrt{\pi}} I \qquad \text{for } \rho \text{ even} \qquad (A.3a)$$

$$= \frac{\rho}{au_u} \frac{1}{\sqrt{\pi}} (2I' - I) \qquad \text{for } \rho \text{ odd} \qquad (A.3b)$$

in which

$$I = \frac{1}{\sqrt{\pi}} \sum_{m=0}^{\rho-1} \binom{\rho-1}{m} \left(-\frac{1}{x}\right)^m \Gamma\left(\tfrac{1}{2}(m+1)\right) \qquad (A.4)$$

and,

$$I' = \int_0^{x^2} e^{-t} \left(1 - \frac{\sqrt{t}}{x}\right)^{\rho-1} \sqrt{t}\, dt \qquad (A.5)$$

where $\binom{\cdot}{\cdot}$ is the binomial coefficient and $\Gamma(.)$ is the gamma function.

REFERENCES

1. Ang, A. H-S., and Tang, W. H., *Probability Concepts in Engineering Planning and Design, Volume I - Basic Principles*, John Wiley and Sons, New York, 1975.

2. Applied Technology Council, *Tentative Provisions for the Development of Seismic Regulations for Buildings*, ATC Publication ATC-3-06, 1978.

3. *Aseismic Design Code for Industrial and Civil Buildings*, TJ 11-78, Chinese Academy of Building Research, 1979 (In Chinese).

4. Atalik, T. S., and Utku, S., "Stochastic Linearization of Multidegree-of-Freedom Nonlinear Systems," *Journal of Earthquake Engineering and Structural Dynamics*, Vol. 4, 1976.

5. Baber, T. T., and Wen, Y. K., "Random Vibration of Hysteretic, Degrading Systems," *Journal of the Engineering Mechanics Division*, ASCE, Vol. 107, No. EM6, Dec. 1981.

6. Benjamin, J. R., and Williams, H. A., "The Behavior of One-Story Brick Shear Walls," *Journal of the Structural Division*, ASCE, Vol. 84, No. ST4, Jul. 1958.

7. Borchelt, J. G., "Analysis of Brick Walls Subject to Axial Compression and In-Plane Shear," *Proceedings of Second International Brick Masonry Conference*, Stoke-on-Trent, Apr. 1970.

8. *Chinese Earthquake Intensity Scale (1980), Commentary*, Institute of Engineering Mechanics, Academia Sinica, Harbin, PRC, 1980 (In Chinese).

9. Haller, P., "Load Capacity of Brick Masonry," *Designing, Engineering, and Constructing with Masonry Products*, Ed. by Johnson, F. B., Gulf Publishing Co., Houston, Texas, 1969.

10. Hegemier, G. A., Nunn, R. C., and Arya, S. K., "Behavoir of Concrete Masonry Under Biaxial Stresses," *Proceedings of First North American Masonry Symposium*, Boulder, Colorado, 1978.

11. Hu, Yuxian, Private communication to Wen, Y. K., 1984.

12. Lai, P. S-S., "Statistical Characterization of Strong Ground Motions Using Power Spectral Density Function," *Bulletin of the Seismological Society of America*, Vol. 72, No. 1, Feb. 1982.

13. Lin, Y. K., *Probabilistic Theory of Structural Dynamics*, Krieger Publishing Co., Inc., Huntington, New York, 1976.

14. Mayes, R. L. and Clough, R. W., "State-of-the-Art in Seismic Shear Strength of Masonry - An Evaluation and Review," *Report No. EERC 75-21*, Earthquake Engineering Research Center, Berkeley, California, Oct. 1975.

15. Mayes, R. L., Omote, Y., and Clough, R. W., "Cyclic Shear Tests of Masonry Piers, Volume 1 - Test Results," *Report No. EERC 76-8*, Earthquake Engineering Research Center, Berkeley, California, May 1976.

16. Meli, R., "Behavior of Masonry Walls Under Lateral Loads," *Proceedings of Fifth World Conference on Earthquake Engineering*, Rome, 1972.

17. Murthy, C. K. and Hendry, A. W., "Model Experiments in Load Bearing Brickwork," *Building Science*, Vol. 1, Pergamon Press, London, 1966.

18. Park, Y-J., Ang, A. H-S., and Wen, Y. K., "Seismic Damage Analysis and Damage-Limiting Design of R. C. Buildings," *Civil Engineering Studies, SRS No. 516*, University of Illinois, Urbana, Illinois, Oct. 1984.

19. Pieper, K. and Trautsch, W., "Shear Tests on Walls," *Proceedings of Second International Brick Masonry Conference*, Stoke-on-Trent, Apr. 1970.

20. Pires, J. E. A., Wen, Y. K., and Ang, A. H-S., "Stochastic Analysis of Liquefaction under Earthquake Loading," *Civil Engineering Studies, SRS No. 504*, University of Illinois, Urbana, Illinois, Apr. 1983.

21. Portillo, M. and Ang, A. H-S., "Evaluation of Safety of Reinforced Concrete Buildings to Earthquake," Ph.D. Thesis, Graduate College, University of Illinois, Urbana, Illinois, Jul. 1976.

22. Priestley, M. J. N., and Bridgeman, D. O., "Seismic Resistance of Brick Masonry Walls," *Bulletin of the New Zealand National Society for Earthquake Engineering*, Vol. 7, No. 4, Dec. 1974.

23. Sahlin, *Structural Masonry*, Prentice-Hall, Inc., Englewood Cliffs, New Jersey, 1971.

24. Scrivener, J. C., "Concrete Masonry Wall Panel Tests - Static Racking Tests with Predominent Flexural Effect," *New Zealand Concrete Construction*, Jul. 1966.

25. Scrivener, J. C., "Static Racking Tests on Concrete Masonry," *Designing, Engineering, and Constructing with Masonry Products*, Ed. Johnson, F. B., Gulf Publishing Co., Houston, Texas, 1969.

26. *Seismic Damage from the Haicheng Earthquake*, Institute of Engineering Mechanics, Academia Sinica, Harbin, PRC, 1979 (In Chinese).

27. Shaanxi Construction Technology Research Institute, "Experimental Study of the

Collapse Resistance of Walls in Buildings," SCTRI, Shaanxi Province, PRC (In Chinese).

28. Sinha, B. P. and Hendry, A. W., "Racking Tests on Storey-Height Shear-Wall Structures with Openings, Subjected to Precompression," *Designing, Engineering, and Constructing with Masonry Products*, Ed. by Johnson, F. B., Gulf Publishing Co., Houston, Texas, 1969.

29. Sues, R. H., Wen, Y. K., and Ang, A. H-S., "Stochastic Seismic Performance Evaluation of Buildings," *Civil Engineering Studies, SRS No. 506*, University of Illinois, Urbana, Illinois, May 1983.

30. Turnsek, V. and Cacovic, F., "Some Experimental Results on the Strength of Brick Masonry Walls," *Proceedings of Second International Brick Masonry Conference*, Stoke-on-Trent, Apr. 1970.

31. *Uniform Building Code, 1985 Edition*, International Conference of Building Officials, Whittier, California, 1985.

32. Wen, Y. K., "Equivalent Linearization for Hysteretic Systems Under Random Excitation," *Journal of Applied Mechanics*, Transactions of ASME, Vol. 47, No. 1, Mar. 1980.

33. Williams, D., *Seismic Behavior of Reinforced Masonry Shear Walls*, Ph.D. Thesis, University of Canterbury, New Zealand, 1971.

34. Williams, D. and Scrivener, J. C., "Response of Reinforced Masonry Shear Walls to Static and Dynamic Cyclic Loading," *Proceedings of Fifth World Conference on Earthquake Engineering*, Rome, Jun. 1973.

35. Woodward, K., "Shear Behavior of Unreinforced Concrete Block Walls," *Proceedings of US-PRC Joint Workshop on Seismic Resistance of Masonry Structures*, Harbin, PRC, May 1986.

36. Xia, J., Ding, S., and Zhou, S., "Tests of Aseismic Behavior of Brick Masonry Wall," *Proceedings of US-PRC Joint Workshop on Seismic Resistance of Masonry Structures*, Harbin, PRC, May 1986.

37. Yang, J. N. and Liu, S. C., "Distribution of Maximum and Statistical Response Spectra," *Journal of the Engineering Mechanics Division*, ASCE, Vol. 107, No. EM6, Dec. 1981.

38. Yang, Y. C., Yang, L., and Gao, Y. X., *Earthquake Damage and Collapse-Resistant Design of Multistory Masonry Buildings*, Institute of Engineering Mechanics, Academia Sinica, Harbin, PRC, 1981 (In Chinese).

39. Zelger, C., "Neue Erkenntnisse bei der Bemessung von Bewehrten Zeigelstürtzen

(Recent Findings in the Design of Reinforced Tile Lintels)," *Die Zeigelindustrie*, Heft 9, 1965.

40. Zhu, B., Wu, M., and Jiang, Z., "Experimental Study on Basic Behavior of Brick Masonry Under Reversed Loading," *Journal of Tung-Chi University*, Shanghai, PRC, 1980 (In Chinese).